Title
CAPACITY FACTORS IN THE PERFORMANCE OF PERFORATED PLATE COLUMNS

Author
Hunt, C.A.

Publication Date
1954-10-01

UCRL 2696

UNIVERSITY OF CALIFORNIA

Radiation Laboratory

BERKELEY, CALIFORNIA

UCRL-2696
Unclassified--Chemistry Distribution

UNIVERSITY OF CALIFORNIA

Radiation Laboratory

Contract No. 7405-eng-48

CAPACITY FACTORS IN THE PERFORMANCE OF PERFORATED PLATE COLUMNS

Charles d'Ancona Hunt

October, 1954

(Thesis)

Berkeley, California

TABLE OF CONTENTS

CAPACITY FACTORS IN THE PERFORMANCE OF PERFORATED PLATE COLUMNS

Charles d'Ancona Hunt
Radiation Laboratory and
Department of Chemistry and Chemical Engineering
University of California, Berkeley, California

October, 1954

ABSTRACT

A study was made of factors affecting the vapor handling capacity of perforated plate liquid-vapor contacting columns. Vapor phase pressure drop across plates, liquid entrainment upward from plate to plate, and plate stability were investigated as functions of operational and geometric column parameters.

Gas phase pressure drop across dry perforated plates was observed to follow functional relationships predicted from available information for single perforations. The presence of liquid on a plate increased the total pressure drop by the equivalent clear liquid head plus a small residue which is nearly constant for a given liquid. This residue was observed to be about 0.4 inches of water, independent of the properties of the flowing gas, with water on the plate, decreasing to less than 0.1 inches of water for hydrocarbons. Within the over-all uncertainty of the measurements the data were reasonably correlated by considering the residue to be the result of energy dissipated in bubble formation in the liquid.

Entrainment was observed to be a function of column gas velocity, independent of gas velocity in the perforations. Entrainment was also found to be proportional to the gas density and inversely proportional to the liquid density and liquid surface tension. For a given system entrainment was observed to be proportional to approximately the third power of the gas velocity divided by the distance between the liquid

surface and the plate above.

The stability of perforated plates was observed to be adequate for many industrial and experimental applications, as also reported in recently published studies, but contrary to qualitative statements found in the earlier literature. Stability was found to increase with decreasing perforation diameter and decreasing total perforation area relative to column cross-sectional area, to increase with greater gas density, liquid surface tension and liquid wetting power, and to be virtually independent of liquid density and viscosity.

Operating limits of vapor throughput are shown for some typical applications of perforated plate liquid-vapor contacting columns.

CAPACITY FACTORS IN THE PERFORMANCE OF PERFORATED PLATE COLUMNS

Charles d'Ancona Hunt
Radiation Laboratory and
Department of Chemistry and Chemical Engineering
University of California, Berkeley, California

October, 1954

INTRODUCTION

The industrial use of perforated plate columns for countercurrent contacting of liquids and vapors has, until recently, been limited mainly to applications where the liquids contained large quantities of solid matter. According to general opinion on column design, the perforated plate type of contacting unit had a narrow stable operating range of gas flow, whereas a bubble-cap unit had no particular lower limit of gas flow except at relatively high liquid flow rates.

Recent studies by Mayfield, et al.,[1] and Arnold, et al.,[2] show that the perforated plate column has definite economic advantages over the bubble-cap plate column and that the possible range of gas and liquid flows for stable operating conditions is sufficiently wide for many applications in the chemical processing field. According to Mayfield, et al., perforated plate columns are being used by the Celanese Corporation for most new applications, and existing bubble-cap plates are being replaced by perforated plates in many units.

The present work is an extension of an experimental program, initiated in 1948 with the work of Jang[3] with the intent of defining the reputedly narrow range of operating limits of perforated plates. The first results showed that in 6-inch diameter columns the perforated plate was surprisingly stable for many configurations, a conclusion also reached by Mayfield, et al.,[1] in later experiments.

Jang's work was concerned with pressure drop and plate stability determinations for the air-water system. Claypool's work[4] also considered pressure drop with other systems besides air-water, but was restricted to single-hole plates to eliminate complications of varying plate geometry. Claypool also investigated the effect of varying the ratio of the length of a perforation to its diameter. He found that the pressure drop in the system depended upon the ratio if the value of length to diameter was less than 0.8 to 0.9.

The present work was undertaken prior to the appearance of References (1) and (2) in order to clear up questions arising from the work of Jang[3] and Claypool[4] related to pressure drop and plate stability. Another objective was to study entrainment in the perforated plate column in order to determine upper limits of gas flow rate in the column imposed by excessive entrainment upward from plate to plate of liquid droplets in the gas stream. The experimental work was done in a 6-inch diameter column.

In columns with liquid flowing across the plate and over a weir, the liquid head on the plate in the stable operating region is determined not only by the height of the overflow weir and the head of liquid required for the flow over the weir but also by the degree of aeration of the liquid on the plate. This aeration is the result of the flow of gas through the body of liquid and is fairly independent of gas flow rate in the stable operating region. However, the phenomenon of aeration is little understood at this time, and the degree of aeration can at best be predicted with a possible error of plus or minus 20%.

In order to eliminate a large share of this uncertainty in the study of pressure drop across perforated plates, the liquid head on the plate was maintained by means of a constant-head tank connected to the column just above the plate. The head was then measured by means of a pressure tap located at the plate level. In this way the effect of many variables upon pressure drop could be determined without any interference from changing aeration of the liquid on the plate. Actually the liquid head on the plate constitutes an important part of the total pressure drop for the gas flowing up the column; so a complete prediction of gas pressure drop requires an accurate knowledge not only of the effect of the variables studied in this work but also of the degree of aeration. The data on aeration presented in References (1) and (2) indicate that this question is one which needs considerably more study.

Because of the unreliability of the performance of liquid overflow weirs in a 6-inch diameter column this study does not include any information on the effect of liquid flow rates across perforated plates. This work does not include any experimental studies of the efficiency of contacting of liquids and vapors.

THEORY REVIEW

Pressure Drop: (Dry Plate)

The total pressure drop for incompressible fluid flow across a nozzle or orifice is proportional to the velocity head of the gas flowing through the orifice, and the only other system variables which enter the pressure drop function are the Reynold's Number and the ratio of orifice area to total duct area for circular symmetrical systems and a given type of orifice or nozzle.

The total pressure drop across orifices and nozzles of various types may be expressed as the sum of the losses due to entrance of the fluid into a restricted cross section of flow and those due to the exit of the resulting jet of fluid into the normal cross section downstream of the constriction.

For a properly designed rounded-entrance orifice (i.e., a nozzle) the fluid flows in a smoothly converging pattern to the minimum diameter of the orifice, and no vena contracta exists downstream. In such a case, entrance losses are negligible, and the exit losses for the nozzle may be expressed in terms of the average flow velocity based upon the minimum cross-sectional area of the nozzle. The exit loss function is the same as that for head loss in flow from a straight section of duct into a length of duct of larger diameter. For such a nozzle then, the total pressure drop is expressed by the following equation:

$$\Delta H = \frac{V_o^2}{2g} \left[1 - \left(\frac{D_o}{D_d} \right)^2 \right]^2 \qquad (1)$$

where ΔH = total pressure drop in feet of fluid flowing

V_o = flow velocity (average) in the minimum cross section of the nozzle or orifice

g = gravity constant

D_d = diameter of duct

D_o = minimum diameter of nozzle

For a sharp-edged thin-plate orifice with the vena contracta clear of the plate experimental work shows that the total pressure drop may again be expressed simply as the exit loss resulting from the flow of the jetting fluid into the downstream section of duct, with entrance losses negligible. For this case the appropriate velocity head is that associated with the flow at the minimum cross section of the vena contracta. The ratio of the minimum diameter in the vena contracta to the orifice diameter is a function only of the ratio of orifice diameter to duct diameter; so again the pressure drop may be expressed by an equation similar to equation (1):

$$\Delta H = \left[\frac{V_o^{\,2}}{2g}\right] \left[1 - \left(\frac{D_o}{D_d}\right)^2\right]^2 \left[\phi\left(\frac{D_o}{D_{vc}}\right)\right] \qquad (2)$$

where D_o = the orifice diameter

D_{vc} = the minimum diameter of the vena contracta

V_o = flow velocity (average) based upon cross-sectional area of orifice

$\phi\left(\frac{D_o}{D_{vc}}\right)$ = an experimentally determined function of $\left(\frac{D_o}{D_d}\right)$

Usually the pressure drop is expressed graphically as follows:

$$\frac{\Delta H}{V_o^{\,2}/2g} = \phi' \left[\frac{D_o}{D_d}\right]$$

where $\phi' \left[\frac{D_o}{D_d}\right]$ = a combination of the two diameter functions in Equation (2), (Reference 5).

Flow through a sharp-edged thick-plate orifice is complicated by the fact that the vena contracta formed downstream of the leading edge of the orifice may be swallowed (or submerged) in the orifice channel before the exit plane is reached. For cases where the vena contracta is submerged the exit loss is expressed in terms of (1) the flow velocity based upon the cross-sectional area of the orifice and (2) the ratio of the orifice diameter to duct diameter. However the total pressure drop for such cases must include the entrance loss associated with the contraction of flow from a straight section of duct to a smaller cross section. This entrance loss is also a function only of the flow velocity in the smaller section and the ratio of the diameters of the two sections. Thus the total pressure drop may be expressed as the sum of two losses:

$$\Delta H_{total} = \Delta H_{entrance} + \Delta H_{exit} \tag{4}$$

$$\text{Or } \Delta H_{total} = \frac{V_o^2}{2g} \left[0.4\left(1.25 - \left\{\frac{D_o}{D_d}\right\}^2\right) + \left(1 - \left\{\frac{D_o}{D_d}\right\}^2\right)^2 \right] \tag{4a}$$

for the case of $(D_o/D_d)^2$ less than 0.715.

Intermediate cases between those of thin sharp-edged orifices and those of definitely thick sharp-edged orifices are not amenable to any detailed analytical treatment, but the total pressure drop in such intermediate cases may be expected to fall in the range between the two extremes noted above.

The question of whether the data for single orifices spaced symmetrically in round ducts are applicable to symmetrical multiple orifices in a duct was answered affirmatively by Baines and Petersen.[5] These observations showed that uniform flow conditions are found within a few orifice diameters upstream and downstream of the individual orifices in a multiple-hole plate, while the total pressure drop can be expressed as a function of the total area of the orifices relative to the total area of the duct with exactly the same function that holds for single orifices. The work on sharp-edged orifices was limited to thin plates having free vena contractas and negligible entrance losses, and the data conformed to Equation (3) as predicted by their theory. No data are available in the literature for flow through multiple sharp-edged orifices in thick plates such as those used in the perforated plate column in the present study.

Thus in perforated plate columns with symmetrically spaced holes the pressure drop across a dry plate can be predicted. However space for liquid flow channels from plate to plate (downcomers) requires that the perforation pattern be unsymmetrical with respect to column walls. The turbulence pattern resulting from this condition will in general persist a few column diameters up from a single plate, and plate to plate spacing is usually less than a column diameter for large columns; hence the pressure drop across such non-symmetrical plates in a series may deviate somewhat from the simple relationships which have been determined for symmetrical systems.[2]

Pressure Drop: (Effect of Liquid on Plate)

The presence of liquid on a perforated plate creates a static head of pressure at the plate surface. This head must be overcome by gas flowing up through the perforations and the body of liquid. The action of the bubbling gas aerates the liquid[1,2,9,10] to an extent primarily dependent upon the gas flow rate and the liquid height. If the liquid level on the plate is maintained by flow over a weir, the equivalent clear liquid head is a function of both weir height and degree of aeration (at low liquid flow rates). The effect of liquid flow rates upon liquid head is a complex and currently unresolved function of many variables in perforated plate systems.[1,2] Therefore in the present work the liquid seal is maintained by means of a constant head tank, so that the head of liquid on the plate is nearly a constant, independent of gas flow rate and other system parameters. Thus the contribution of liquid head to total pressure drop of gas flowing across the plate may be determined readily and subtracted from the total to give the portion of pressure drop resulting from turbulence of the gas phase and bubbling phenomena in the liquid region.

The turbulent expansion loss for gas flow across a dry plate would probably be little changed by the presence of a turbulently agitated liquid on the plate. Hence the total pressure drop for gas flow across a plate with liquid present would be expected to be at least as great as the sum of the equivalent clear liquid seal and the dry plate pressure drop. If a significant amount of energy must be used to form the gas bubbles in the liquid and generate turbulence in the liquid, then an additional contribution to the total pressure drop would be observed.

Recent papers[11-13] have considered the question of the size of bubbles formed at single orifices. Use of the correlations presented in these papers allows the calculation of bubble diameters for single-hole perforated plates, but for multiple-hole perforated plates such as those used in the present work the violent turbulence in the liquid region undoubtedly has a primary effect upon reducing the ultimate size of bubbles rising through the liquid. The size of a bubble formed at an orifice is a complex function of several factors, as is shown in the following analysis:

(1) Formation of a static, nearly hemispherical bubble at an orifice requires an excess of pressure in the gas below the orifice to balance the liquid static head at the plate and the surface tension forces restraining the hemispherical bubble. The surface tension forces restraining the bubble are at the maximum possible value under these conditions; and there are no upward buoyant forces due to static liquid pressures upon the surface of such a bubble. The gas bubble is stable and stationary under these conditions of equal forces upward and downward.

(2) Any slight increase of gas pressure, however small, will create an excess of force upward at the gas-liquid interface. This unbalance of forces can only be restored by an acceleration of the liquid upward and by the pressure drop of the gas flowing through the orifice into the enlarging bubble.

(3) As soon as the bubble size has increased at all, the shape is no longer hemispherical. If the liquid were motionless at the start of this action, the bubble shape would change such that buoyant forces due to static liquid head differences would have upward components over the portions of the bubble surface below the plane of maximum diameter which now must exceed the orifice diameter.

(4) The bubble will continue to enlarge, but the neck of the bubble will be under the influence of surface tension forces which act to close off the neck in this region of the gas-liquid interface.

(5) The inertia of the liquid moving inward overcomes this unbalance of static forces near the surface of the plate, and the resulting motion of the liquid proceeds until the bubble is separated from the orifice.

(6) If the rate of bubble formation is sufficiently rapid to create significant liquid turbulence and interference between bubbles rising in the liquid, then the size of the bubble becomes dependent upon the rate of formation of bubbles. Whether liquid density and viscosity enter significantly would depend upon the relative magnitude of the shear and inertia forces in the moving liquid. If local disturbances in the liquid are in the fully turbulent regime, then these two liquid properties would not enter. Data presented by Harris et al.[12] indicate that density and viscosity do not enter significantly as variables. Van Krevelen et al.[11] give data showing that liquid surface tension enters as a variable in relatively static systems, but the data of Harris et al.[12] show no effect of surface tension for comparable conditions.

(7) On multiple-orifice perforated plates the liquid turbulence is so violent that the initial bubble formed at any hole is probably quite unstable and may be reduced to several smaller bubbles as the gas flows up through the aerated liquid region. Since the energy required for bubble formation depends upon the ultimate surface area formed during the passage of a given quantity of gas, the ultimate average bubble size is the figure of importance in estimating pressure drop requirements resulting from the generation of liquid-gas interfacial area. A detailed analysis based upon the complex hydrodynamic action on a multiple perforation plate cannot be made at this time; however

the experimental data obtained in the present work lead to certain hypotheses concerning this action. These speculations are presented later in the discussion of the experimental results.

Regardless of the mechanism of bubble formation, however, a given pressure drop is required for the generation of bubbles of a given ultimate size. This requirement may be estimated with the aid of certain simplifying assumptions, as shown in the following development:

The generation of spherical bubbles of a particular diameter requires the formation of a definite amount of gas-liquid interfacial area for a given volume of gas. Thus the surface area of a spherical bubble is:

$$A_s = \pi \ d^2$$

where d = the diameter of the bubble

A_s = surface area of spherical bubble

And the volume of this bubble is

$$V = \pi \ d^3/6$$

The work required to generate the interfacial area is equal to the product of the area times the surface tension; and the pressure drop requirement for the flowing gas creating the bubble is then the work required divided by the volume of the bubble:

$$\Delta P = A \ \gamma/V = \frac{6\gamma \ d^2 \pi}{d^3 \pi} = 6 \ \gamma/d$$

where ΔP = pressure drop occurring in flowing gas as a result of bubble formation,

γ = gas-liquid surface tension.

Pressure Drop: (Fluctuations in measurements of pressure drop)

The component of pressure drop due to factors other than equivalent liquid static seal on a perforated plate may be determined by measuring the total pressure drop across an operating plate and subtracting from this value the measured liquid head on the plate as shown by a manometer connected between the surface of the plate and the static pressure tap above the aerated liquid region in the column. Unfortunately the violent turbulence in the aerated liquid region is of such a character that large scale fluctuations are observed in the reading of the liquid head manometer. The question of what type of average or mean pressure to determine from these fluctuating pressures is by no means an easy one to answer.

If fluctuations in a measured variable are large compared to the total value of the variable, a significant variation may be obtained between average values determined in different ways. Furthermore, unless the fluctuations are of a known characteristic nature, the differences between the various types of averages cannot be interpreted quantitatively.

Thus for example the use of manometers which are primarily viscous damped yields different results than use of manometers which are mainly inertia damped. Viscous damped manometers will react to sudden changes in pressure more rapidly than inertia damped manometers, since viscous damping does not come into play until the observed reading begins to change and viscous resistance to motion is encountered in the manometer fluid. Inertia damping, on the other hand, acts to resist any change in observed reading upon sudden change in pressure, so that a large pulse of short duration may have much less effect in producing a change in manometer reading in this type of damping compared to viscous damping.

If all the fluctuations in liquid head at the plate are of such short duration that they may be damped out by suitable design of the manometers, the question must be decided concerning which type of average to use in determining the appropriate pressure drop for the design of columns employing liquid downcomers. Downcomers contain a considerable amount of flowing liquid when operating near the maximum allowable pressure drop from plate to plate; therefore an average liquid head determined experimentally in a system without downcomers probably should be obtained with inertia-damped manometers, rather than with viscous damped systems.

Entrainment:

Souders and Brown[6] present a semi-empirical correlation of entrainment data for column operation in the region of extremely low entrainment. The entrainment under such conditions is assumed to be dominated by viscous hydrodynamic ("Stoke's Law") drag of liquid droplets carried upward in the vapor stream. The constants in the published correlation are based entirely on qualitatively observed column operating characteristics, and no attempt is made to propose a detailed physical model suitable for calculated estimates of liquid entrainment. The correlation is in general use in the chemical and petroleum industries and seems to provide reasonable upper limits of vapor rates for cases where entrainment must be kept to a minimum. An example of such a case is the distillation of a feed containing solid particles which could impart a color to the top-product of a distillation column.

However, if no special reasons require low entrainment rates, then entrainment can be considered as an upward flow of liquid that reduces the efficiency of the separation on each plate in a column. Colburn[8] presents an analysis of the effect of entrainment per se upon plate efficiency and shows that the efficiency is not lowered significantly until entrainment reaches values as much as 100 times greater than those predicted as allowable upper limits by Souders and Brown. Many applications of distillation involve feed streams and product qualities that would not limit operation by the conditions for which the Souders and Brown correlation was developed; yet there are no data in the literature that would allow quantitative predictions of entrainment under conditions approaching the limits predicted by Colburn.

Mayfield, et al.,[1] present qualitatively determined upper limits of operation for conditions of high entrainment and they state that the upward flow of liquid droplets appears to be primarily due to splashing action at the liquid-vapor interface. If entrainment under conditions of high vapor velocity is the result of splashing rather than hydrodynamic drag, then a correlation of the type proposed by Souders and Brown would presumably be inapplicable.

The purpose of the present work is to present quantitative data for entrainment for a wide variety of operating conditions in order to provide a framework for a reasonable analysis of the physical situation involved. Since the analysis must be based upon the observed results of the present study, presentation of the discussion concerning the mechanism of entrainment at high vapor rates is included with the later section concerned with the data.

If all the fluctuations in liquid head at the plate are of such short duration that they may be damped out by suitable design of the manometers, the question must be decided concerning which type of average to use in determining the appropriate pressure drop for the design of columns employing liquid downcomers. Downcomers contain a considerable amount of flowing liquid when operating near the maximum allowable pressure drop from plate to plate; therefore an average liquid head determined experimentally in a system without downcomers probably should be obtained with inertia-damped manometers, rather than with viscous damped systems.

Entrainment:

Souders and Brown[6] present a semi-empirical correlation of entrainment data for column operation in the region of extremely low entrainment. The entrainment under such conditions is assumed to be dominated by viscous hydrodynamic ("Stoke's Law") drag of liquid droplets carried upward in the vapor stream. The constants in the published correlation are based entirely on qualitatively observed column operating characteristics, and no attempt is made to propose a detailed physical model suitable for calculated estimates of liquid entrainment. The correlation is in general use in the chemical and petroleum industries and seems to provide reasonable upper limits of vapor rates for cases where entrainment must be kept to a minimum. An example of such a case is the distillation of a feed containing solid particles which could impart a color to the top-product of a distillation column.

However, if no special reasons require low entrainment rates, then entrainment can be considered as an upward flow of liquid that reduces the efficiency of the separation on each plate in a column. Colburn[8] presents an analysis of the effect of entrainment per se upon plate efficiency and shows that the efficiency is not lowered significantly until entrainment reaches values as much as 100 times greater than those predicted as allowable upper limits by Souders and Brown. Many applications of distillation involve feed streams and product qualities that would not limit operation by the conditions for which the Souders and Brown correlation was developed; yet there are no data in the literature that would allow quantitative predictions of entrainment under conditions approaching the limits predicted by Colburn.

Mayfield, et al.,[1] present qualitatively determined upper limits of operation for conditions of high entrainment and they state that the upward flow of liquid droplets appears to be primarily due to splashing action at the liquid-vapor interface. If entrainment under conditions of high vapor velocity is the result of splashing rather than hydrodynamic drag, then a correlation of the type proposed by Souders and Brown would presumably be inapplicable.

The purpose of the present work is to present quantitative data for entrainment for a wide variety of operating conditions in order to provide a framework for a reasonable analysis of the physical situation involved. Since the analysis must be based upon the observed results of the present study, presentation of the discussion concerning the mechanism of entrainment at high vapor rates is included with the later section concerned with the data.

EXPERIMENTAL PROCEDURE

Pressure drop, entrainment, and stability criteria were studied in a 6-inch diameter perforated plate column, using a non-flow constant-head system to maintain liquid on the plate and a totally enclosed gas circulation system to provide gas flow through the perforated plate.

The variables measured were the following:

(1) total pressure drop across the plate,

(2) liquid head on the plate,

(3) gas pressure upstream of the plate,

(4) gas temperature upstream of the plate,

(5) pressure drop in a standard ASME orifice gas-flow measuring system,

(6) gas pressure upstream of the orifice,

(7) gas temperature upstream of the orifice,

(8) amount of liquid entrained from the primary plate to a similar plate above it in the column, and

(9) amount of liquid dumping through plate perforations.

The system parameters investigated were:

(1) gas velocity in the perforations and the column,

(2) liquid head on the plate,

(3) perforation diameter,

(4) perforation pattern,

(5) total perforation area relative to column cross-section area,

(6) gas properties,

(7) liquid properties,

(8) damping in manometer systems,

(9) length of perforation relative to its diameter, and

(10) plate spacing and distance from liquid surface to the plate above.

A diagram of the experimental system is shown in Figure 1. Both the gas circulation system and the liquid constant-head system were enclosed and vented to the column in order to allow the use of other gases and liquids besides air and water. Provision was made for purging of manometers in the plate system with the liquid in use. A heat exchanger cooled by tap water served to remove heat added from the work of compression of the gas-circulation blower. Since the orifice measured the flow of gas between the blower and the heat exchanger, gas properties at both the orifice and the plate were measured in order to avoid significant systematic errors in gas density determination. The orifice was assembled according to ASME standard specifications, 15 diameters downstream of flow straightening screens designed to provide a 20:1 improvement in the flow distribution at the entrance of the section. The orifice was 9 diameters upstream of a short radius turn.

Gas entered the column through a trap designed to prevent the liquid which dumped through the perforations from filling up the gas ducts, flowed through a set of straightening screens designed to provide a 15:1 improvement in flow distribution, and impinged upon the primary plate with a fairly uniform flow profile in the column. The column was constructed of 1/16" thick wall brass with plastic windows provided for observation of plate action and dumping. Pressure taps 6 inches below the plate and 18 inches above the plate were constructed to avoid any possibility of drops of liquid affecting the pressure reading.

The liquid entrained from the primary plate was collected on a similar plate higher in the column and drained continuously into a vented receiver which was calibrated for determination of the volume of the liquid entrained as a function of time. Less than 1% of the liquid reaching this upper plate could be further entrained out of the tapered, baffled column section above this plate. All entrainment data were taken under conditions which assured little or no dumping of liquid from the catcher plate to the primary plate. The plate spacing was increased by adding glass spacer sections to the column just below the entrainment catcher plate. After the completion of the pressure drop measurements, the metal portion of the column above the plate was shortened to 8 inches in order to allow the determination of entrainment at small plate spacings.

The gas pressure at the entrance to the blower was maintained slightly greater than atmospheric pressure in order to prevent in-leakage of air in runs using other gases and to prevent excessive leakage of these gases through the inadequate seal around the blower shaft. Gas flow velocity was controlled by means of a simple slide valve in the 4-inch ducting used throughout the remainder of the system. Liquid head on the plate was maintained constant within 0.3 inches by means of the adjustable overflow weir in the constant head tank. The liquid was continuously circulated from a storage tank through the constant head tank.

The manometers connected to the column and plate were assembled with glass and transparent plastic tubing in order to make visible any gas bubbles in lines which should have been full of liquid. The inertia-damped manometers were 3/4 inches in diameter and vertical; the viscous-damped manometers were 3/16 inches in diameter and inclined to a shallow angle in order to give a multiplication of 2.5 to the scale reading. The large diameter vertical manometers could be read to the same degree of precision as the narrow inclined manometers (namely ± .02 inches of H_2O), and with greater reliability. The pressure drop at the orifice was measured with a standard Uehling Inclined Manometer.

Gas temperatures were measured with unstandardized iron-constantan thermocouples immersed in the gas stream. Sufficient accuracy for the purposes of this work was provided by this arrangement.

Plates of 20% relative perforation area were so unstable with respect to dumping that stabilizing screens had to be installed above these plates in order that a suitable liquid head could be maintained. The stabilizer consisted of three concentric cylinders, about 6 inches long, composed of 1/16-inch gauge wire woven into a 1/4-inch mesh screen. The stabilizer had no effect on pressure drop measurements.

EXPERIMENTAL RESULTS

Dry Plate Pressure Drop:

All the experimental data were obtained with aluminum perforated plates. The thickness of these plates was such that the length of the perforations was always equal to the diameter, since Claypool's work[4] showed that consistent results could be obtained with values greater than about 0.9 of the parameter defined as length of perforation divided by its diameter. Such values of this parameter are of practical usefulness, because many perforated plate column designs require the use of plates which are self-supporting over a span of a few feet.

Results for dry plate pressure drop measurements (Figures 2 through 9) show that the only significant variables are (1) average hole velocity of the flowing gas and (2) the ratio of total perforation area to column cross-sectional area for symmetrically arranged holes. As shown in Figures 5 and 9 there is a slight effect of hole diameter, in that 3/8-inch and 1/2-inch diameter perforations show a slightly higher pressure drop than do 1/4-inch and 1/8-inch diameter perforations. This discrepancy is probably due to the fact that minor differences in the velocity distribution in the gas at the exit of the perforations may occur between different hole sizes, and such differences would mean that gas velocities based upon average flow rates in the perforations would not be exactly comparable. The possibility that column wall effects might enter was eliminated by changing the pattern of holes in a 1/2-inch plate in order to position most of the holes very close to the wall. The results for this plate with modified hole spacing with respect to the wall were exactly the same as for the plate with holes spaced normally.

As predicted by the theory, dry plate pressure drop may be expressed as a linear function of the square of the average gas velocity in the holes, with relative hole area as a parameter. Although the experimental results were an average of 14% higher than the predicted values, the discrepancy was uniform and independent of column geometry. A quantitative evaluation of the error involved would not be possible without data on the actual velocity distribution at the exit plane of the perforations in question.

All data for gases other than air followed the same functional relationship as did air (Figure 11). This result is in accord with the theory, since Reynold's Numbers in all cases were much greater than 100. The gases tested were Freon 12, Argon, Carbon Dioxide and Methane.

Pressure Drop with Liquid on Plate:

As shown in Figures 2 through 10 for the system air-water, a plot of Total Pressure Drop minus Measured Liquid Head versus the Square of the Average Gas Velocity in the perforation yields a function which may best be described as a straight line somewhat above and nearly parallel to the dry plate pressure drop line. Even at very low velocities, this relationship seems to hold.

The over-all uncertainty in measured values of the liquid head varies from 0.1-inch of water at low gas velocities to 0.3-inch of water at high velocities; hence there is a corresponding uncertainty in the pressure drop obtained by subtracting this measured head from the total drop across a plate. This uncertainty is the result of fluctuations in the level of the liquid-head measuring manometer of such long and irregular cycle time that the manometer damping is not effective. Such irregular changes in observed liquid heads introduce into the precision of the data an uncertainty of a definite maximum amount, since the average damped liquid level reading may actually lie anywhere between the limits of the long-period fluctuations.

A further systematic discrepancy between average liquid head readings occurs between data taken with viscous-damped manometers compared to those with inertia-damping. As shown in Figure 3-A for the air-water system with 1/4-inch perforations, a 6% difference exists between data taken with two types of manometers. The over-all uncertainty in absolute value of the liquid head due to the long cycle fluctuations described above is actually greater than this 6% difference; so no definite conclusions can be drawn concerning this point. An effort was made in all cases however to record the approximate average liquid head during the long-cycle variations which do not respond to either viscous or inertia damping; so the difference noted in the data obtained with each type of damping is probably the result of reading a different sort of average of the rapid fluctuations which do respond to the damping methods employed. As suggested in the earlier section on Theory, the recommended correlation for pressure drop design data is based upon the type of data that is characteristically obtained with inertia damping of manometers.

Despite the over-all uncertainty in manometer readings a set of data for any particular system shows considerably greater precision. This apparent precision is the result of the fact that in taking the data, an observer tends to read some consistent average of the long-cycle fluctuations, although this average may not be the true best reading. Thus the differences shown in Figures 5 and 9 between pressure drop as a function of velocity for different hole sizes are less than the absolute uncertainty in the data. Whether the differences noted are the result of systematic errors in recording of liquid head readings or are the result of real differences in hydrodynamic phenomena cannot be answered definitely. High speed photographs (Appendix III) of the formation of bubbles at the plate and of the frothing action in the liquid region indicate that no significant hydrodynamic differences occur.

Thus the photographs show that the bubbles as formed at the plate are quite distorted in shape and obviously very unstable. These large bubbles of a wide variety of shapes and sizes, appear to be broken into many smaller ones very rapidly, and all pictures of the froth region show bubble size distributions which are quite independent of perforation diameter, gas velocity, and total perforation area relative to column cross-sectional area. Further, a calculation of the required pressure drop for the generation of the bubbles as shown in the froth photographs gives a result of 20 to 30 feet of air, assuming all the flowing gas ultimately forms bubbles of the size photographed. This figure checks quite well the observed excess of pressure drop over dry plate requirements.

A definite effect of perforation area relative to column cross-sectional area may be observed in Figure 10, with 1/4-inch plates as shown as the example. This effect is <u>not</u> within the absolute uncertainty of the data; so it is probably not just due to manometer fluctuations. The photographs, however, show no apparent differences between the two systems. What neither the photographs nor visual observation can confirm or deny, however, is whether or not all the flowing gas forms the small bubbles characteristic of the froth, since larger bubbles, although unstable, could possibly rise so rapidly that they would not be apparent at the walls of the column. Presumably, then, with relative hole area of 20% a sizeable portion of the larger bubbles formed at the plate rise through the froth without being reduced to the ultimate size observed at the wall of the column, whereas with 5% hole area nearly all of the large initial bubbles are reduced to typical froth bubbles. The physical explanation for such a phenomena lies in the fact that the amount of liquid available for turbulent agitation of the gas flowing in the column is proportionally less for larger hole areas; hence there is a greater possibility of proportionally less bubble breaking action.

Variation of gas properties in the system was accomplished by using different gases with a range of viscosity of 3:1 and a range of density of 8:1. The difference between the total pressure drop minus liquid head and the total dry-plate pressure drop is shown in Figure 11 to be nearly a constant loss, independent of gas properties. Dividing this difference measured in feet of fluid flowing by the density of the fluid yields a value of mechanical energy loss that is constant within the over-all accuracy of liquid head determinations. The gas viscosity does not appear to enter.

Liquid properties were varied in the system in order to determine the nature of this constant energy loss measured in the water system. By suitable choice of liquids, the following properties were changed:

(1) Viscosity, over a range of 80:1, other properties remaining nearly constant,

(2) Surface tension, over a range of 4:1,

(3) Density, over a range of 2:1,

(4) Interfacial tension between the aluminum plate and the liquid, as measured by the spreading of a given volume of liquid on a level aluminum plate.

The liquids used were:

(1) water, low wettability,

(2) water, good wettability,

(3) glycerine-water, viscosity equal to 10 cp and 80 cp,

(4) n-butyl alcohol,

(5) carbon tetrachloride,

(6) n-hexane,

(7) kerosene, (approximately C-12).

The results for pressure drop using these liquids are shown in Figure 12. The uncertainty in the data is indicated on the plot; thus at low velocities liquid level variations are about 0.1-inch total, and at high velocities variations from 0.3-inch (for water) to 0.4-inch (for CCl_4) are noted. Within the over-all uncertainty of the data the only properties which could have an effect consistent with the observations are the surface tension of the liquid, possibility the wettability of the liquid with respect to the plate, and to a slight extent the density of the liquid. The viscosity of the liquid has no clear effect upon the pressure drop. At high velocities the data diverge widely, probably because of the large uncertainties in liquid head observations; so probably the most reasonable correlation would be one based upon straight lines drawn parallel to and above the dry-plate pressure drop line.

There is not enough information to confirm or deny the possible effects of liquid density and wettability, and there are no a priori reasons, based upon observations of the hydrodynamics involved, for including these variables in any correlation of the data. That the surface tension is of primary importance, however, seems unquestionable. Thus the work (and thus the gas pressure drop) required to break the gas flow into bubbles of a given size is directly proportional to the liquid surface tension. It is quite possible that other liquid properties affect the ultimate size of the bubbles formed, but since the data can be correlated adequately without considering other properties at the present time, the predicted values of excess pressure drop requirements shown in Figure 12 are based upon surface tension considerations only.

EXPERIMENTAL RESULTS AND DISCUSSION

Entrainment:

Entrainment data for the system air-water, with 1/4-inch diameter perforations in the plates, are shown in Figure 13. These results correlate very well on a single line when entrainment is plotted against the average gas velocity in the column, even though gas velocities in the perforations range from approximately 50 ft/sec to 100 ft/sec for each of the three plates used. Thus at a gas velocity in the column of 11 ft/sec, data coincide where the gas velocity in the perforations is 110 ft/sec for the 10% hole area plate and 55 ft/sec for the 20% hole area plate. The plate spacing for these runs was 20 inches with 1.8 inches of liquid head on the plate.

Figure 14 shows entrainment data for a variety of plate spacings, with entrainment again plotted against gas velocity in the column. Where possible the gas velocity was increased to whatever value was necessary to achieve an entrainment of approximately 20 weight percent liquid relative to gas flow rate, but pressure drop in the gas flow system limited the maximum gas velocity in the column to 11 to 12 ft/sec. There is a very sharp increase in entrainment with decreasing plate spacing, as shown in Figure 15, where entrainment is plotted against plate spacing, with various gas velocities as constant parameters.

In order to determine whether or not the plate spacing should be considered as the actual distance from the liquid surface (as maintained by a weir) to the plate above, runs were made at various combinations of liquid head and plate-to-plate spacing. Figures 14A and 14B show the results of these runs. The true position of the liquid surface in the column used in this work is not indicated directly by the observed liquid head on the plate because of the phenomena of aeration. Quantitative data on aeration in multiple hole perforated plate columns is presented by Jang,[3] Mayfield et al.,[1] and Arnold et al.[2] The data obtained in those works scattered a good deal, and this scatter would cause serious uncertainty in the prediction of pressure drop for gas flow in a perforated plate column. However, for purposes of estimating the position of the liquid surface for a given liquid head used in this study, an average value of the aeration factor could be chosen as 0.5 without causing an average error greater than one inch in the position of the surface. As a check on the data referred to above, the column used in the present work was modified temporarily to include a liquid-overflow weir and downcomer system in order to observe aeration effects. The aeration factor in the 6-inch diameter column consistently lay in the range 0.4 to 0.6 at liquid levels of 4 inches and greater, and was independent of gas velocity and the nature of gas used.

Figure 15A shows a replotting of the data of Figure 15 with the effective plate spacing plotted as the independent variable, instead of the distance between plates. The effective plate spacing is the plate distance minus the height of aerated liquid on the plate. The average slope of the straight lines obtained is 3.1, varying from 2.6 to 3.8, showing that the effect of plate spacing is very nearly the same as the effect of gas velocity in the column. Therefore a reasonably good correlation of all the air-water system data can be obtained by plotting the entrainment against an independent variable consisting of the gas velocity divided by the effective plate spacing. Figure 15B shows all the air-water data represented in this manner. The abscissa is arbitrarily multiplied by the number 16 in order to have a reference line that coincides with the data for the column configuration used most frequently in this study. A limiting velocity based upon excessive entrainment determined by the position of this reference line would give a conservative value for use in column design. The maximum error would be 25%, and the average would be 10%, with all errors in the safe direction.

The fact that entrainment is such a sharp function of effective plate spacing shows conclusively that hydrodynamic drag of liquid droplets by the upward flowing gas stream is not the major contributing cause of entrainment in a perforated plate column. Such a drag would be constant, at constant gas velocity in the column, independent of plate spacing; yet there is little indication that entrainment is approaching a constant value as plate spacing increases. Thus any analysis of entrainment observed under conditions similar to those involved in the present work should presumably be concerned with the phenomena related to splashing at the liquid surface above the plate.

Considerable visual observation of the column action confirms the fact that at plate spacings of 8 inches and 12 inches the entrainment is largely due to irregular splashing upward of drops of liquid approximately 1/4 inch in diameter. High-speed photographs (Appendix III) of the entraining liquid droplets indicate that the same situation holds at larger plate spacings. Figure 16 is a tracing of a photograph taken across the column, 20 inches above the plate, with a gas velocity in the column of 11.5 ft/sec. Drag calculations based on the assumption of spherical droplets showed that the largest drop that would be carried upward by the gas flow at this velocity is 1/50 inches in diameter. Such a drop is indicated on the tracing, but drops of smaller size show up only inconsistently in the photographs.

The largest drop present is 0.2 inches in diameter, and its volume accounts for 90% of the total volume of liquid visible in the photograph. Drops of this size occur in about 1/3 of the photographs; so about 75% of the entrained liquid is probably carried up in such large drops, which could only be thrown up by violent splashing. Figure 17 shows a plot of drop size distribution versus drop diameter for this photograph. The other photographs which do not show large drops have similar distributions up to a diameter of 0.1 inch.

That entrainment is a function of gas velocity in the column rather than in the perforations is probably due to the fact that the splashing of liquid at the surface above the plate appears to be the result of the sudden rupture of large (ca 2 to 3-inch diameter) bubbles rising through the froth. These bubbles are far enough from the perforations so that their velocity appears to be closer to that of the average gas velocity in the column rather than that in the perforations. Visual observation of the column action, plus examination of many high-speed photographs of the liquid surface, indicate that the frothy surface of these larger bubbles ruptures with sufficient violence to cause even 1/4-inch diameter liquid drops to be thrown as much as 24 inches above the plate.

The energy for this process is presumably available in the form of potential energy stored up in the liquid-gas interfacial area that is generated by the bubbling action discussed in the previous section on "Pressure Drop". Hence the degradation of the mechanical energy removed from the gas as a consequence of the formation of gas-liquid interfacial area probably involves a step in which some of this energy is transformed briefly into kinetic energy of liquid droplets. Since the physical action involved is quite complex, no detailed accounting of the mechanism can be presented here; however a calculation of the work required to lift the entrained liquid from plate to plate shows that even under conditions of 20 weight percent entrainment less than 10 feet of air pressure drop would be required to provide energy for the entrainment process.

The effect of perforation diameter upon entrainment is shown in Figure 18. In the range of velocities studied, entrainment with 1/2-inch perforations is about 4 times greater than that with the smaller perforation diameters. Visual observation of the surface of the liquid indicates that the splashing is quite irregular with 1/2-inch holes compared to the action with the other sizes; so the relatively larger entrainment is probably related to this irregularity.

Figure 19 shows the data for the systems Freon 12-water, air-water and methane-water. Figure 20 presents the entrainment results for the systems air-carbon tetrachloride, air-kerosene, air-hexane and air-water. In these figures the volumetric rate of liquid entrainment is plotted against gas velocity in the column. The results show that entrainment is proportional to gas density and inversely proportional to liquid density and liquid surface tension.

A general correlation of all the entrainment data taken with a given perforation diameter, plate spacing, and liquid head is presented in Figure 21. The data plotted as weight percent entrainment times a relative surface tension ratio versus gas velocity in the column fall on a single line with a maximum deviation of 35% and an average deviation of 15%. The data show that the gas flow rate in a column may be much greater at conditions of limiting entrainment defined by Colburn[8] than at conditions of limiting entrainment predicted by Souders and Brown[6] for cases where entrainment must be kept to a minimum. The Souders and Brown equation is generally used at present, however, in a modified form in which the empirical constants employed are such that a satisfactory upper limit of operation is obtained, even though entrainment may not be the limiting factor in design. These upper limits may also be imposed by factors such as excessive pressure drop and loss of contacting efficiency of liquids and vapors. Furthermore the equation is applicable to bubble-cap trays only, whereas no data has been published concerning perforated-plate operational upper limits resulting from factors other than excessive entrainment.

DISCUSSION OF RESULTS

Plate Stability:

Perforated plate stability was studied by measuring the quantity of liquid dumping through the perforations and observing the effect of column operating parameters upon this quantity. As shown in Figures 22 through 28, for the air-water system, the amount of liquid dumping through the perforations increases sharply in a narrow range of decrease in gas velocity for any given configuration. The region of sharpest change in liquid dumping rate as a function of gas velocity is noted on each curve, and this region is used as the lower limit of the perforated plate stable operating range. A complete specification of lower operating limits would have to include a study of plate efficiency drop with reduction in gas velocity, since the lower operating limits determined by dumping criteria are visibly associated with relatively poor contacting between the gas and liquid. Plate efficiency was not studied in this work, however; so lower limits of plate stability will be specified by the average gas velocity associated with a sharp change in liquid dumping rate.

The data presented in Figures 22 through 28 show that increasing liquid level on perforated plates decreases the plate stability, however the effect is not consistent. For example, the most stable plate (II, 1/8-inch diameter perforations, 5% hole area) is operable down to less than 5 ft/sec gas velocity in the perforations with a liquid head of one inch. At higher liquid heads however the effect is comparable to results found for other plate configurations. The effect of liquid head upon plate stability becomes more marked with increase in total area of perforations for a given hole diameter, as may be seen by comparison of Figures 22 and 23 and also Figures 25 and 26.

No exact rule can be formulated for predicting the effect of hole diameter, since this effect differs with change in total perforation area. In general, however, increasing hole diameters decreases the plate stability. An exception is found with the 5% hole area plates, in which group the 1/2-inch diameter perforations showed greater stability than did the 1/4 inch. Since most of the dumping through perforations occurs in those nearest the column walls, a second 1/2-inch plate was constructed with the same hole area but larger spacing. This spacing placed the outer row of holes within 1/2 inch of the column walls, as was the case with the 1/4-inch and 1/8-inch diameter holes. Figure 28 shows that this modified plate gave stability criteria that fell in line with the general rule observed on the 1/4-inch and 1/8-inch plates. Table III-A tabulates the stability results as a function of perforation diameter and total area.

The sensitivity of plate stability with respect to perforation spacing near the column walls indicates that the design of perforated plate columns should take this factor into account. More random dumping across the plate will occur if the holes are at least two diameters away from the wall of the column, and this random dumping will usually occur at lower operating limits than will edge dumping.

The investigation of the effect of changing liquid and gas properties was carried out entirely with 1.8 inch of liquid head on plate III, with 1/4-inch diameter perforations and 5% total hole area. Table III presents the data for the systems studied, and Tables III-B and III-C present cross tabulations to show the effect of specific variables.

Tests with methane, air and Freon-12 show that gas density apparently affects the stability, in that the gas velocity corresponding to the stability criteria is approximately inversely proportional to the square root of the density. Tests with air flowing through n-butyl alcohol, carbon tetrachloride, kerosene, and n-hexane represent a group of liquids with about the same surface tension but with different wetting characteristics. Wetting characteristics were determined by noting the diameter to which a given volume of liquid would spread on a level plate. A definite correlation appears between increased wettability and increased plate stability. A similar set of tests with air flowing through water and various glycerine-water mixtures represents another group of liquids with approximately constant surface tension but varying wettability. A similar correlation is obtained.

There can be no direct comparison of varying surface tension at constant wettability for these liquids; however the fact that the glycerine-water mixtures gave greater plate stability than alcohol and carbon-tetrachloride despite a lower wettability shows that increasing the surface tension has a direct effect upon improving the plate stability.

The data indicate that liquid density and liquid viscosity have no noticeable effect upon stability of perforated plates.

The results obtained in this study provide a reasonable basis for accepting a physical model based on a balance of forces acting upon the liquid in the perforations at the condition of critical stability. Thus the effect of gas density may be explained by the fact that impact of the gas upon the liquid moving in a turbulent manner on the plate tends to keep the liquid from flowing into the perforations: for a given impact head, the velocity is related to the reciprocal of the square root of the gas density. If liquid does start to fill a perforation and form a drop below the bottom of the plate, then the force tending to hold the drop from falling is proportional to the surface tension of the liquid, for complete wetting conditions. If the liquid does not wet the plate well, the positive contact angle between the suspended drop and the inside of the perforation reduces the effectiveness of the surface tension forces, in proportion to the cosine of this angle. The data indicate that the contact angle of wetting is of considerable importance in its effect upon plate stability, as is the nature of the liquid circulation on the plate in the vicinity of the column walls. Since these two factors will depend upon column design and materials of construction to a large extent, prediction of exact stability criteria for new designs is not possible. Pilot plant data on fairly small scale equipment such as was used in the present work should provide fairly reliable information, however.

COMPARISON TO OTHER STUDIES

Pressure Drop, Dry Plate:

As a preliminary study to further work on large scale equipment the pressure drop across perforated plates in a 6-inch diameter column was measured by Mayfield et al.[1] The results obtained for the 6-inch column show that the dry-plate pressure drop is the same function of gas velocity in the perforations as was found in the present work. However the results of Mayfield et al.,[1] lie 14% lower. The relative hole area to column area is not reported; so an exact comparison is not possible. If the hole area in that work is of the order of 5% of the column cross section, however, then those results lie within 1% of the values predicted by the theory outlined in the present work. Such discrepancies between two apparently similar systems may be ascribed partly to slight differences in pressure tap configuration, differences in "standard" orifice systems used to meter gas flows, and mainly to small errors in perforation diameters.

The continuation of pressure drop measurements on a 6.5-foot diameter column show the same results as those obtained with the 6-inch diameter column, for 1/4-inch perforation diameters. For the 3/16-inch diameter holes the pressure drop was approximately a function of the velocity to the 1.8 power, with values higher than those in the 6-inch column at low flow rates and lower at high flow rates. For 1/8-inch perforations, the pressure drop was the same function of velocity as in the 6-inch column, but values were 50% high, a discrepancy attributed to worn drills and burrs around the holes in the large tray. A reduction of drill diameter of .013 inches would be required to account for this difference, providing the holes were appropriately sharp-edged. Since this much wear seems unlikely, burrs on the perforation edges must account for some of the error. The plate thickness is not reported for the one large tray which was used for all the data taken; so no effect of variable ratio of perforation length to diameter (L/D) can be inferred.

The measurements of pressure drops made by Arnold et al.[2] were carried out in a 1.5-foot diameter column with plates of a single thickness, 0.29 inches; hence values of L/D vary as hole diameter changes. The range of L/D covered in that work is 0.76 to 0.09, compared to the value of L/D of 1.0 used in the present work and to the minimum value of 0.9 found by Claypool[4] to be a requirement for consistent results independent of L/D in a given system. The results of the studies reported by Mayfield et al.[1] and Claypool[4] both show inconsistent effects of L/D in the region of L/D less than 0.9; so no proper comparison of such data can be made with that obtained in the present work for L/D of 1.0. Neither study reported any influence of variable L/D upon the functional relationship of pressure drop versus velocity; however Arnold, et al.[2] report that pressure drop is a consistent function of the gas velocity in the perforations to the 1.8 power, whereas all of the results of the present work and most of those shown by Mayfield,[1] Jang[3] and Claypool[4] indicate that the gas velocity enters to the 2 power as predicted by the theory.

The discrepancy between the two functions is probably caused by the fact that in the column used by Arnold et al.[2] nearly 1/3 of the cross-sectional area was occupied by liquid downcomers instead of perforations, a condition which creates a non-uniform over-all turbulence pattern in the flow of gas up the column from plate to plate. No reason is apparent for the fact that some of the results reported by Mayfield et al.[1] for the 6.5-foot diameter column (which does contain downcomers occupying about 25% of the column area) agree functionally with those of Arnold et al.,[2] but most of the results agree with those predicted by theory.

Comparing results of Arnold et al.,[2] for L/D of 0.76 to those of this work shows that pressure drops in the former case vary from 5% to 15% higher than those reported herein. The difference in values of L/D between the two systems might account for this variation, according to Claypool's[4] results. A greater uncertainty in the validity of comparing the two systems lies in the fact that no definite relative hole area can be chosen for a column whose cross-section is only 2/3 occupied by the perforation pattern. Thus a plate with 7.7% hole area in the perforated region has only 4% free area based on the entire column cross section. A point of question in regard to certain of the data by Arnold[2] is that, whereas a normal effect of pressure drop as a function of relative hole area to column area is observed for most of the plates, no effect is noted in changing from 20% perforation area to 30% (based on the perforation region). This phenomenon is inconsistent with the theory and with the observations reported in all other work discussed here.

The data for dry-plate pressure drop reported by Jang[3] and Claypool[4] (for values of L/D greater than 0.9) lie about 10% higher than the theory, compared to the 14% found in the course of the present work. This difference of 4% is small enough to be well within the absolute accuracy of the experimental results, since gas flow measurements are made with standard but uncalibrated orifice configurations.

Pressure Drop, Liquid on Plate:

The preliminary study on a 6-inch diameter column by Mayfield et al.[1] also included measurements of the total pressure drop across perforated plates with various quantities of liquid present. The report states that the total pressure drop was very nearly equal to the sum of the dry-plate pressure drop plus the equivalent clear liquid head. This equivalent head was assumed to be that height of clear liquid which corresponds to the known quantity added to the column. The data for the system air-water shows the total pressure drop to be about 0.2 inches of water greater than the sum of dry-plate drop plus assumed liquid head. Data for the system air-absorption oil (specific gravity of 0.83) shows the total to be within 0.1 inch of water of this sum, and for the system air-glycol-water (viscosity of 8 cp) to be equal to this sum. These results are within 0.2 inches of water of the pressure drop data obtained in the present work, a difference within the over-all absolute uncertainty of the results reported here.

The work done with the 6.5-foot diameter column and reported by Mayfield et al.[1] shows that the equivalent clear liquid seal on the plate, calculated as the difference between total pressure drop and dry-plate pressure drop, was a complicated function of overflow-weir height, assumed liquid head over the weir (calculated on the basis of the Francis weir formula for clear liquid flow), and gas flow rate. An aeration factor was defined as the apparent liquid seal divided by the calculated liquid seal. This aeration factor was found to be a function of the above parameters in such a complex way that the effect of any one of them was in turn dependent upon the other two; so no attempt was made in that report to draw any conclusions concerning a possible universal correlation of the aeration factor as a function of column operating factors. The only system investigated for pressure-drop in the large column was air-water.

The experimental work reported by Arnold et al.[2] includes the measurement of actual liquid seal with manometers for only one plate configuration (5% hole area and L/D of 0.09). The total pressure drop was observed to about 0.3 inches of water greater than the sum of dry-plate drop plus measured liquid seal, a result in agreement with those obtained in the present study. Apparently these measurements were restricted to this particular plate, for no other observations of this type are reported. The rest of the data on pressure drop is correlated on the basis of an aeration factor which is based upon calculated versus observed total pressure drop. There is no indication of any attempt to separate dry-plate pressure drop from the liquid aeration phenomena. This aeration factor based upón total pressure drop was observed to be a function of gas flow rate and weir height, for low liquid flow rates involving negligible calculated head over the weir. The report states that efforts to include in the correlation data taken at larger liquid flow rates were unsuccessful. No systems other than air-water were studied.

Jang[3] and Claypool[4] present data which show that the total pressure drop for the system air-water exceeds the sum of dry-plate drop plus measured liquid head by 0.3 to 0.4 inches of water. This result is in good agreement with that found in the course of the present work.

COMPARISON TO OTHER STUDIES

Entrainment and Plate Stability:

None of the published studies on perforated plate performance include any quantitative information on entrainment rates or liquid weeping rates; however the report of Mayfield et al.,[1] tabulates a qualitative estimate of the range of stable plate operation for two plate configurations. For 3/16-inch diameter perforations of 7% hole area relative to column area, they report an upper limit of 7.5 ft/sec air velocity (with water as the liquid) in the column (109 ft/sec in the perforations) and a lower limit of 2.2 ft/sec in the column (33 ft/sec in the perforations). They define the lower limit as the gas velocity at which liquid begins to weep through the perforations. The upper limit corresponds to an entrainment rate (estimated from data obtained in the present work) of only 0.2 weight percent entrained water relative to air flow. According to the results obtained in the present work a maximum air flow rate of 10 or 11 ft/sec in the column would not cause excessive entrainment by standards proposed by Colburn.[8] The lower limit of velocity of 33 ft/sec in the perforations is difficult to compare to data obtained in the present work, since the minimum column velocity is stated to be that at which liquid just starts to weep through the perforations. This condition is not necessarily the appropriate one for defining a lower limit of operation, as may be seen in the comparable data shown in this work (Figure 26), for there may be a significant difference between the gas velocity at the condition of incipient weeping and that at the condition of a sudden increase in the quantity of liquid dumping through the perforations.

For a plate with 3/16-inch diameter perforations but with 4.5% hole area, Mayfield et al.,[1] tabulate the same upper limit as for the other configuration but a minimum velocity for stable operation of 17 ft/sec gas velocity in the perforations. The marked difference in lower limit for this plate compared to that for the plate with approximately twice the hole area, is larger than would be expected if the lower limit were specified in the manner recommended in the present work. Reference to Figures 25 and 26 shows that as hole area is reduced, the lower limit specified by Mayfield et al.,[1] approaches more closely the limit determined by the sudden increase in dumping rate; so the discrepancy indicated above is probably explained by this change in the nature of the liquid dumping curves.

Although Mayfield et al.,[1] report no significant change in lower operating limit with increase in calculated liquid head on the particular try reported on in detail, the general results of both their study and the present work shows a definite and important relationship between liquid head on the plate and lower limit of operation. Figure 29 shows the correlation of Mayfield et al.,[1] for weep point on the plate with 3/16-inch perforations; they get a fair correlation plotting dry tray pressure drop for the gas velocity at the point of incipient weeping versus calculated liquid depth on the plate. The data of the present work are shown on the same graph and show a wide variation in slope of dry-tray pressure drop versus liquid level, although some of the plates show the same type of function. The fact that the phenomena associated with liquid dumping are very sensitive to slight changes in column design causes difficulty in making any absolute comparison of data between different systems.

Entrainment is not considered in the report published by Arnold et al.[2] However they do indicate qualitatively-determined operating conditions corresponding to incipient weeping of liquid through the perforations. These points occur at gas velocities in the perforations of about 40 ft/sec, but show no consistent relationship to hole size, total hole area, or liquid head on the plate. There is no quantitative information presented concerning plate stability.

A large amount of data for entrainment from bubble-cap plates is reported by Holbrook and Baker[9] for the steam-water system, by Sherwood and Jenny[7] for the air-water system, and by Peavy and Baker[10] for the alcohol-water system. Holbrook and Baker used an 8-inch diameter column with only two bubble caps per plate, but they do not indicate the liquid level on the plate. They report no significant effect of slot velocity; in fact, the effect of slot velocity was found to depend both in magnitude and direction upon the plate spacing. Data are presented for entrainment as a function of gas velocity in the column, as shown in Figure 30, for several different plate spacings. Entrainment data from the present work is also shown for comparison, although lack of information on the actual effective spacing makes exact comparison difficult. The detailed drawing of the equipment of Holbrook and Baker indicates that the liquid level on the plate was probably about 2 inches; therefore their data for a plate spacing of 18 inches should have the same effective spacing as that of the present study for an effective spacing of 16 inches. Also shown in Figure 30 is a plot of entrainment versus plate spacing and also versus effective spacing, at constant velocity.

Sherwood and Jenny[7] employed an 18-inch diameter column with 7 bubble caps per plate. They observe some effect of slot velocity, but the effect is no more than that shown by Holbrook and Baker.[9] Their data for various plate spacings is shown in Figure 31, and a comparison to the data of the present work is shown for an effective spacing of 16 inches. Again, Figure 31 shows a plot of entrainment versus plate spacing and also versus effective spacing, at constant velocity.

Peavy and Baker[10] used an 18-inch diameter column and present entrainment data at one liquid level and a single plate spacing. The data are shown in Figure 32, and compared to the data of the present study for a comparable effective spacing.

Figure 33 presents a comparison of representative data from these three references with comparable data from the present work. The data of Sherwood and Jenny[7] and of Peavy and Baker,[10] both for an 18-inch diameter column, compare closely, and they lie above the data of the present work by a factor of about six. The data of Holbrook and Baker[9] lie closer to those of this study, and the entrainment is a steeper function of gas velocity than for any of the other cases. The fact that columns of different diameter were used makes comparison difficult because of the uncertain magnitude of the wall effect, but the fact that the entrainment increases with increasing column diameter is in qualitative agreement with the expected direction of any wall effect. The disagreement in slope between the data of Holbrook and Baker[9] and all the rest of the data is probably due to the fact that only two bubble caps were used in that study, an experimental condition which could have a serious effect upon the uniformity of surface splashing across that particular tray compared to trays with several caps. Whether all of the difference between the various sets of data is the result of wall effect in the columns is not known; however, a portion of the difference between the entrainment observed in the present study on perforated plates and that observed in the work on bubble-cap plates may be due to a difference in the splashing action at the surface of the liquid on the two types of plates. Thus, Mayfield et al.,[1] report that bubble-cap plates appear to be entrainment-limited at a lower gas velocity than do perforated plates in an otherwise identical column. No quantitative information accompanies that statement however.

Figure 33 also presents a comparison of the data of the present work with those available for bubble-cap plate studies which shows that entrainment is nearly the same function of effective spacing for all cases reported.

APPLICATION OF PERFORMANCE DATA TO COLUMN DESIGN

The data presented in this study were all obtained with a six-inch diameter perforated plate column; however, extrapolation of the data to the design of larger columns is probably well justified in view of the agreement of the results presented here with those presented by Mayfield et al.,[1] and Arnold et al.[2] Actually, the allowable upper limits of operation of columns cannot be defined accurately without the aid of pilot plant information on the particular system involved because of lack of knowledge beforehand on such questions as foaming of the liquid phase, density of the liquid in the downcomer, maximum allowable liquid crest over the weir, etc.

Within a predetermined framework of policy decisions with respect to such factors, however, the operating characteristics of perforated plate columns as presented here may be used to define operating limits of column operation. The data used for this purpose are undoubtedly valid for such purposes to as great a degree as the *a priori* "policy" assumptions regarding such factors as liquid density in downcomers for a given system.

As noted previously in this work the largest degree of uncertainty lies in the prediction of plate stability with respect to liquid weeping through the perforations. This uncertainty is the result of the sensitivity of this factor to minor changes in the distribution of perforations at the periphery of a plate, and pilot plant data would be required in cases where the stability limits are of importance in the design. For many applications stability is of secondary importance in column design, as can be seen in many of the examples illustrated below.

A very convenient method of presenting column operating limits involves a simple plot of vapor velocity (based upon plate area not including downspouts) as a function of liquid flow per unit length of weir. For a given liquid flow an allowable upper and lower limit of vapor flow can be calculated, while maximum and minimum liquid flows can also be specified.

As shown in Figure 34 (and all subsequent figures), a simple graphical picture of column operating characteristics is the result. The construction of each graph requires the specification of the following:

(1) Column Diameter

(2) Weir Length

(3) Relative area of perforations to plate area (minus downcomers)

(4) Plate Spacing

(5) Weir Height

(6) Downspout Outlet

(7) Vapor Density

(8) Liquid Density

(9) Liquid Surface Tension

(10) Perforation Diameter

Operating lines for given ratios of liquid to vapor flow may also be shown. One graph can conveniently be used for more than one ratio of weir length to plate area; so each operating line represents a different ratio of liquid to vapor flow for each value of the ratio of weir length to plate area.

Calculations of operating limits are made as follows:

(1) Maximum vapor flow limited by entrainment:

An upper limit of percent entrainment is arbitrarily chosen for the particular case (e.g., 20 wt. percent liquid relative to vapor flow). As shown in Figure 21 and Figure 15B, the upper limiting vapor velocity can be determined if the effective spacing between liquid surface and plate above is known. The spacing is calculated as the plate spacing minus the sum of weir height and liquid crest over the weir (as predicted by the standard Francis Weir Formula). Thus for each liquid flow in a given column there is a particular effective spacing which controls the allowable upper limit of vapor flow for the entrainment limiting conditions. This limit is independent of perforation area relative to plate area but is a function of plate spacing, weir height, gas density, liquid density, and liquid surface tension, as well as liquid flow rate.

(2) Maximum vapor flow limited by flooding:

The flooding limit is defined as that point where the gas phase pressure drop across the plate is equal to the driving force of liquid head available in the downcomer for overcoming this pressure drop. Thus the expression for this condition is:

$$\Delta P_{total} = \Delta P_{DP} + h_{liq} + \Delta P_x = C\ (S + H_{weir}) - h_{liq} - h_d$$

Where

ΔP_{DP} = gas pressure drop across the dry plate

$\Delta P_x = \Delta P_{total} - h_{liq} - \Delta P_{DP}$

ΔP_{total} = total gas pressure drop, liquid on plate

C = an arbitrary constant to allow for foaming in the downcomer

S = plate spacing

H_{weir} = weir height

h_{liq} = head of liquid on plate

$$(h_{liq} = \left[H_{weir} + H_{w.c.}\right] \alpha)$$

$H_{w.c.}$ = height of liquid crest over weir according to Francis Weir Formula

h_d = liquid head loss for flow out downspout outlet

α = aeration factor

Figures 2 through 12 present the pressure drop data from which the vapor velocity in the perforations may be obtained. Vapor velocity based on plate area is then calculated, knowing the ratio of perforation area to plate area.

For every liquid flow rate, then, there is a maximum allowable vapor flow rate limited by flooding.

The position of this line is also a function of perforation area relative to plate area, plate spacing, weir height, downspout outlet, gas and liquid densities, and (to a very slight degree) liquid surface tension.

(3) Minimum vapor flow limited by liquid weeping through the plate perforations:

This point is defined as the vapor velocity in the perforations corresponding to the sharp change in liquid weep rate as a function of gas velocity. Figures 22 through 28 present the data obtained in the six-inch diameter column for the air-water system, and Table III (Appendix IV) presents the data for systems with other liquids and gases. The data show that minor changes in perforation spacing near the edge of the plate makes considerable difference in the performance of the column in the unstable regions of operation; hence the lower limits shown in Figures 34 through 48 may require revision in the light of pilot plant data obtained for a given system under investigation.

The position of this line is a function of gas and liquid densities, liquid surface tension, perforation diameter, and relative area of perforations to area of plate.

(4) Maximum liquid flow, limited by weir capacity:

This flow rate is defined arbitrarily here as the liquid flow corresponding to 2 1/2 inches of calculated liquid crest height over the weir. At sufficiently high vapor rates, where liquid entrainment rates become significant, the liquid load caused by cycling of liquid upward by entrainment reduces the allowable net flow of liquid down the column. The position of this curve is a function of the ratio of weir length to plate area, but only rarely is this fact of any importance in column design. The position of the line is also a function of the gas and liquid densities.

(5) Minimum liquid flow, limited by splashing of liquid over the weir:

In order to maintain the designed head of liquid on the plate to maintain contacting efficiency, a minimum liquid flow is required to overcome that thrown over the weir by splashing resulting from bubbling action. The figure of 10 gpm per foot of weir is an estimate based upon semi-quantitative observations on a small weir installed in the six-inch diameter column. The limit is shown tentatively as independent of vapor velocity, but in any case this limit need never be a factor of importance in new column design, since a reduction in weir length in a given column can be accomplished easily. Where a column already in existence is being checked for use with a new system, more accurate knowledge of this lower limit may be required. In such a case pilot plant data would be required, as this limit would be expected to be some function of column layout.

Contacting efficiency is frequently a limiting factor in the design of bubble-cap plates; however the preliminary results of a study parallel to the present work and concerned with contacting efficiencies of perforated plates show that plate efficiency is only a slight function of vapor velocity at moderate to high rates of vapor flows. The work is part of the, as yet, unpublished Ph.D. thesis of R. D. Lee.

According to Mayfield et al.,[1] hydraulic gradient is not significant in the operation of perforated plate columns.

As a typical case for a general exposition of the effect of the variables to be considered in the design of perforated plate columns, a system characteristic of hydrocarbon distillation is taken first. Figure 34 shows the graphical presentation of the operating limits of the column used as the example.

Of particular interest is the fact that the flooding limit cuts off sharply at liquid flow rates considerably less than the maximum allowable flow over the weir. This condition is caused by the rapidly increasing head loss involved in liquid flow out the downspout opening which is only 3/4 inches high. Figure 35 shows the effect on the flooding limit of increasing the weir height from 1 inch to 2 inches in order to increase the height of the downspout outlet to 1 and 1/2 inches. The head loss for liquid flow out the downspout no longer provides an undesirably limiting factor in the operating limits of the column.

The increase in plate stability in changing from 1/4-inch diameter to 1/8-inch diameter perforations is shown in Figures 34 and 35. Since the use of the smaller perforations involves greater fabrication cost for the plates, the choice of small perforations over large ones would presumably be made only when plate stability is important in column operation.

The particular column configuration used for Figure 35 results in a flooding limit 20% lower than the entrainment limit. Figure 36 presents operating limits for the same column with different values of perforation area relative to plate area. Since the entrainment limit is independent of this parameter, while the flooding limit is dependent upon vapor velocities in the perforations, the relative positions of the entrainment and flooding lines shift with change in percent perforation area. The stability limit is also a function of vapor velocities in the perforations as well as percent perforation area; so the stability lines change markedly. Hence as percent perforation area increases, the ratio of maximum to minimum allowable operating limits significantly decreases after the flooding limit exceeds the entrainment limit.

Figure 37 shows the operating limits for the standard column of Figure 35 with different plate spacings. Both the entrainment and flooding limits change with change in plate spacing, but the stability limit remains the same. Of interest to note is the fact that the flooding limit is less sensitive to changes in plate spacing than is the entrainment limit. Increasing the plate spacing not only increases the capacity of a column but also increases its relative stability. Comparison of Figures 36 and 37 shows that the determination of optimum column design with respect to plate spacing and percent perforation area can be accomplished rapidly and easily with the aid of such graphs. Furthermore, the relative stability of the column for a given operating condition may be determined readily by means of the operating line superimposed on the chart for the appropriate relative rates of gas and liquid flow and relative length of weir to plate area.

Figure 38 presents the operating limits for the standard column operating with gases of various densities. Since the weight percent entrainment is independent of gas density, the entrainment limit is unchanged; however the flooding limit and stability limit change approximately in proportion to the inverse square root of the gas density. Thus as the gas density is reduced, the flooding limit becomes less important. In general, then, columns with light gases will be more likely to be entrainment limited than will columns handling dense gases. The effect of gas density upon the position of the operating line is also shown on this chart, with the conclusion evident that columns handling light vapors might have too much weir length even if the column were properly designed in that respect for dense vapors.

The effect of liquid density upon the operating limits of the standard column is shown in Figure 39. The chart makes clear the fact that with an increase in liquid density the greater driving force available in the downcomer for overcoming vapor phase pressure drop raises the flooding limit significantly. The entrainment limit remains constant because of the fact that weight percent entrainment is independent of liquid density. The data on plate stability obtained with the six-inch diameter column showed no effect of liquid density upon plate stability.

Figure 40 presents operating limits for the standard column showing the effect of a change in surface tension. The flooding limits are changed only slightly, but the entrainment limit increases markedly with the threefold change in surface tension. An important increase in plate stability also accompanies an increase in surface tension.

The effect on the standard column (Figure 35) of changes in the ratio of plate area to weir length is shown in Figure 41. There is a minor effect upon maximum weir capacity, but the most important effect is the change in position of the operating line with change in this ratio. Three different operating lines are shown, and each one is valid for a particular relative liquid to vapor flow for each value of the ratio of plate area to weir length. Increasing the weir length in a given column moves the operating line counterclockwise, while increasing the liquid flow relative to vapor flow shifts the position of operating line clockwise.

Figure 42 shows the operating limits for a typical double-weir modification of the standard column operating with a high ratio of liquid flow to vapor flow (typical rectified absorber operation). The 10% perforation area configuration is seen to provide a narrow range of maximum to minimum allowable flows in this column under these columns; so additional operating limits are shown for 5% and 2 1/2% perforation area designs. The relative stability of the column increases with decreasing perforation area; so considering the 5% column design to be sufficiently stable, a set of operating limits for this column with different plate spacings is presented in Figure 43.

These curves demonstrate the reduction in flooding limit with reduction in plate spacing, and the concomitant decrease in relative plate stability. The ultimate column design will depend upon policy decisions with respect to general column proportions of height and/or diameter as well as with respect to stability considerations; hence such graphical presentations assist in the rapid analysis of the problem of cost estimating and sizing the possible column configurations fitting the over-all policy limitations.

Figure 44 presents operating limits for another variation of the original conditions illustrated in Figure 35. In this case a gas four times as dense as in the former case is considered. Operating limits for different plate spacings are shown, and the effect of changing from a single to a double weir configuration is illustrated. To be noted here is the fact that the change to a double weir column markedly increases the relative stability of the column at only a small cost in reduced maximum throughput (the reduced throughput results from the reduction in net plate area which more than compensates for the increased vapor throughput based upon net plate area). Here again use of such charts assists in the rapid analysis of the problem of optimizing the design of a perforated plate column.

The design characteristics of a typical vacuum column is illustrated in Figure 45 which presents the operating limits for the standard column operating with a gas of one-sixteenth the density of the former case shown in Figure 35. The column is entrainment limited at all the plate spacings considered, and the effect of the low gas density upon the position of the operating line for a typical rectifying section (i.e., equi-weight flows) is such that stable operation indicates the use of 1/2 or 1/4 the length of a maximum single weir.

A problem of importance in the distillation of light hydrocarbons under pressure is the design of the stripping section of such columns. Here the gas density is so high that the liquid density may be only 6 times as great as that of the gas. Naturally, flooding problems become critical. With bubble caps the solution reportedly lies in the use of large plate spacings; however, as shown in Figure 46 and Figure 47, satisfactory perforated plate designs lie in the same general region of column characteristics for operation with less critical conditions of relative gas and liquid density. The extrapolation of the data obtained in the present work to the design problem discussed above represents a 25-fold increase in density of vapor above the maximum used in this study. Despite the magnitude of this extrapolation, the conclusions to be drawn from this discussion are probably quite valid, since flooding limits are not susceptible to any changes of a fundamental nature just because of changes in vapor density.

As an example of a design for which column proportions are of major importance, operating conditions typical of liquid air distillation are illustrated in Figure 48. The column is similar to the standard column except for the very small plate spacing of 6 inches, consistent with the requirement that liquid air columns be relatively squat in over-all proportions in order to optimize the design with respect to heat leak. Operating limits for three values of percent perforation area are shown, as are operating lines for maximum length of single weir and one-half this length of single weir. The 5% perforation area with the latter weir length provide a column configuration that appears to be quite useful. The ratio of maximum to minimum flows is three, a figure which ought to be quite adequate for a system like a liquid air distillation unit which must operate near a given designed throughput in order to obtain designed over-all energy efficiencies.

Perhaps the most striking factor in the design of perforated plate columns evidenced in the above discussions is the simplicity of design methods based upon the data obtained in the present work and in other studies on the same subject. Elimination of problems related to bubble cap design, hydraulic gradient, loss of contacting efficiencies between vapor and liquid, and general uncertainties related to factors limiting vapor throughputs in bubble cap columns reduce the problem of perforated plate column design to a rapid process of optimization of design within policy limitations, using graphical techniques illustrated above as a guide to a clear understanding of the important limiting factors in each design problem encountered.

APPENDIX

BIBLIOGRAPHY

(1) F. D. Mayfield, W. L. Church, Jr., A. C. Green, D. C. Lee, Jr., and R. W. Rasmussen, "Perforated Plate Distillation Columns," Ind. Eng. Chem. 44, No 9, 2238 (September, 1952).

(2) D. S. Arnold, C. A. Plank, and E. M. Shoenborn, "Performance of Perforated Plate Distillation Columns," Chem. Eng. Prog. 48, No. 12, 633 (December, 1952).

(3) R. Jang, "Operating Characteristics of Perforated Plate Columns," M.S. Thesis, University of California, unpublished, 1949.

(4) D. C. Claypool, "Variables Affecting the Pressure Drop in Perforated Plate Distillation Columns," M. S. Thesis, University of California, unpublished, 1951.

(5) W. D. Baines and E. G. Petersen, "An Investigation of Flow Through Screens," Trans. ASME 73, No. 5, 467 (July, 1951).

(6) M. Souders, Jr. and G. G. Brown, "Design of Fractionating Columns: I, Entrainment and Capacity," Ind. Eng. Chem. 26, No. 1, 98 (January, 1935).

(7) T. K. Sherwood and F. J. Jenny, "Entrainment in Plate Columns," Ind. Eng. Chem. 27, No. 3, 265 (March, 1935).

(8) A. P. Colburn, "Effect of Entrainment on Plate Efficiency in Distillation," Ind. Eng. Chem. 28, No. 5, 526 (May, 1936).

(9) G. E. Holbrook and E. M. Baker, "Entrainment in a Bubble-Cap Distillation Column," Ind. Eng. Chem. 26, 1063 (1934).

(10) C. C. Peavy and E. M. Baker, "Efficiency and Capacity of a Bubble-Plate Fractionating Column," Ind. Eng. Chem. 29, 1056 (1937).

(11) D. W. Van Krevelen and P. J. Hoftijzer, "Gas Bubble Formation: Calculation of Interfacial Area in Bubble Contactors," Chem. Eng. Prog. 46, No. 1, 29-35 (1950).

(12) B. L. Harris, A. I. Johnson, and C. J. Quigley, "Size and Mass Transfer Studies on Gas Bubbles," preprint of paper presented at AIChE Conference, Toronto, Canada, April 26, 1953.

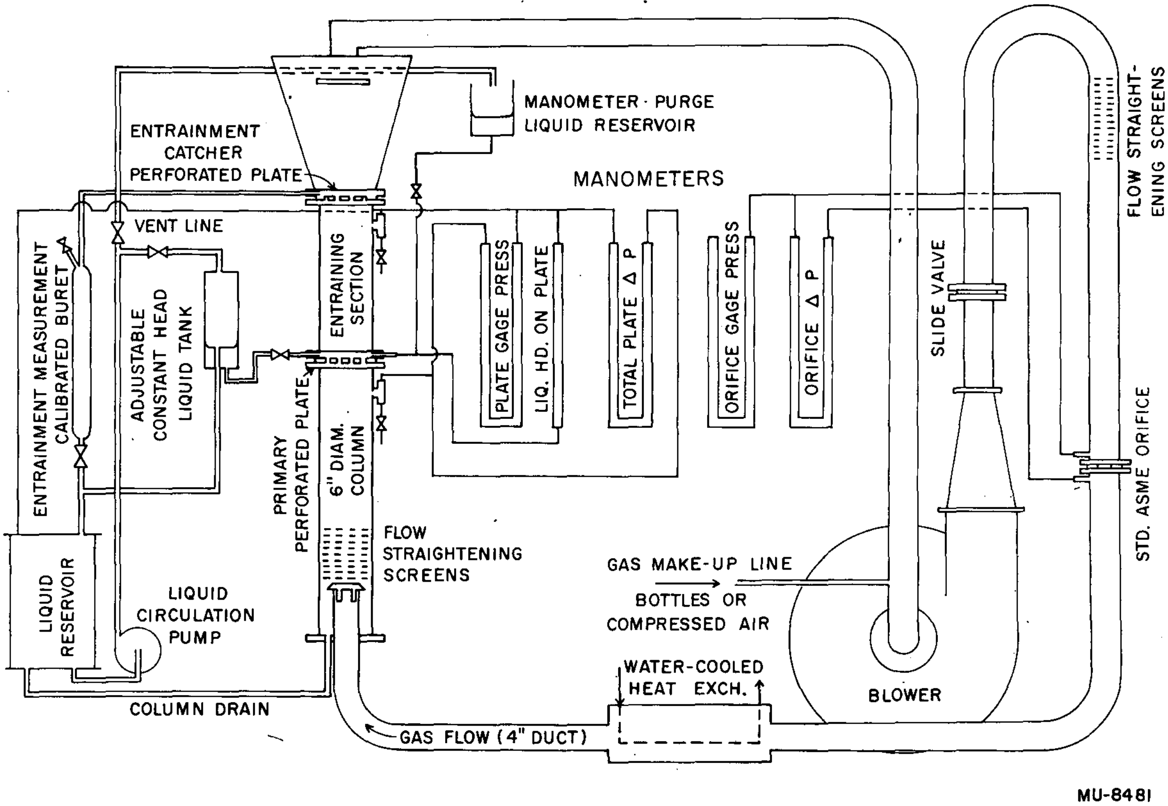

Fig. 1. Schematic Diagram of Experimental Equipment.

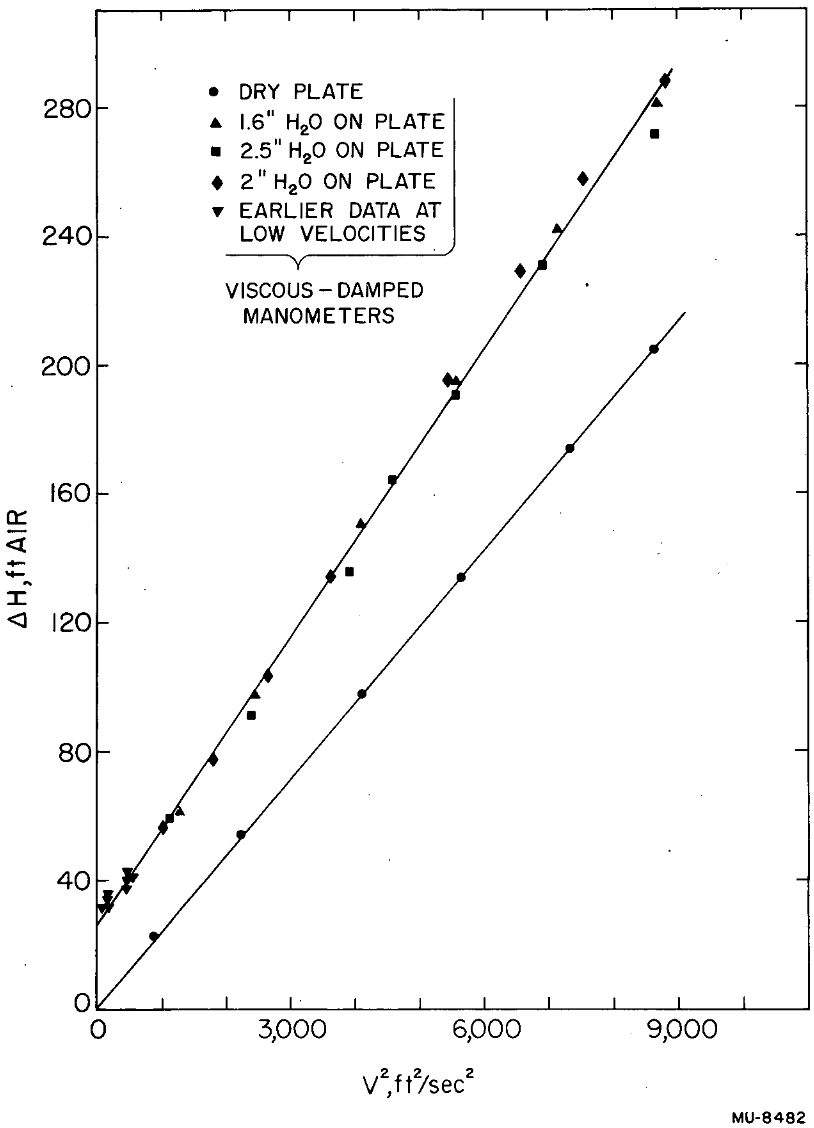

Fig. 2. Pressure Drop Across Perforated Plates. Plate IIA 1/8 inch holes at about 4 diameter spacing (4.9% hole area). Pressure drop (minus head of liquid on plate) vs hole velocity squared. System Air-H_2O.

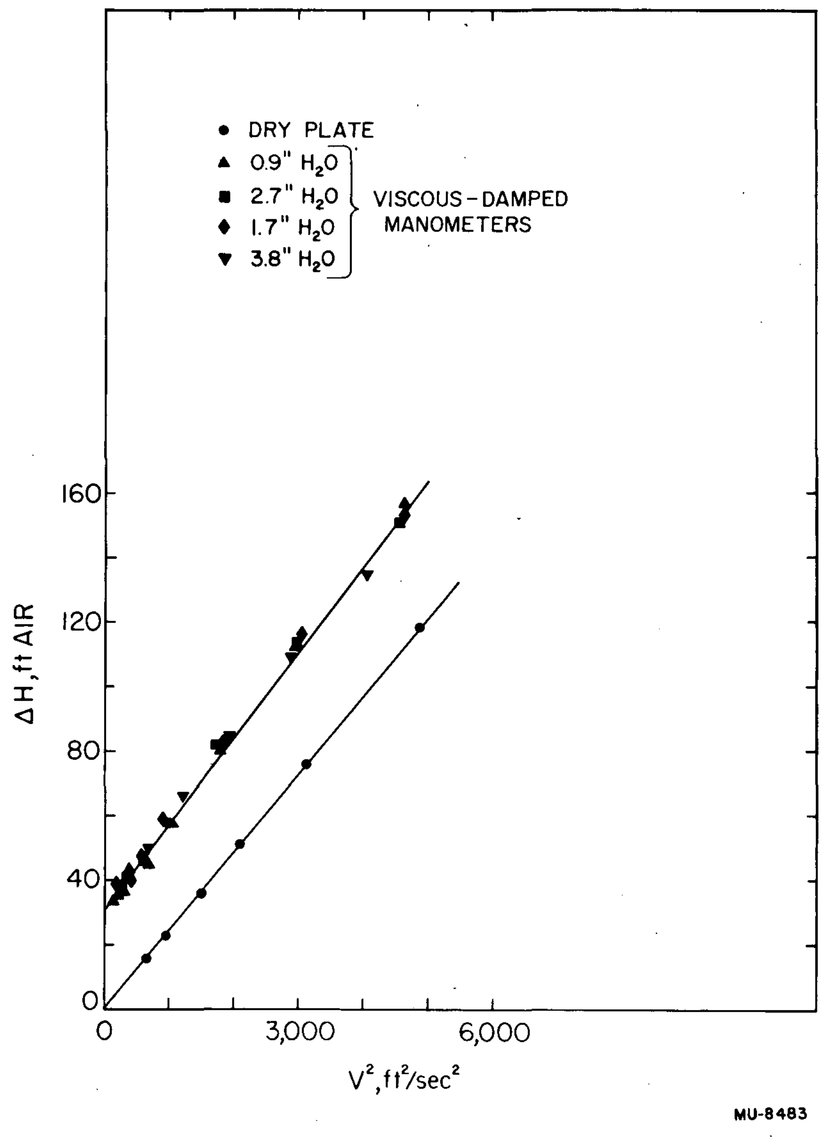

Fig. 3. Pressure Drop Across Perforated Plates. Plate III 1/4 inch holes at about 4 diameter spacing (5.4% hole area). Pressure drop (minus liquid head) vs hole velocity, squared. System Air-H_2O.

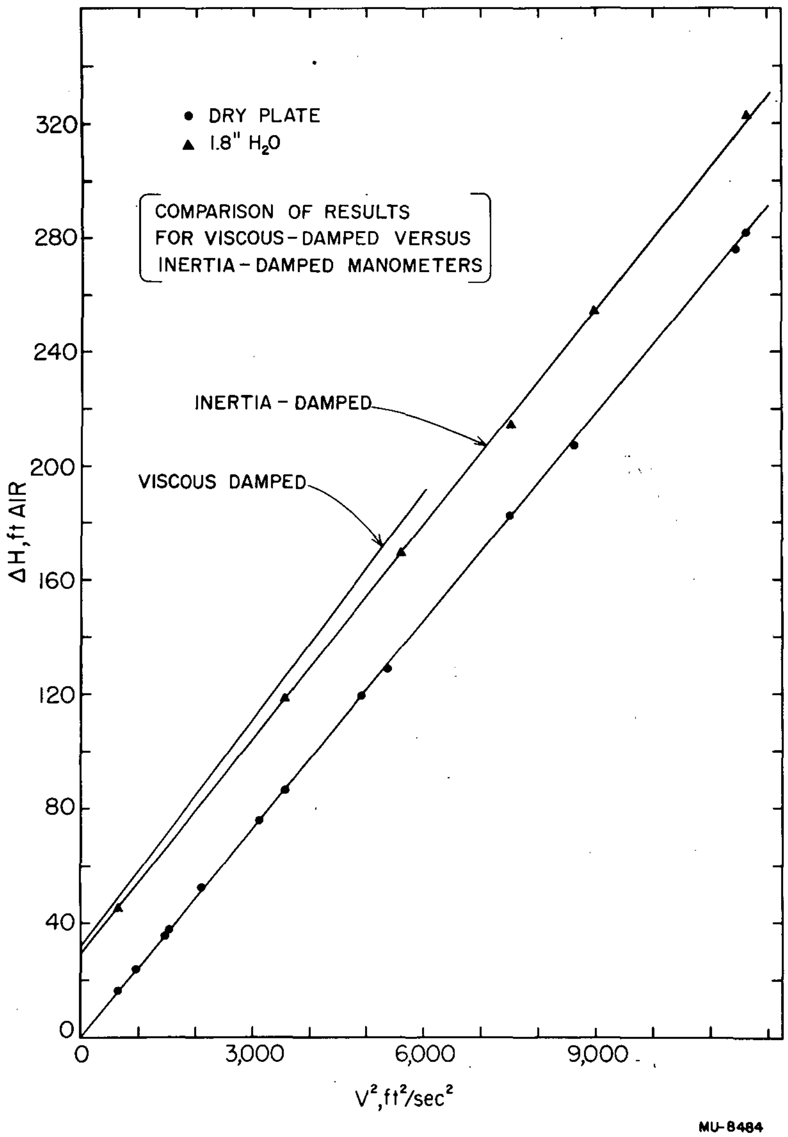

Fig. 3a. Pressure Drop Across Perforated Plates. Plate III 1/4 inch holes at about 4 diameter spacing (5.4% hole area). Pressure drop (minus liquid head) vs hole velocity squared. System Air-H_2O.

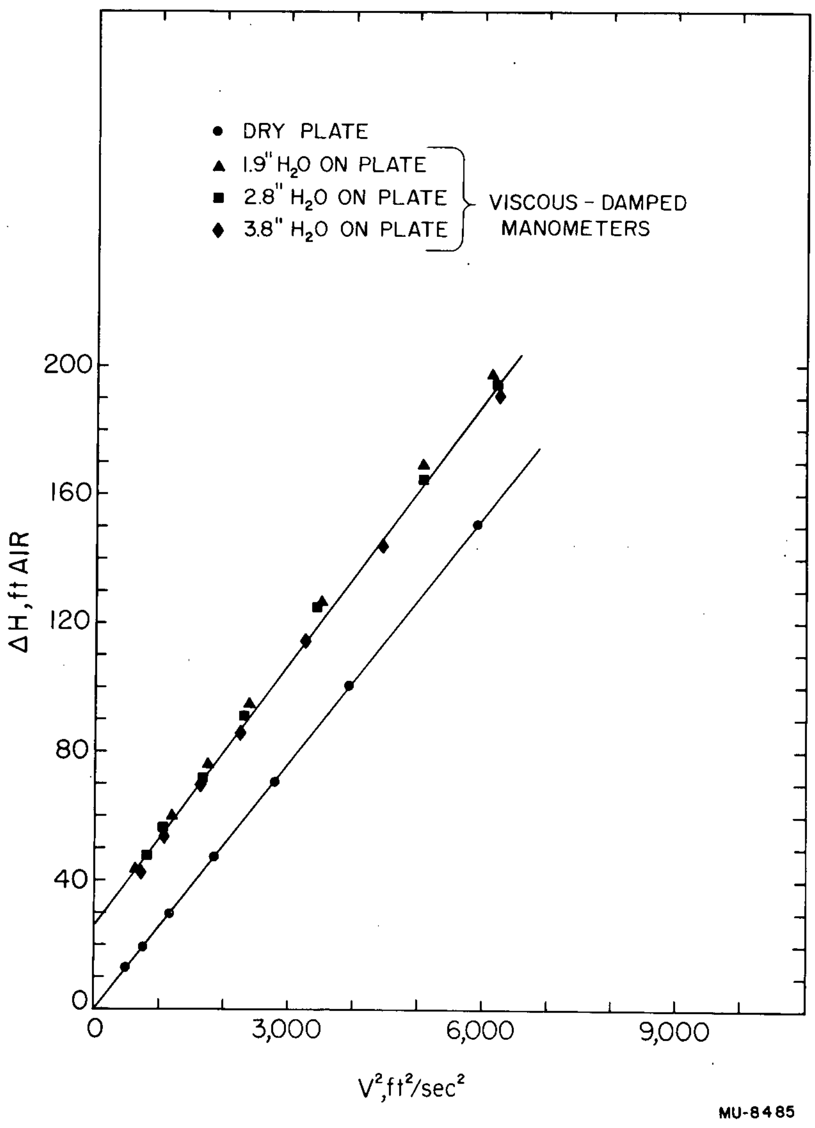

Fig. 4. Pressure Drop Across Perforated Plates. Plate V 1/2 inch holes at about 4 diameter spacing (4.9% hole area). Pressure drop (minus liquid head) vs hole velocity, squared. System Air-H_2O.

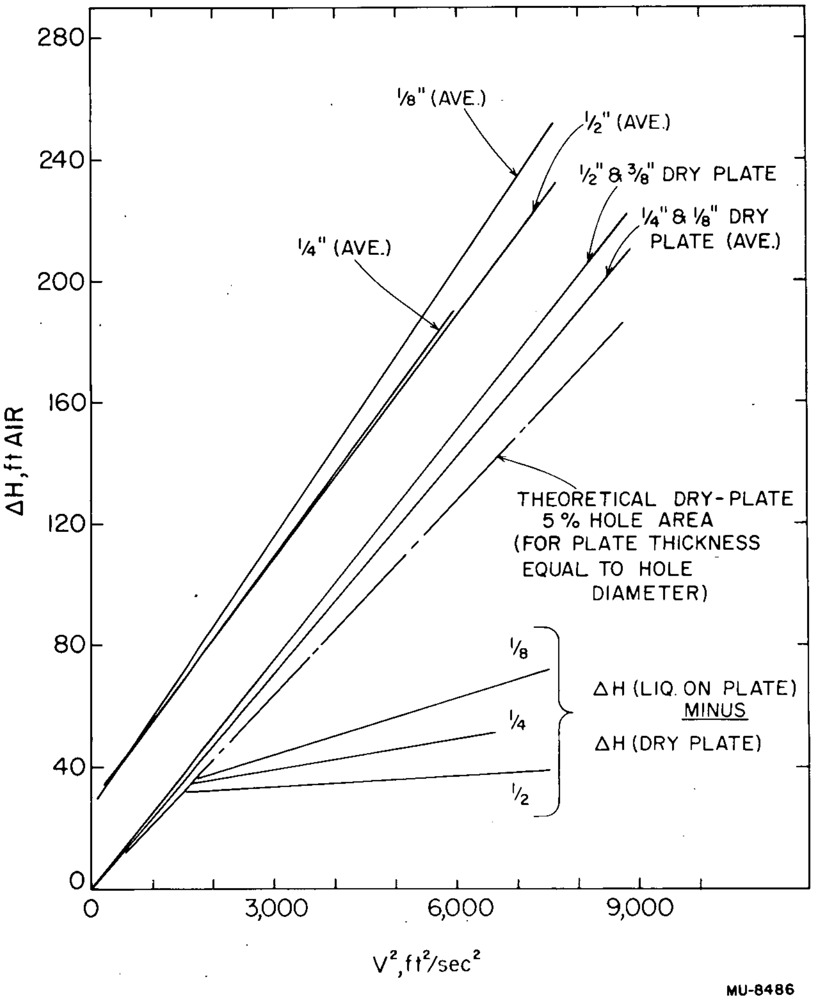

Fig. 5. Pressured Drop Across Perforated Plates. Effect of Hole Size (1/8 inch-1/4 inch-1/2 inch diameter holes at about 4 diameter spacing) (approximately 5% hole area). Pressure drop (minus liquid head on plate) vs hole velocity, squared. System $Air-H_2O$. Viscous-damped Manometers.

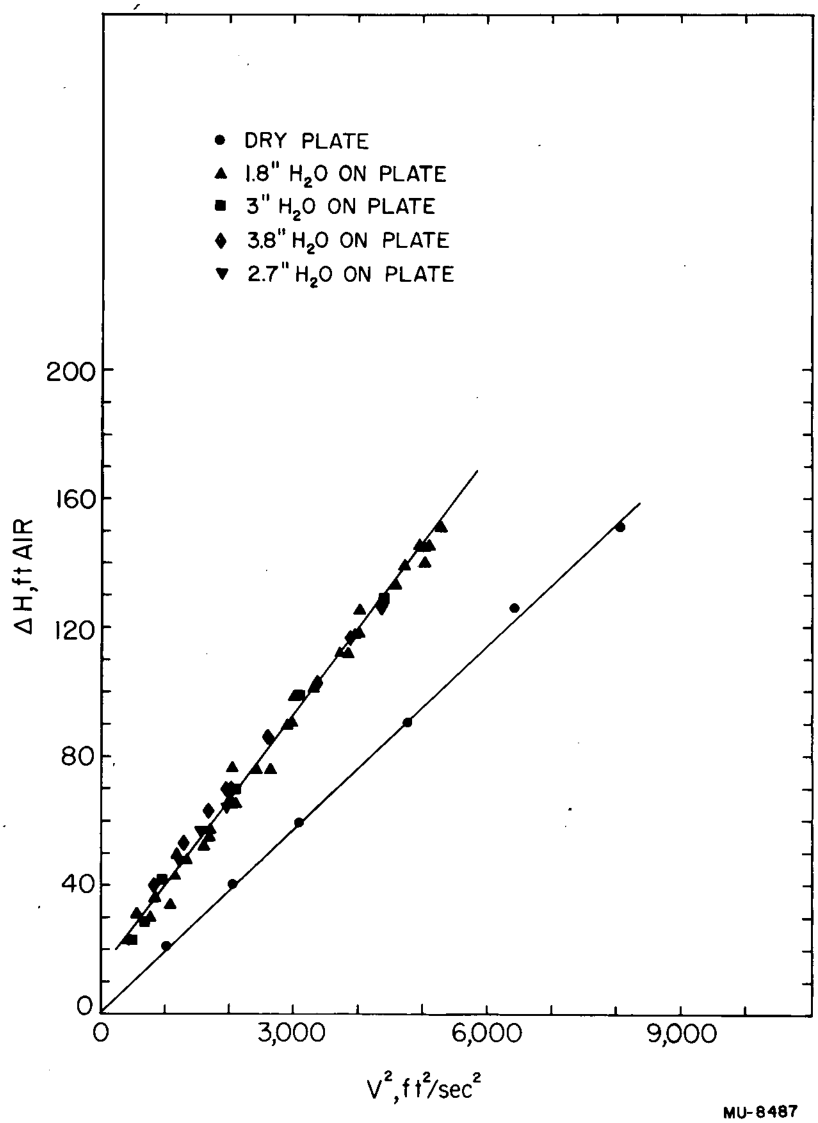

Fig. 6. Pressure Drop Across Perforated Plates. Plate I 1/8 inch holes at about 2 diameter spacing (18.8% hole area). Pressure drop (minus liquid head on plate) vs hole velocity, squared. System Air-H_2O. Viscous-damped Manometers.

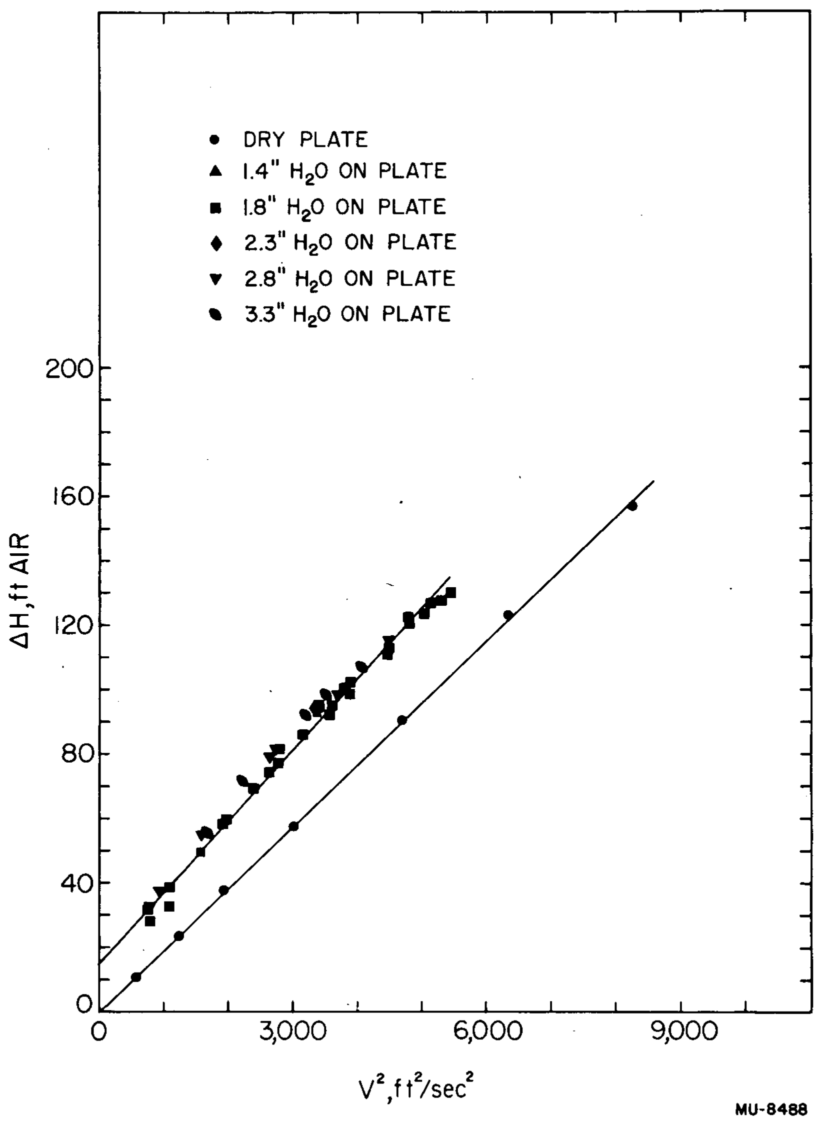

Fig. 7. Pressure Drop Across Perforated Plates. Plate IV 1/4 inch holes at about 2 diameter spacing (19.0% hole area). Pressure drop (minus liquid head on plate) vs hole velocity, squared. System Air-H_2O. Viscous-damped Manometers.

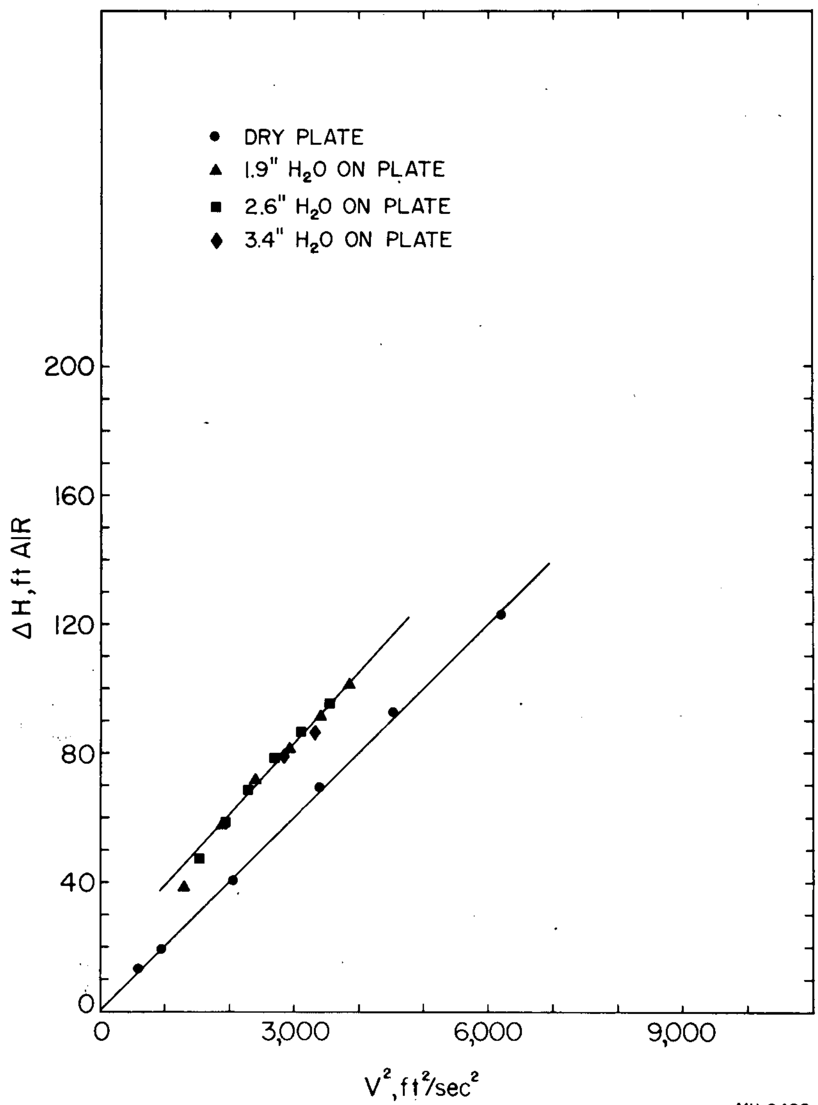

Fig. 8. Pressure Drop Across Perforated Plates. Plate VI 1/2 inch holes at about 2 diameter spacing (21.5% hole area). Pressure drop (minus liquid head on plate) vs hole velocity, squared. System Air-H_2O. Viscous-damped Manometers.

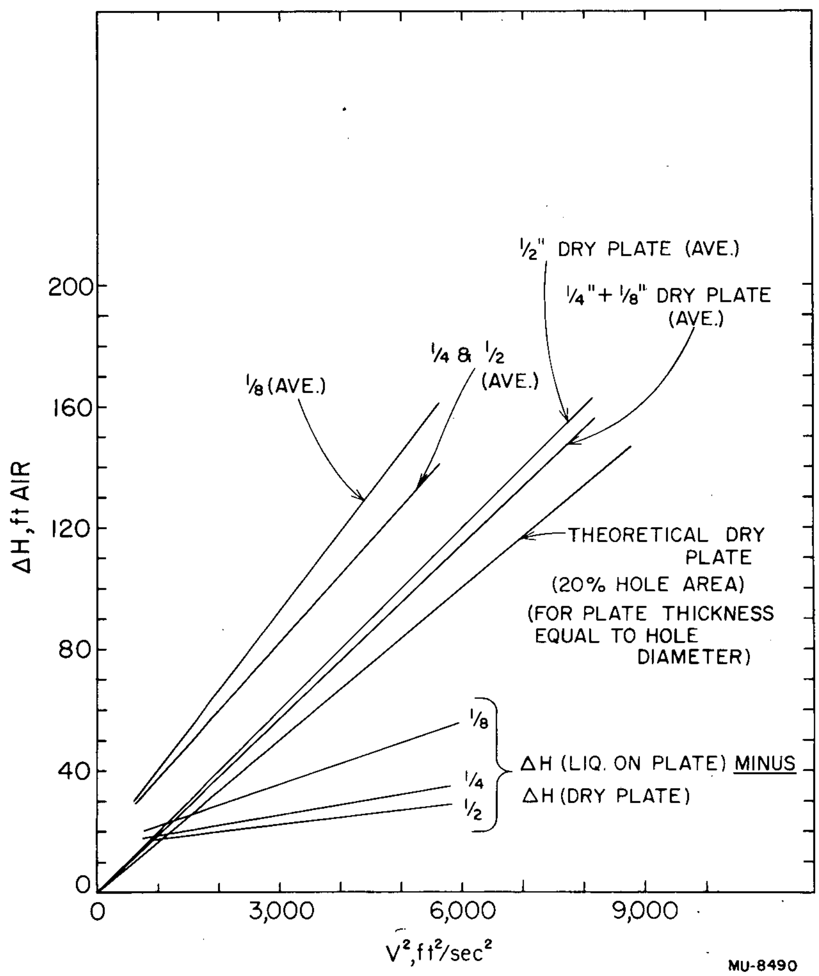

Fig. 9. Pressure Drop Across Perforated Plates. Effect of hole size (1/8 inch-1/4 inch-3/8 inch-1/2 inch diameter holes at about 2 diameter spacing)(approximately 20% hole area). Pressure drop (minus liquid head on plate) vs hole velocity, squared. System Air-H_2O. Viscous-damped Manometers.

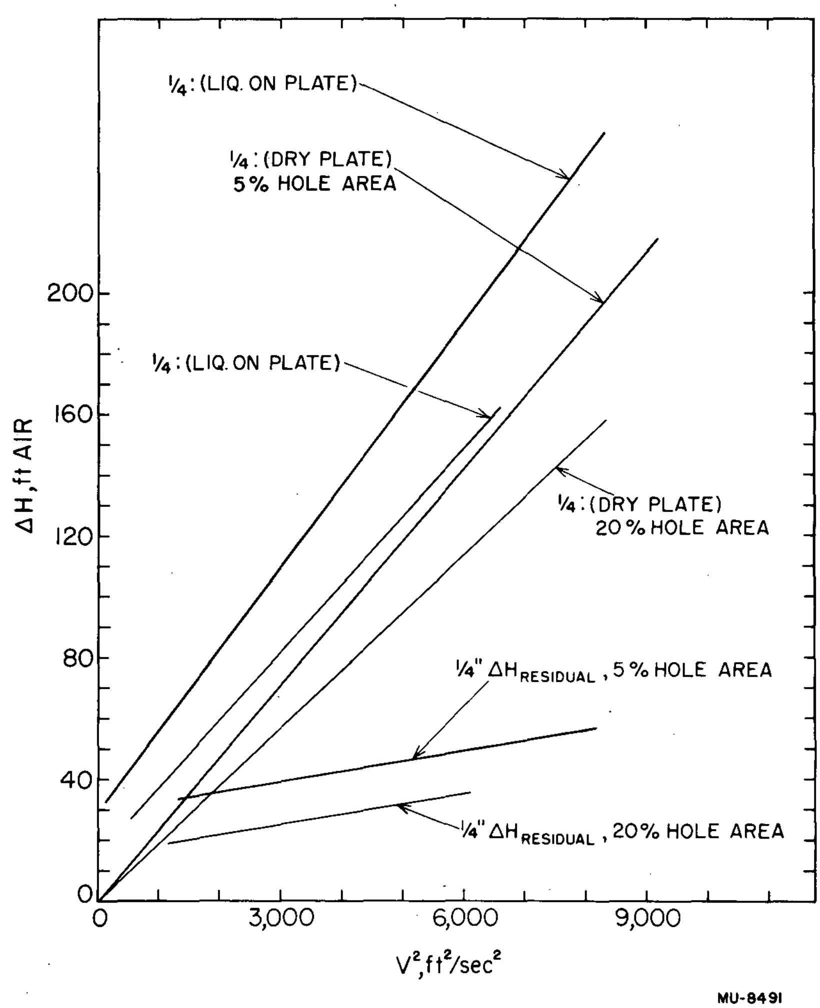

Fig. 10. Pressure Drop Across Perforated Plates. Effect of Hole Area (Using 1/4-inch holes as example). Pressure drop (minus liquid head on plate) vs hole velocity (squared). System Air-H_2O. Viscous-damped Manometers.

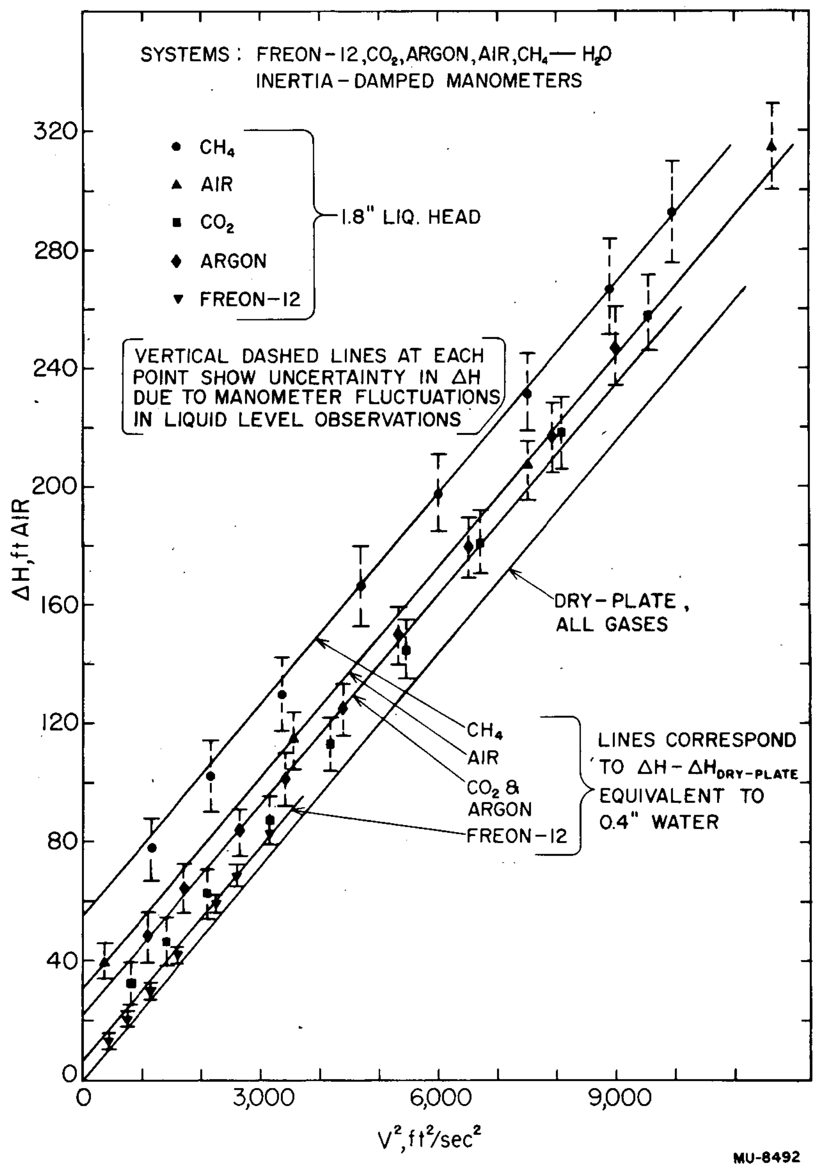

Fig. 11. Pressure Drop Across Perforated Plates. Effect of Using Various Gases. Pressure drop minus liquid head vs hole velocity squared.

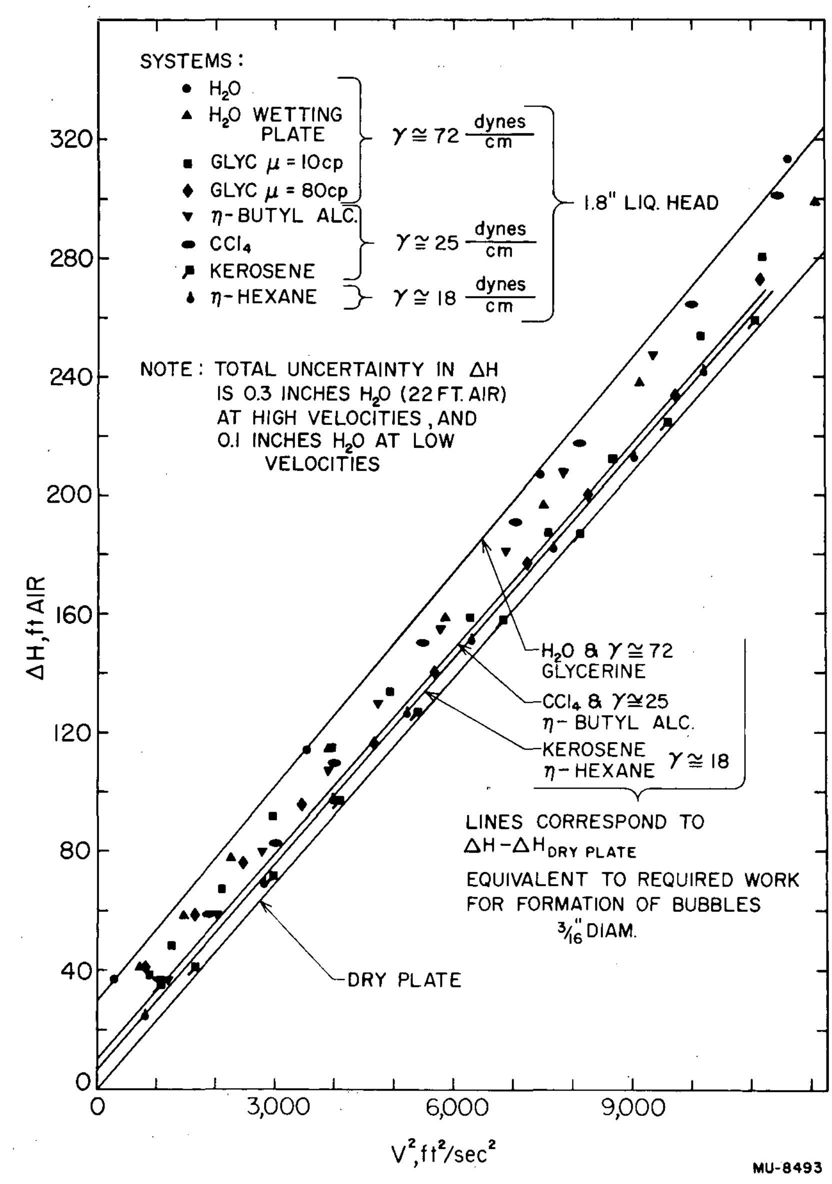

Fig. 12. Pressure Drop Across Perforated Plates. Effect of Using Various Liquids. Pressure drop -minus liquid head- vs hole velocity squared.

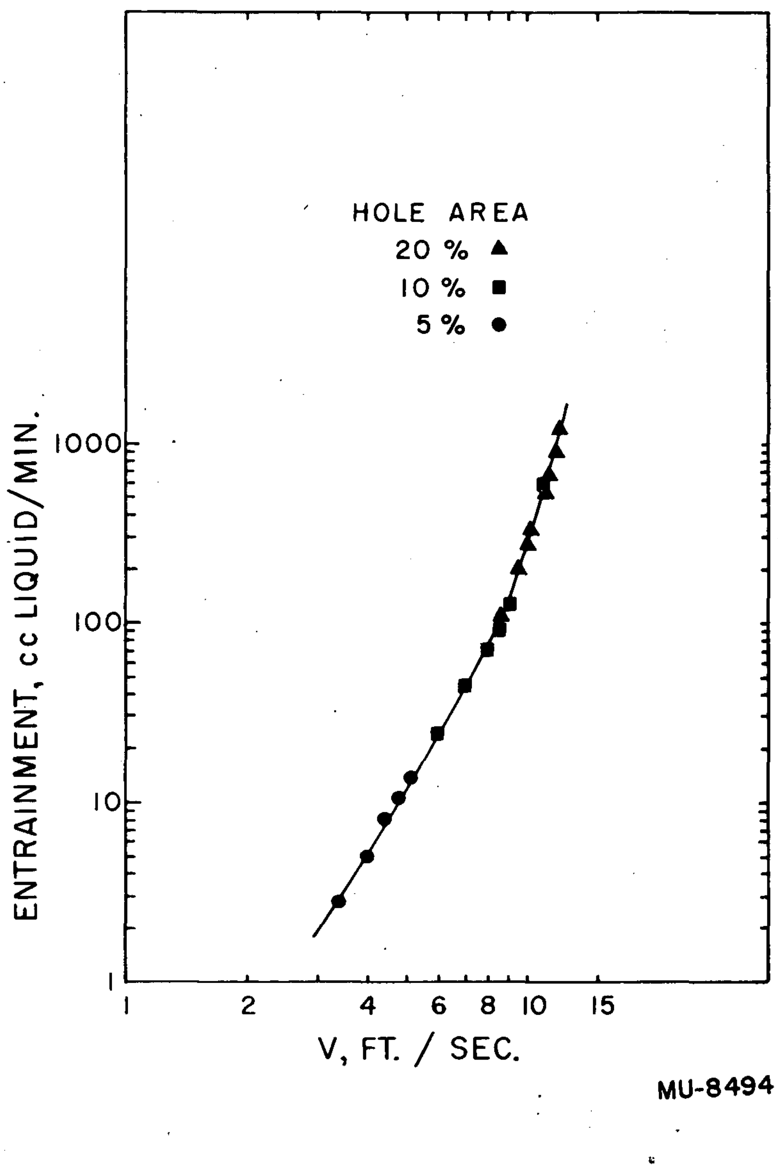

Fig. 13. Entrainment vs Average Velocity of Vapor in Column, Air-H_2O System, 1/4-inch diameter perforations, 1.8-inch liquid head on plate, 20-inch plate spacing.

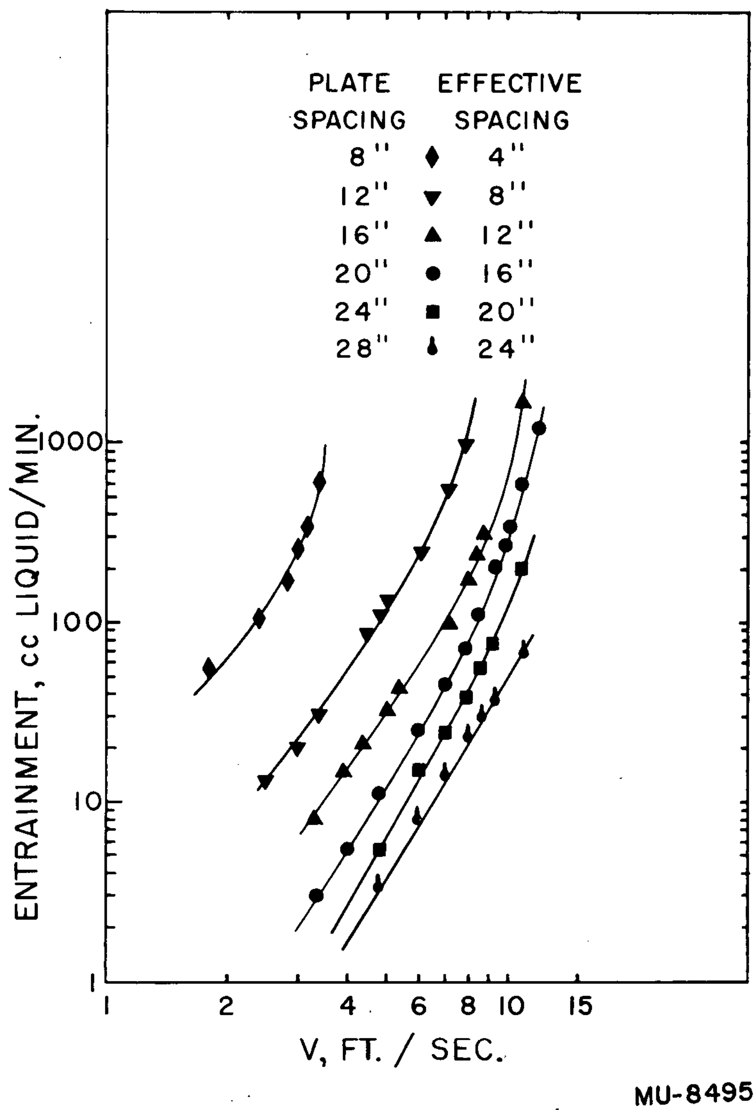

Fig. 14. Air-Water Entrainment Data for Various Plate Spacings (1.8-inch liquid head on plate); entrainment vs column vapor velocity.

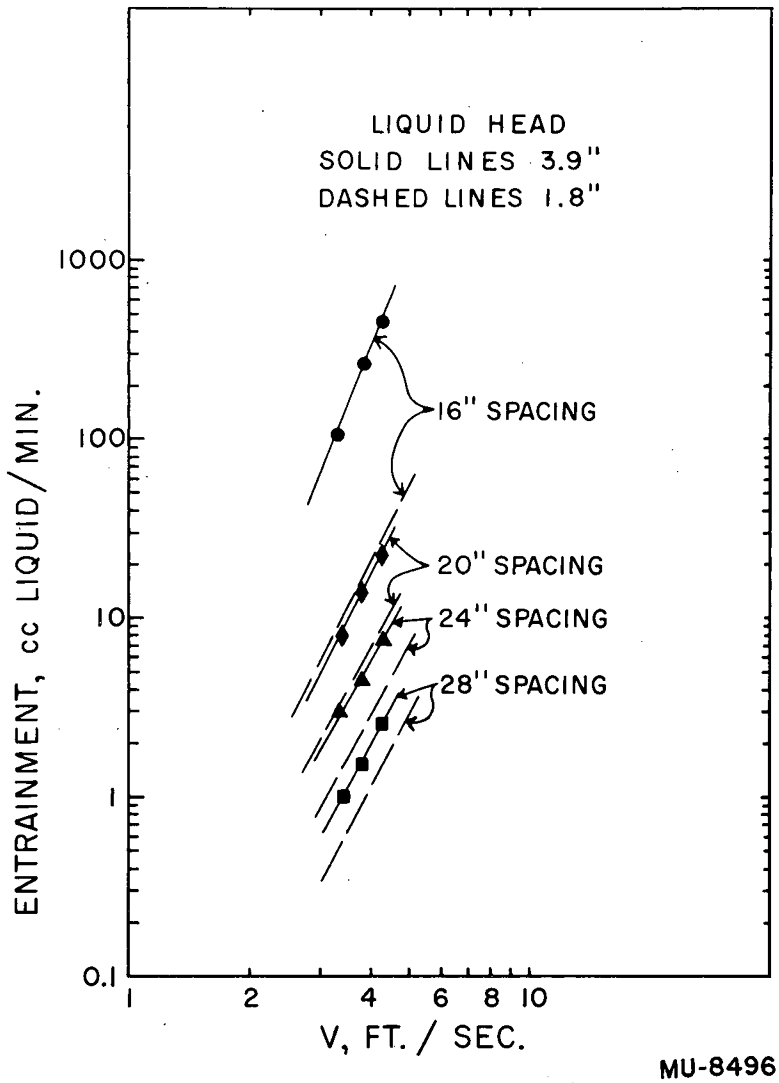

Fig. 14a. Effect of Liquid Level on Entrainment at Various Plate Spacings, Plate III, Air-H_2O System. Entrainment vs Vapor Velocity in column.

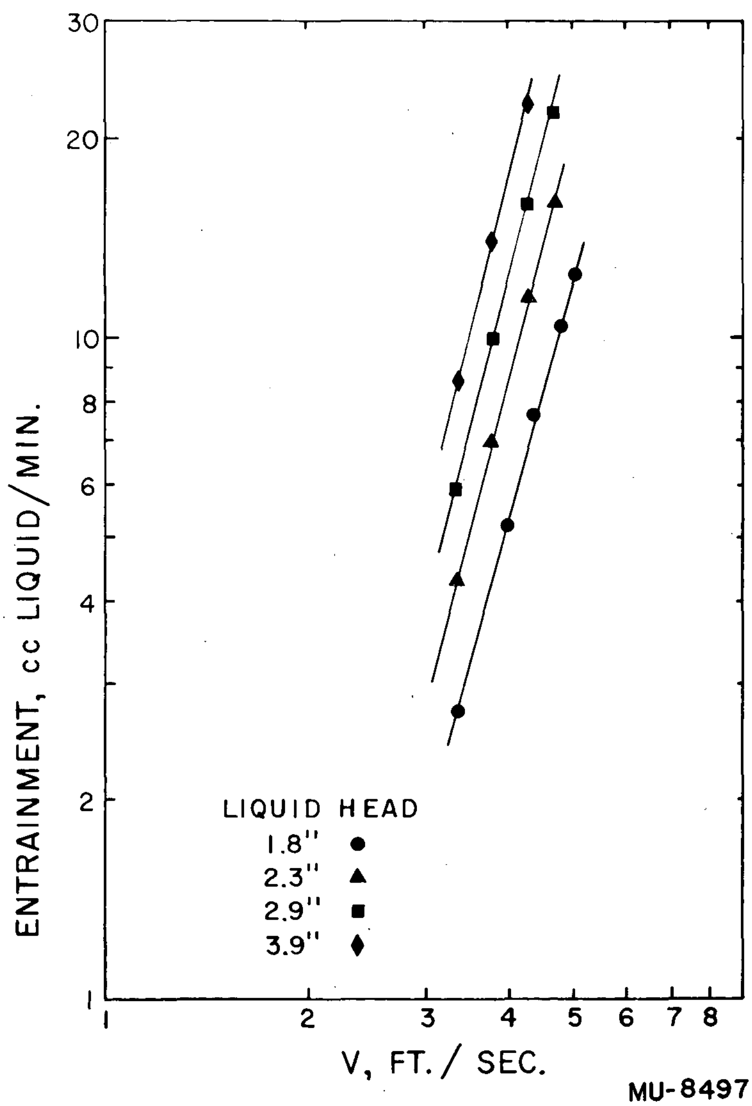

Fig. 14b. Effect of Liquid Level on Entrainment, at about 20-inch plate spacings, Plate III, Air-H_2O System. Entrainment vs Vapor Velocity in Column.

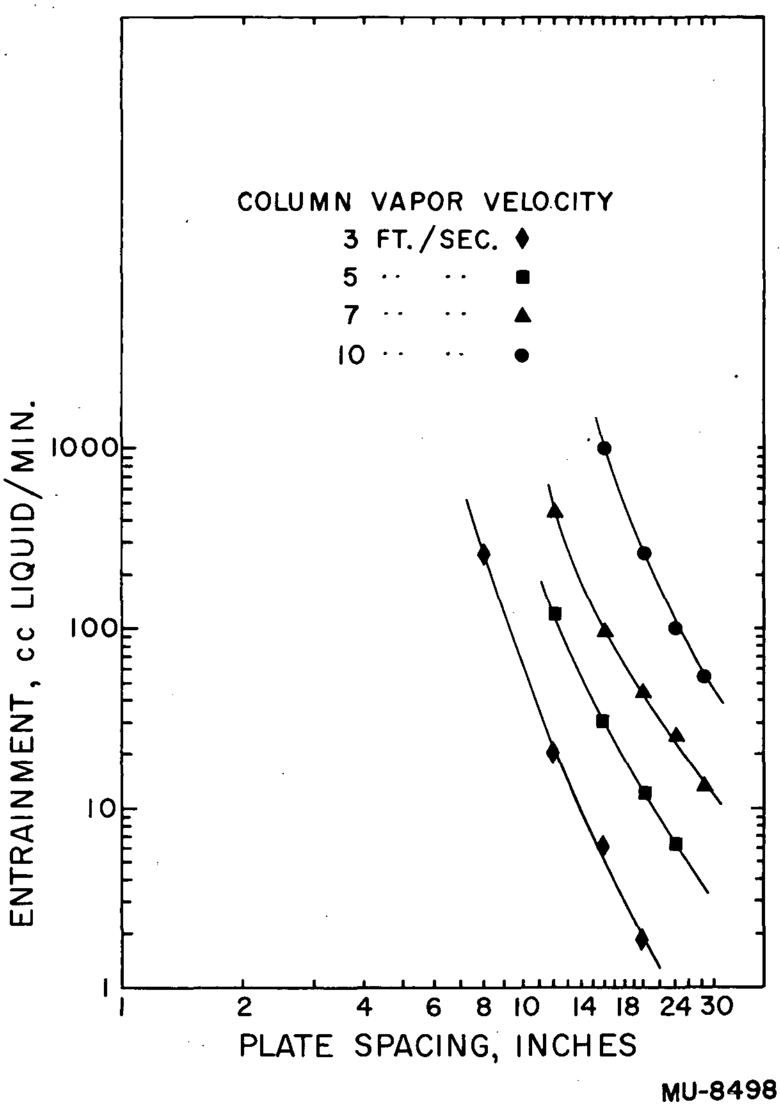

Fig. 15. Effect of Plate Spacing on Entrainment, Plate III, Air-H_2O System, 1.8-inch liquid level, at about various vapor velocities in column. Entrainment vs Plate Spacing.

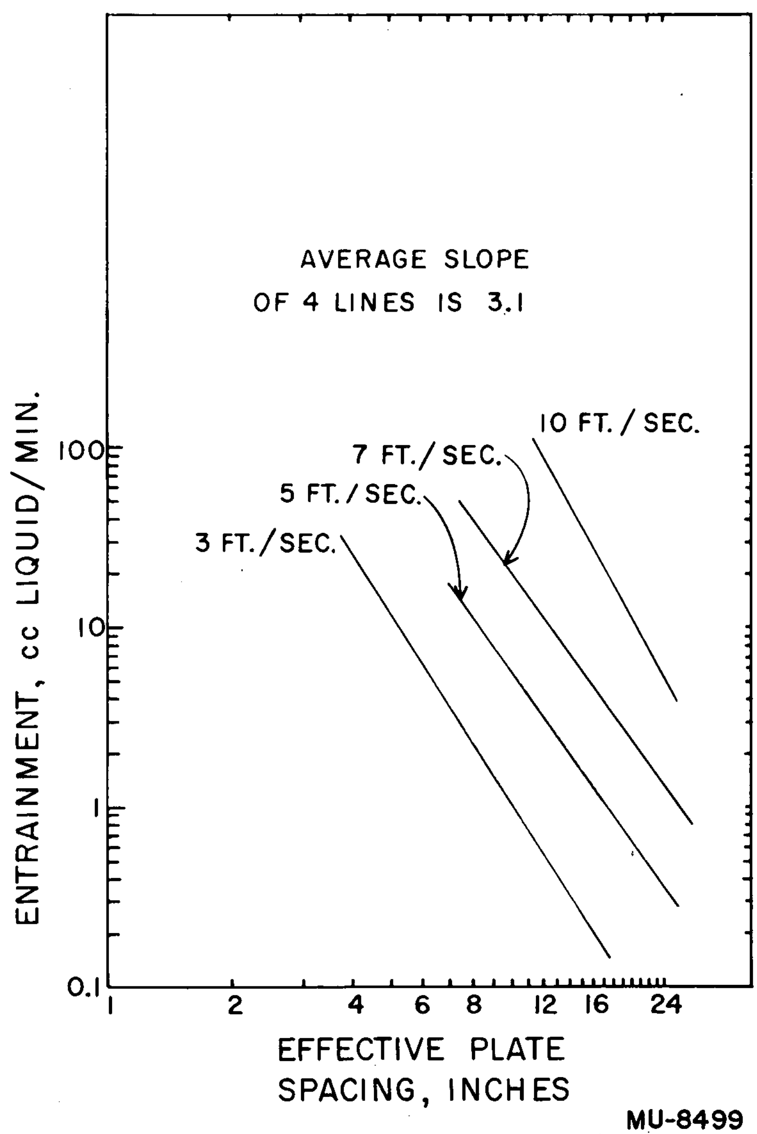

Fig. 15a. Effect of Effective Plate Spacing on Entrainment, 1.8-inch liquid head, Air-H_2O System. Entrainment vs Effective Plate Spacing. (At constant vapor velocity in column)

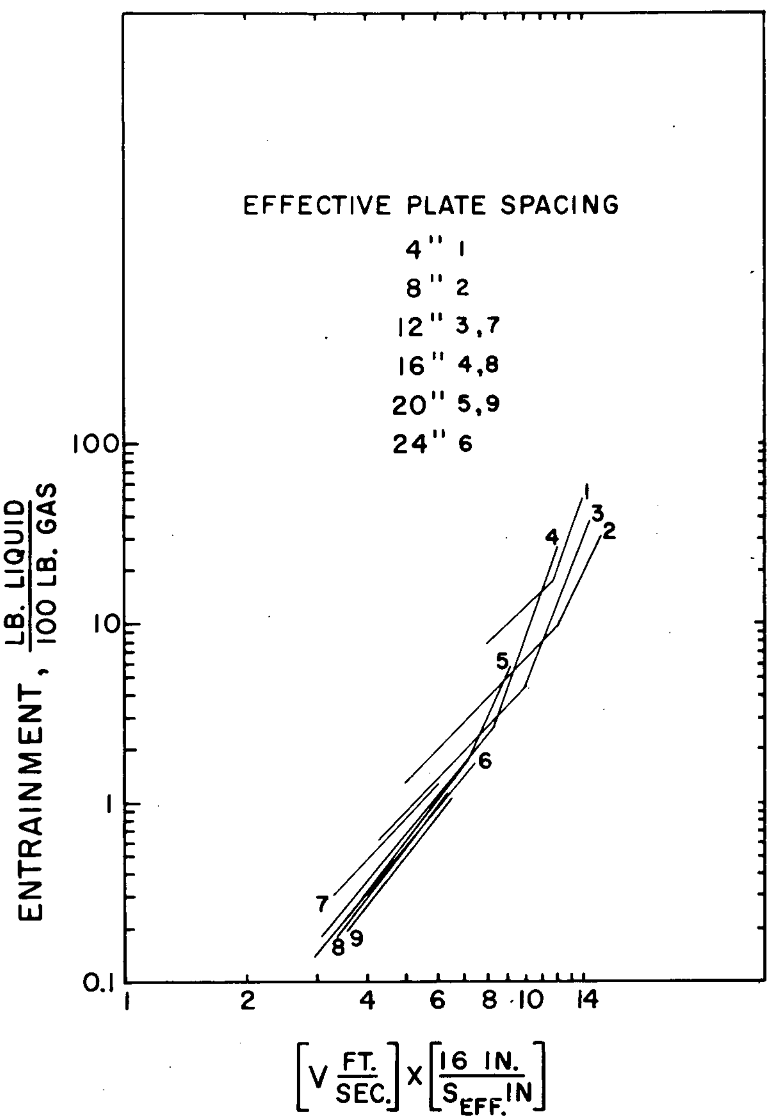

MU-8500

Fig. 15b. Correlation of Entrainment Data for Different Effective Plate Spacings. Entrainment vs Column Vapor Velocity Divided by Relative Effective Spacing.

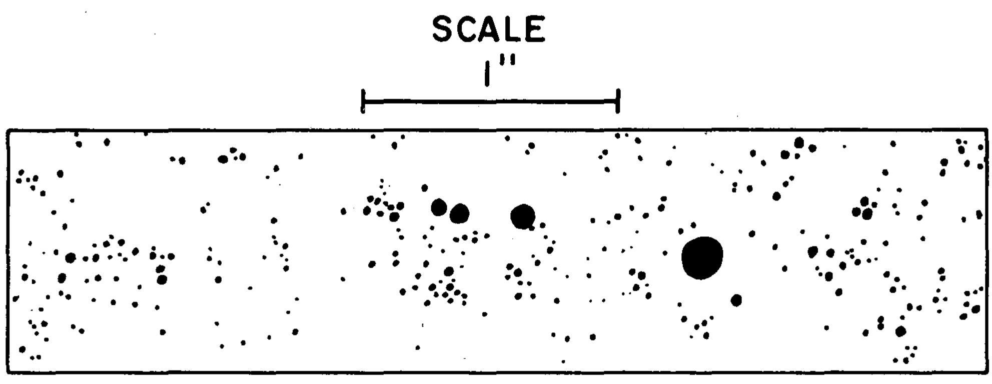

MU-8501

Fig. 16. Tracing of Photograph of Entrained Liquid Drops, Air-H_2O System, Velocity = 11.5 ft/sec; Liquid level = 1.8-inch on plate; Bottom of picture 20 inches above plate, approximately 1/4 of column cross section is included in this picture. Entrainment rate = 20% by weight. Drops less than 1/50-inch diameter do not show up consistently in photograph.

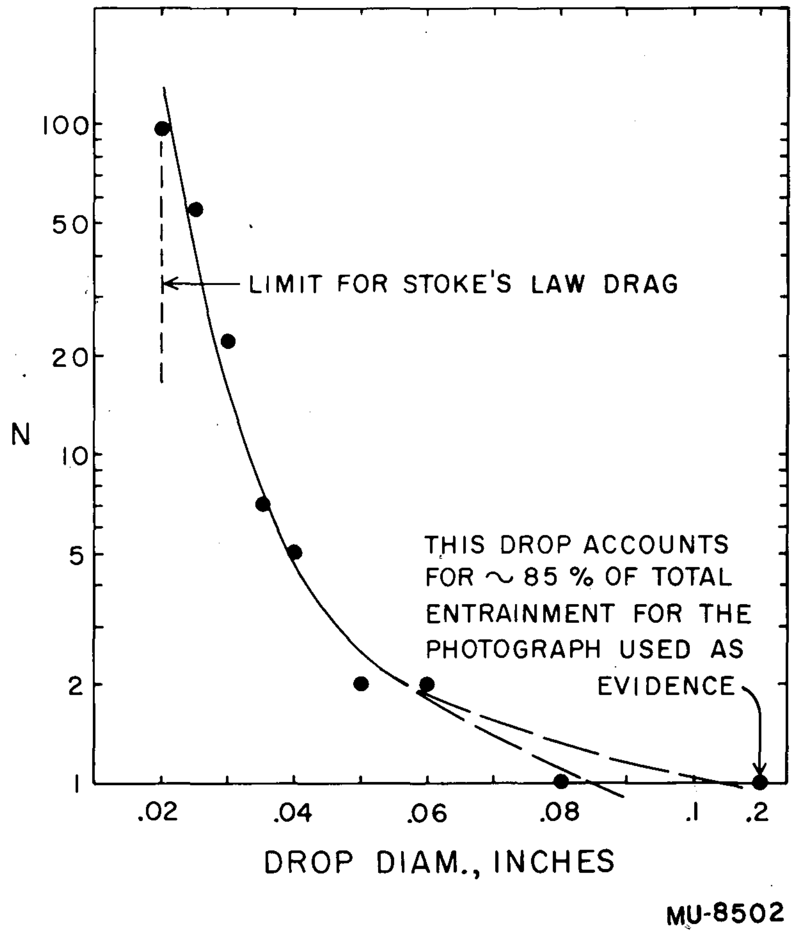

Fig. 17. Drop Size Distribution of Entrained H_2O in Air at about 12 ft/sec col. velocity.

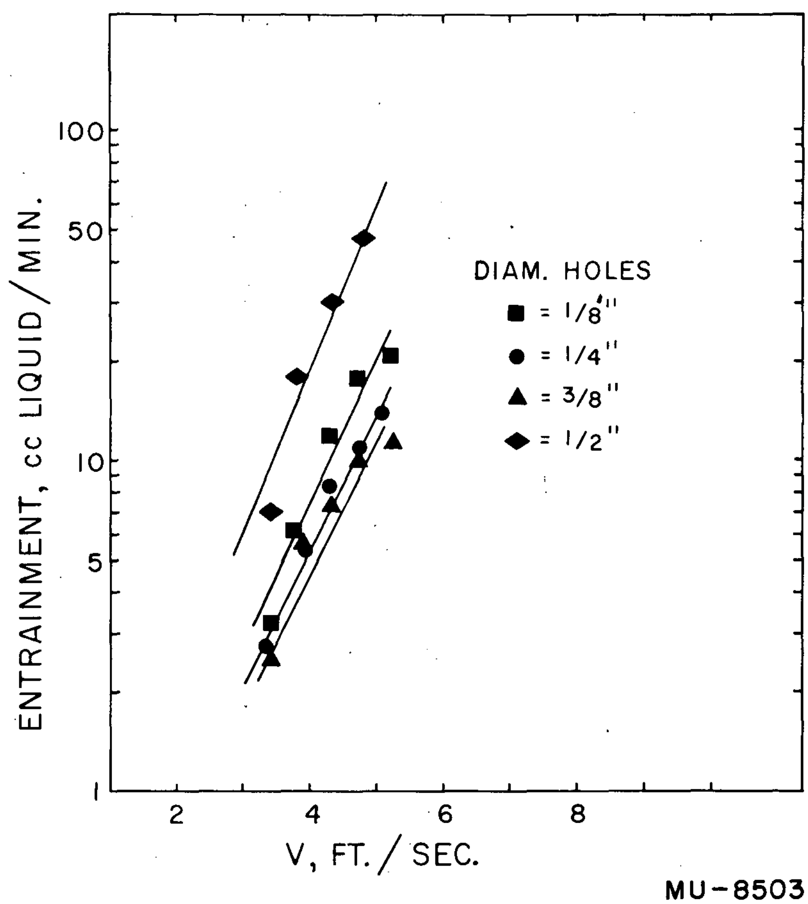

Fig. 18. Effect of Hole Size on Entrainment, Air-H_2O System, Plate III, 1.8-inch liquid on plate, 5% hole area. Entrainment vs. Vapor Velocity in Column.

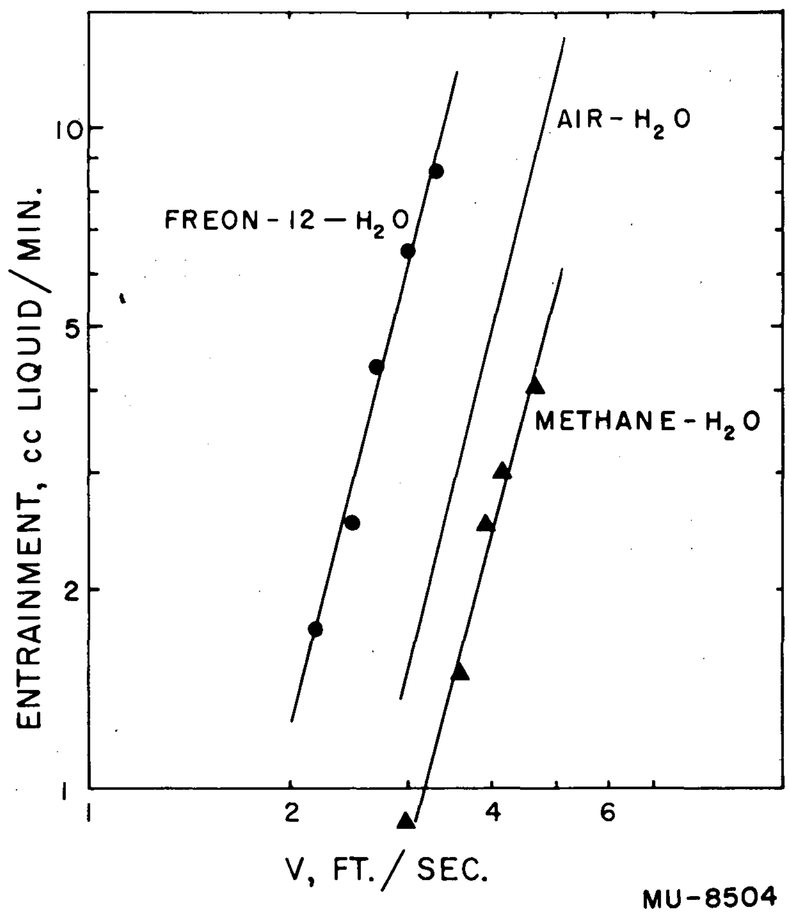

Fig. 19. Effect of Gas Density on Entrainment, Plate III, Air-H_2O System, 1.8-inch liquid level, 20-inch plate spacing. Entrainment vs Vapor Velocity in Column.

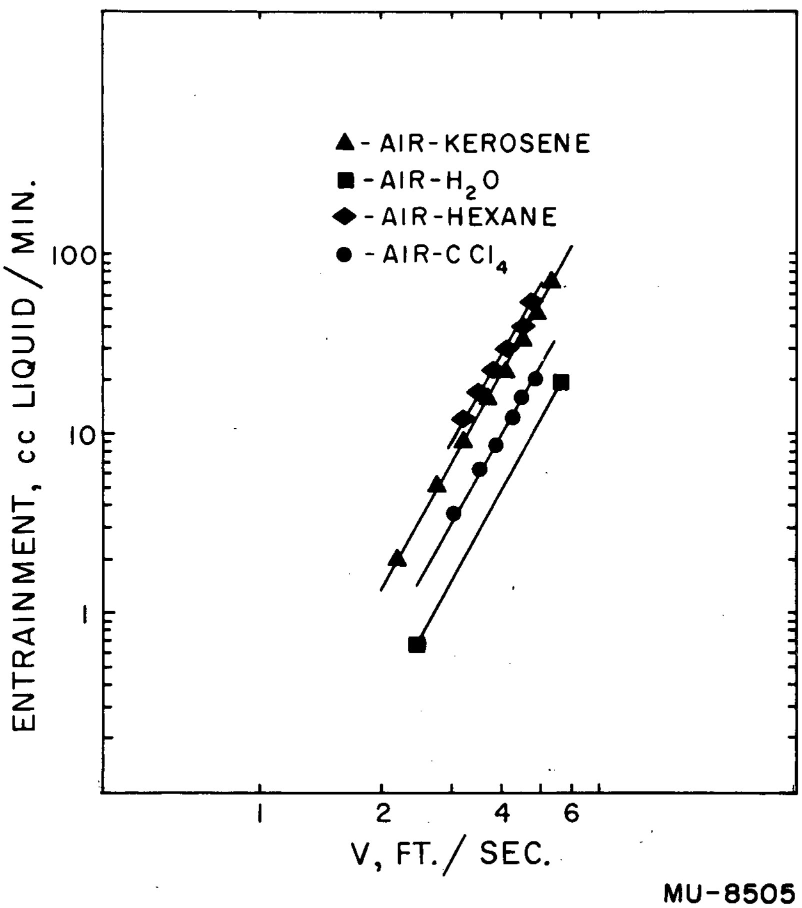

Fig. 20. Effect of Liquid Properties on Entrainment, Plate III, 1.8-inch liquid level, 20-inch plate spacing. Entrainment vs Vapor Velocity in Column.

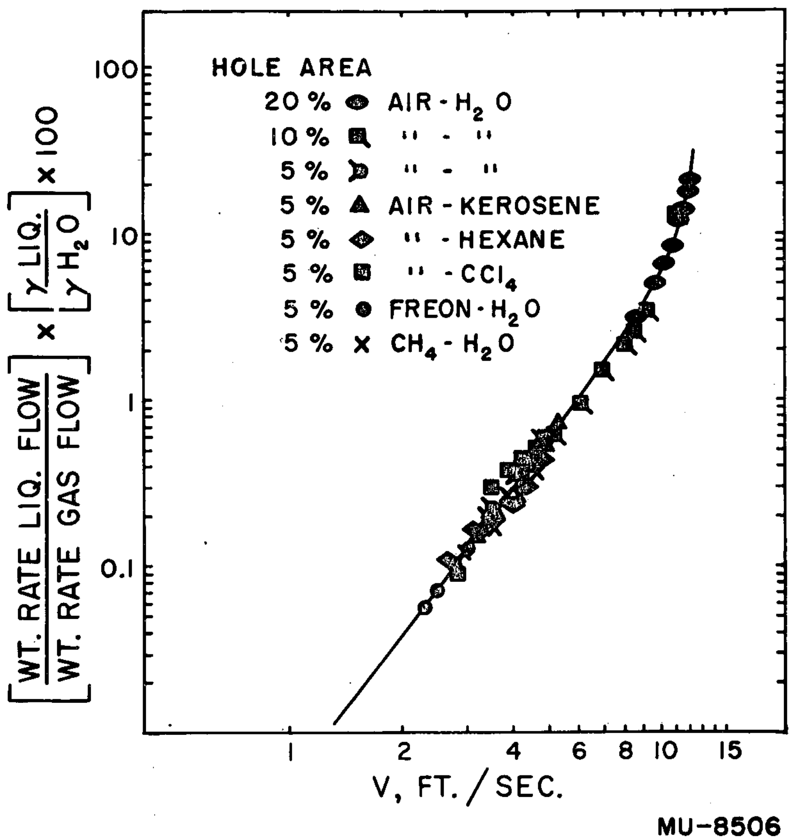

Fig. 21. General Entrainment. Correlation for 1/4-inch holes, with 1.8-inch liquid on plate and 20-inch plate spacing. Entrainment vs Column Vapor Velocity.

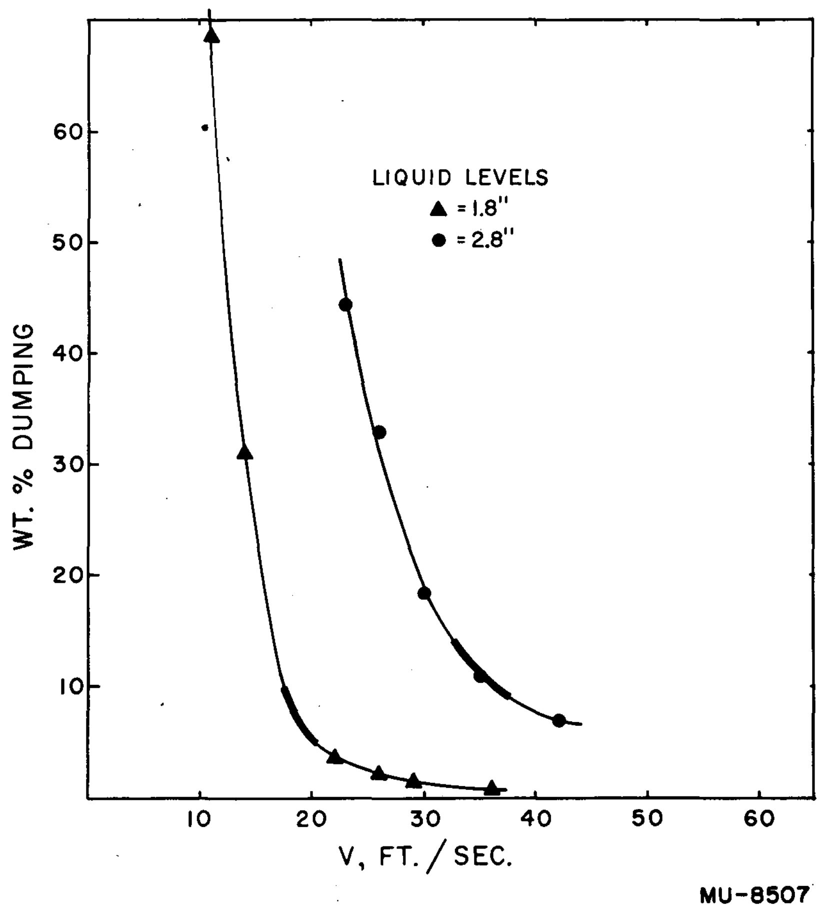

Fig. 22. Wt. % Dumping vs Gas Velocity in Perforations. Air-H_2O. 1/8 x 2 D (Plate I) 20% hole area.

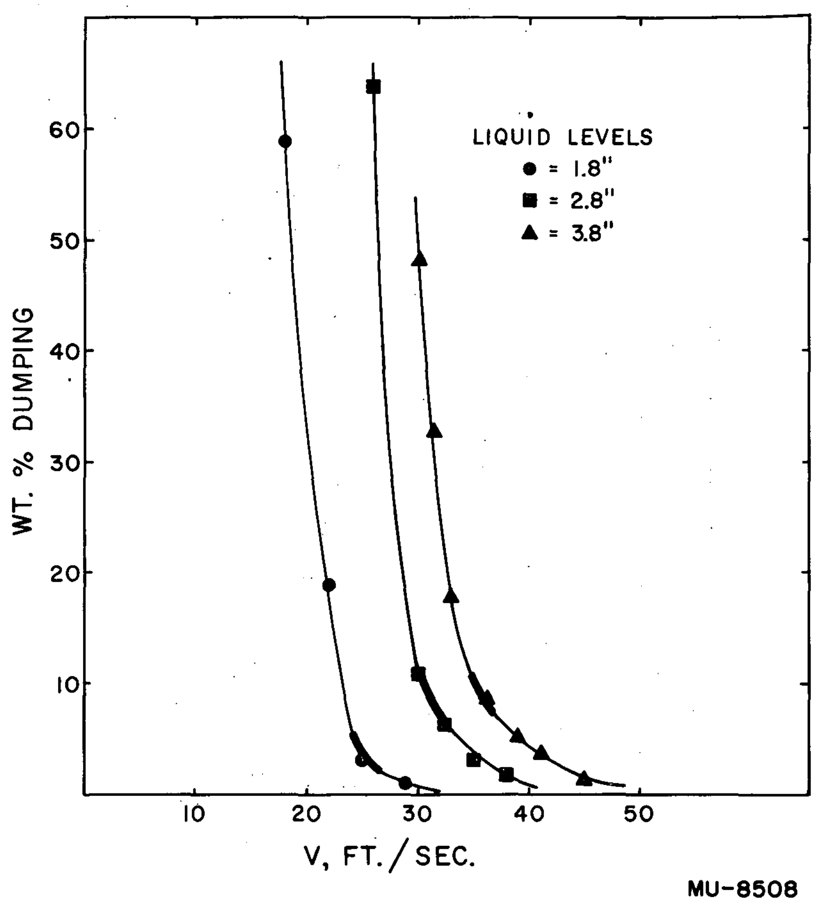

Fig. 23. Wt. % Dumping vs Gas Velocity in Perforations. Air-H_2O. 1/8 x 4 D (Plate II) 5% hole-area.

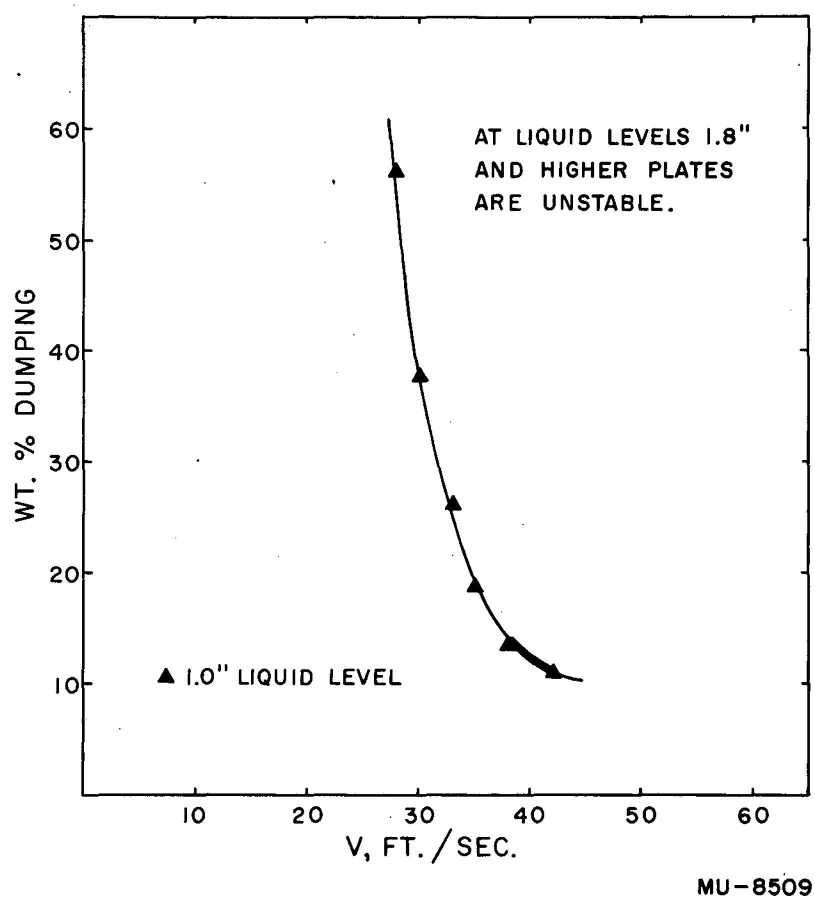

Fig. 24. **Wt. % Dumping Rate** vs Gas Velocity in Perforations. Air-H_2O. 1/4 x 2 D (Plate IV) 20% hole area.

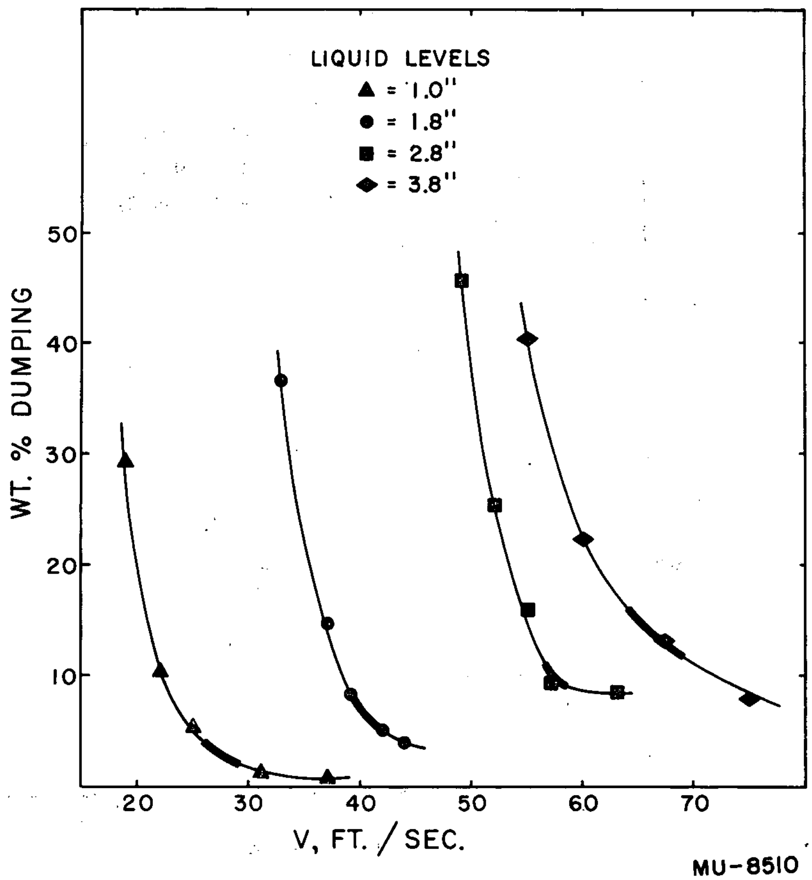

Fig. 25. Wt. % Dumping Rate vs Gas Velocity in Perforations. Air-H_2O. 1/4 x 3 D (Plate VIII) 10% hole area.

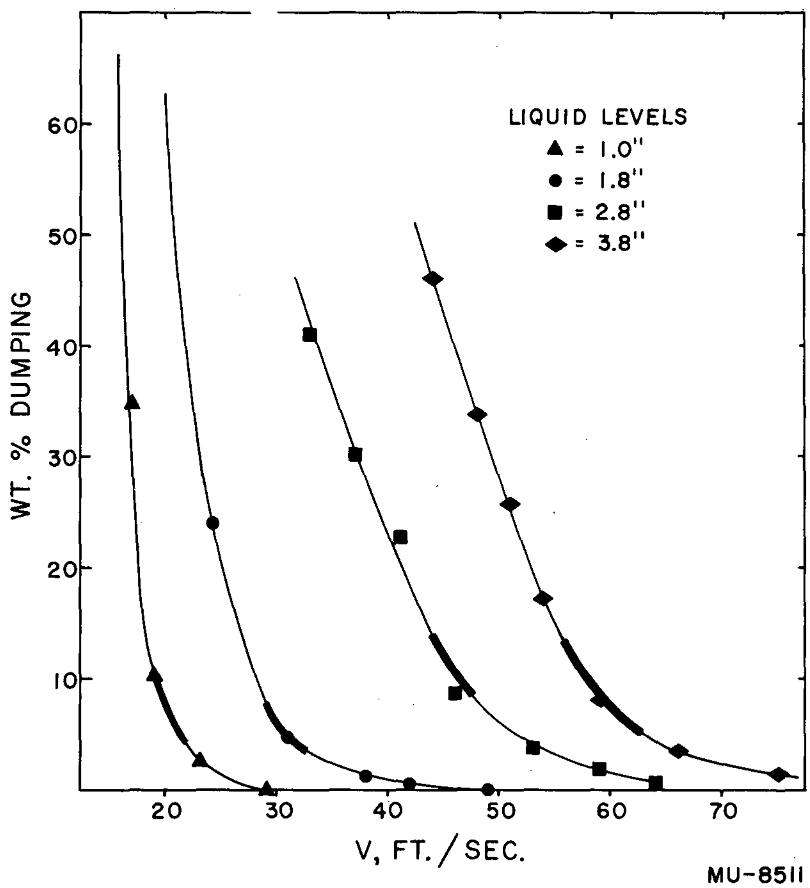

Fig. 26. Wt. % Dumping Rate vs Gas Velocity in Perforations. Air-H_2O. 1/4 x 4D (Plate III) 5% hole area.

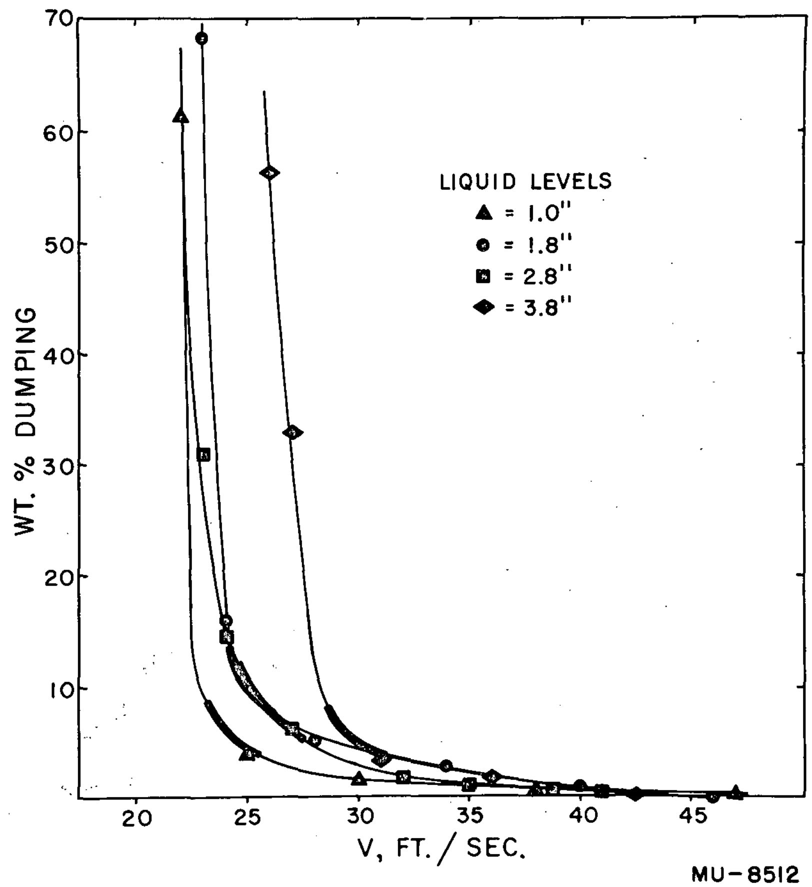

Fig. 27. Wt. % Dumping Rate vs Gas Velocity in Perforations. Air-H_2O. 1/2 x 4 D (Plate V) 5% hole area.

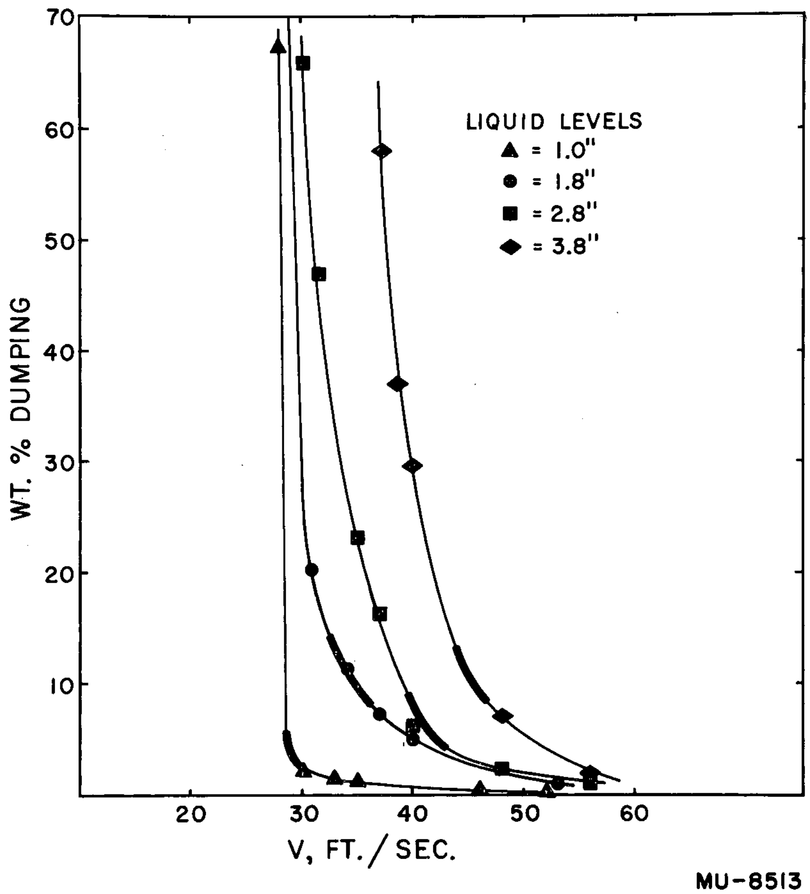

Fig. 28. Wt. % Dumping Rate vs Gas Velocity in Perforations. Air-H_2O. 1/2 x 6 D (Modified Plate V: holes next to column wall) 5% hole area.

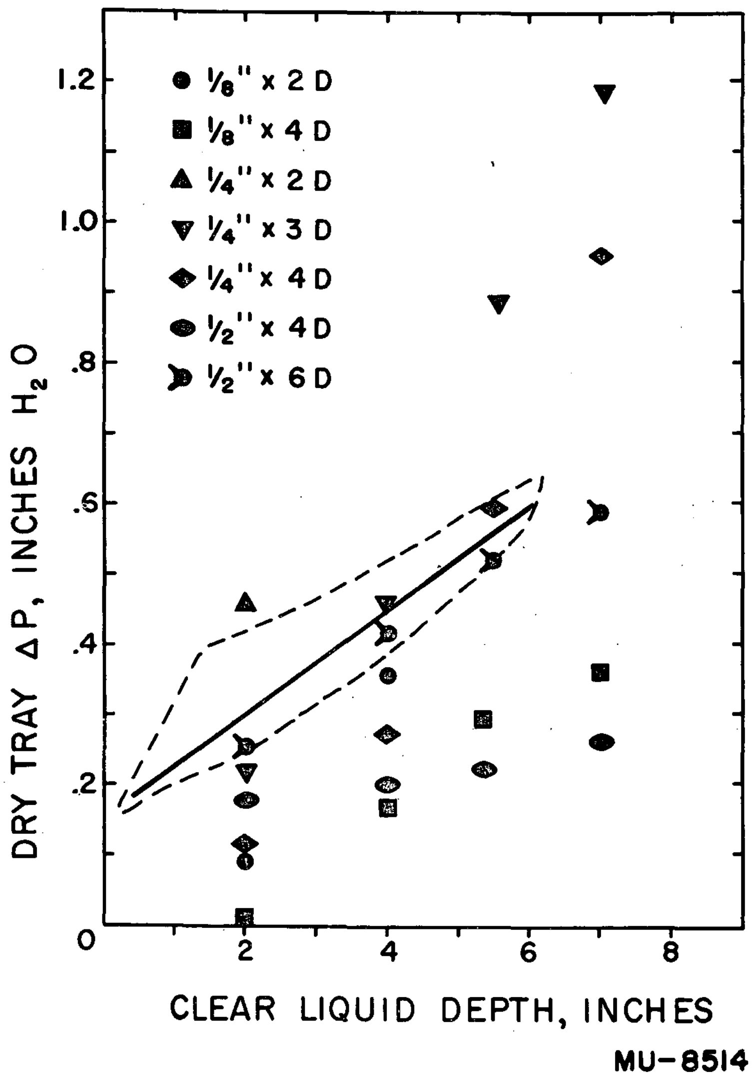

Fig. 29. Comparison of Stability Data to that of Mayfield, et al., I.E.C. 44, 2238 (1952) for "Weep Point" Correlation, 6.5-foot-diameter perfor. tray, air-H_2O System, 3/16-inch diameter holes.
Note: Dotted lines show total scatter of Mayfield's data; Solid line same as Mayfield's recommended line.

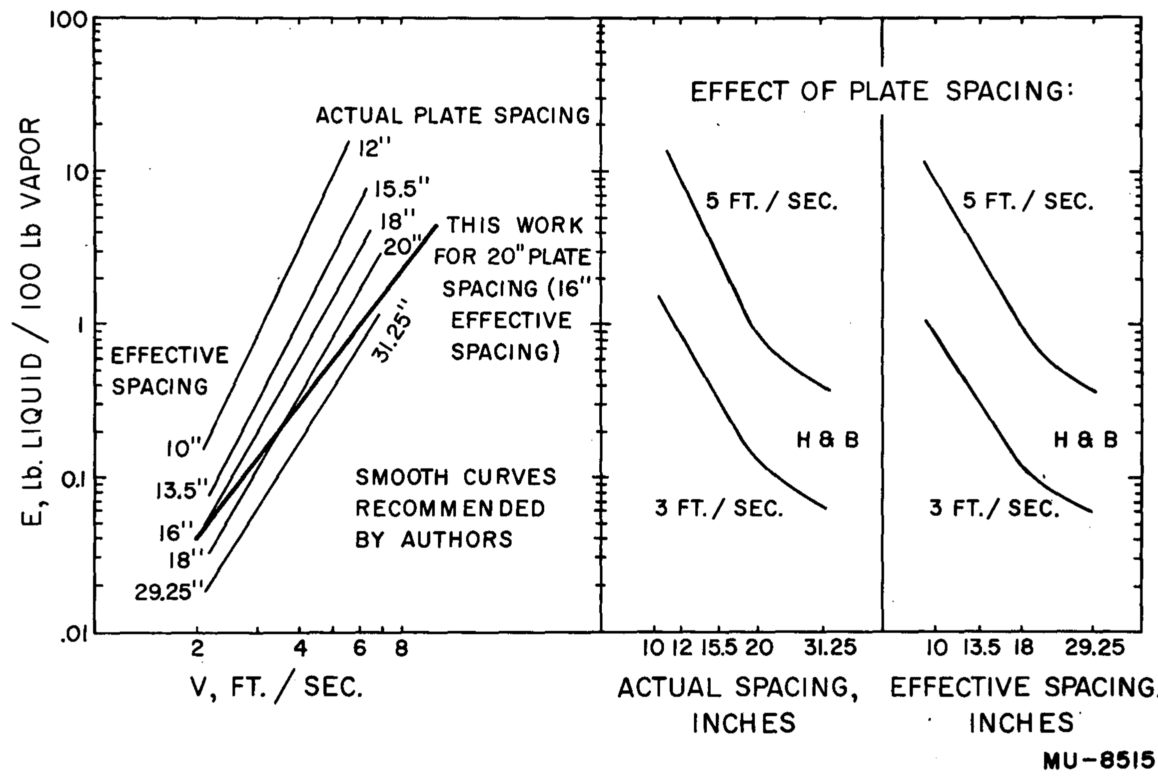

Fig. 30. Holbrook and Baker, IEC 26, 1063 (1934).
Entrainment vs. Column Velocity. Steam-Water.
2-inch Liquid Level.

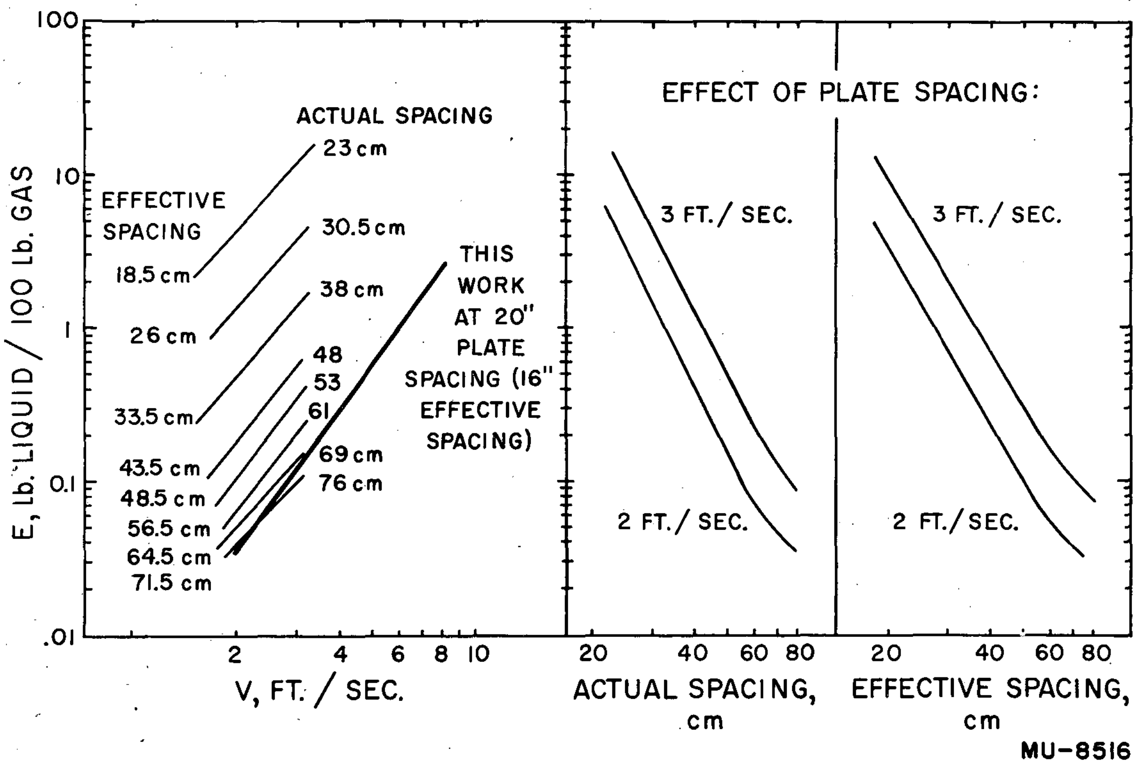

Fig. 31. Sherwood and Jenny, I.E.C. 27, 265 (1935). Entrainment vs Column Velocity. Air-Water. 4.5 cm Liquid Level.

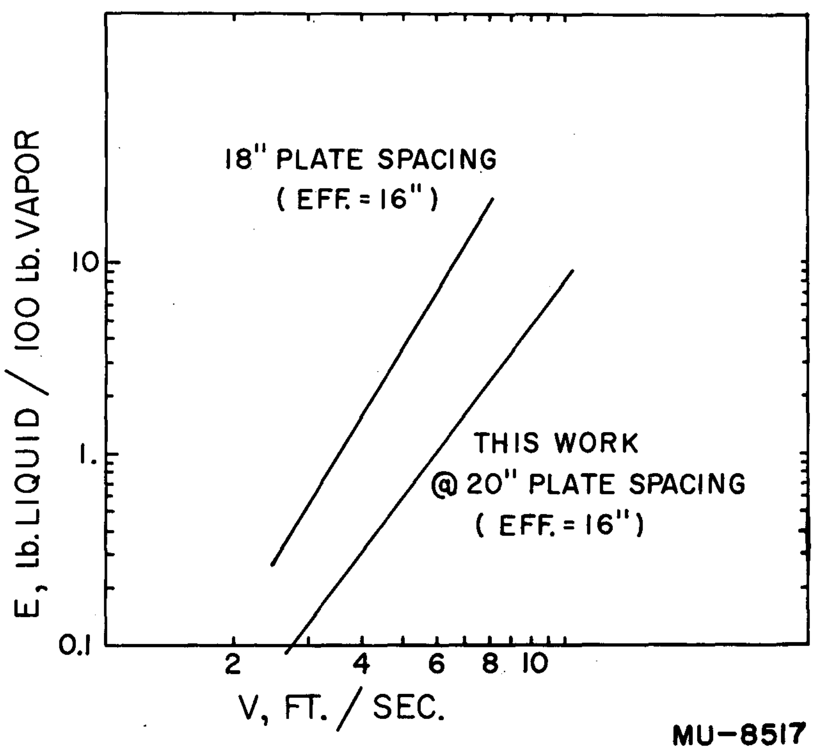

Fig. 32. Peavy and Baker, I.E.C. 29, 1056 (1937). Entrainment vs Column Velocity.

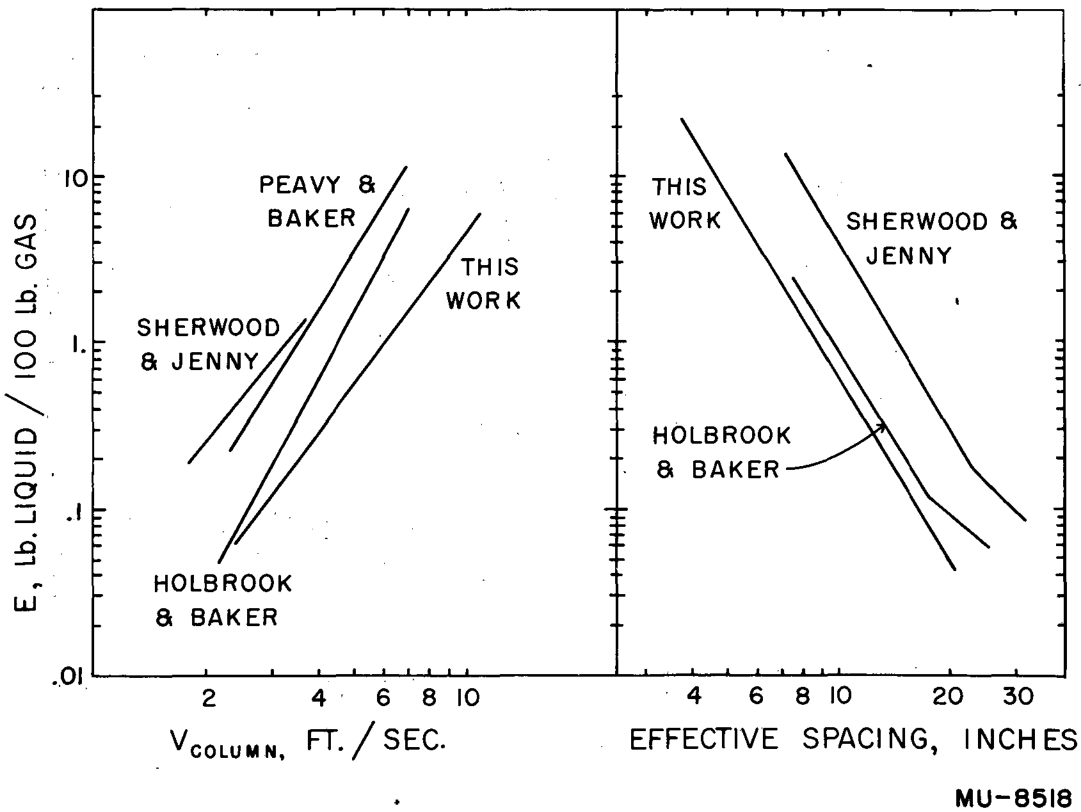

Fig. 33. Comparison of Data on Entrainment. All at 16-inch effective spacing between liquid surface and plate above. References: Holbrook and Baker, Peavy and Baker, Sherwood and Jenny.

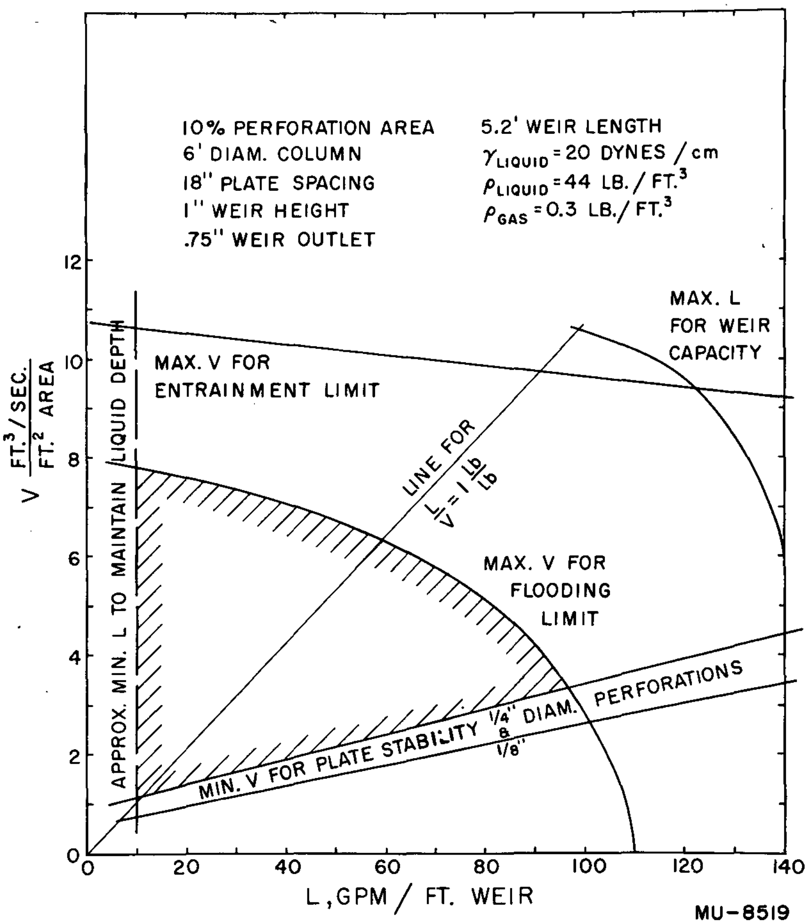

Fig. 34. Perforated Plate Column Operating Limits.

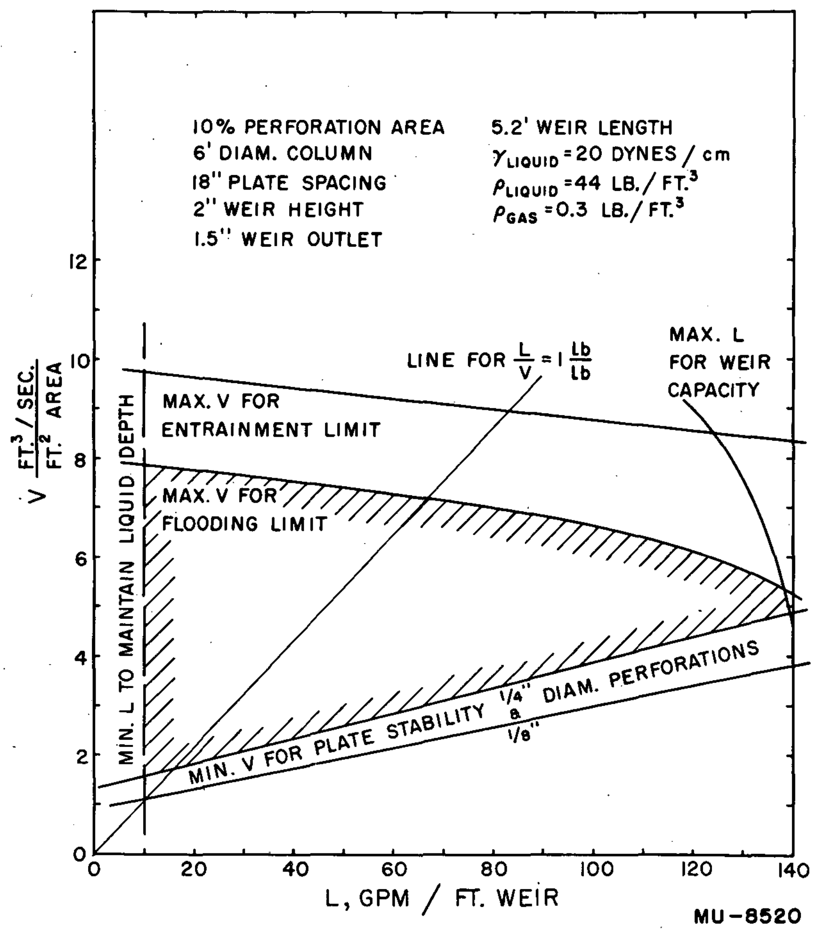

Fig. 35. Perforated Plate Column Operating Limits.

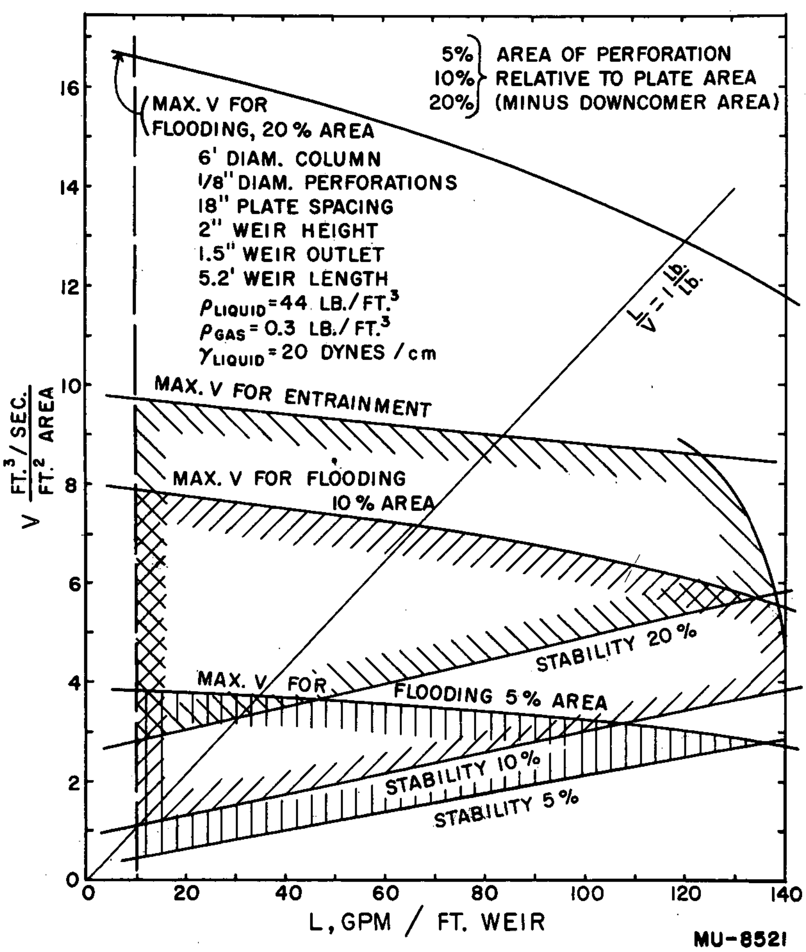

Fig. 36. Perforated Plate Column Operating Limits.

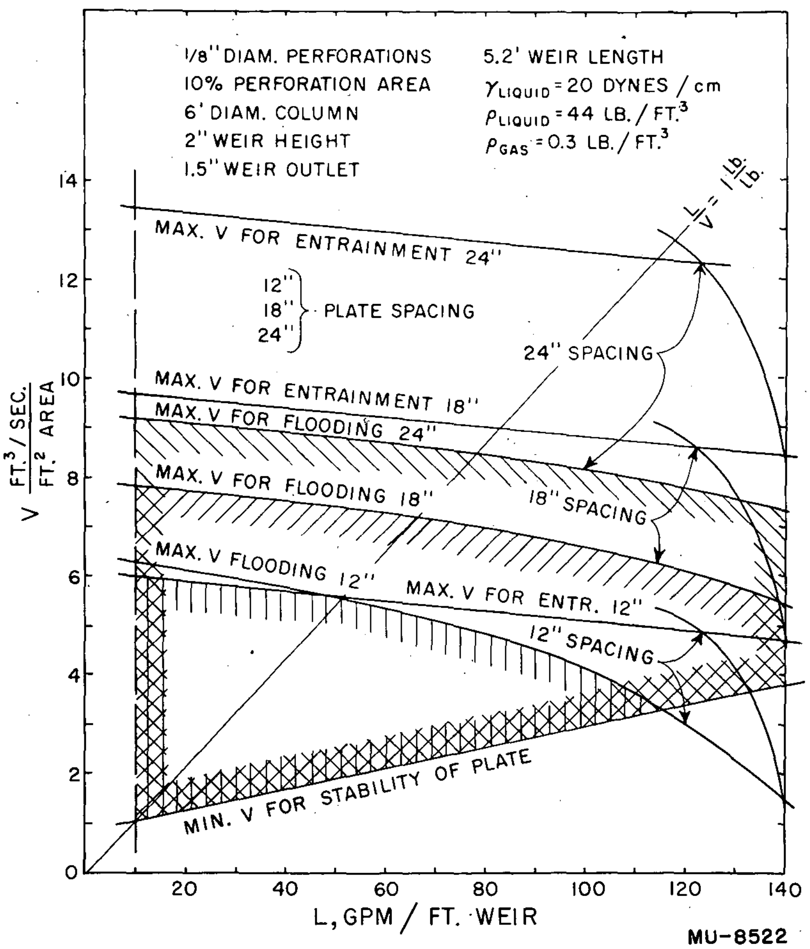

Fig. 37. Perforated Plate Column Operating Limits.

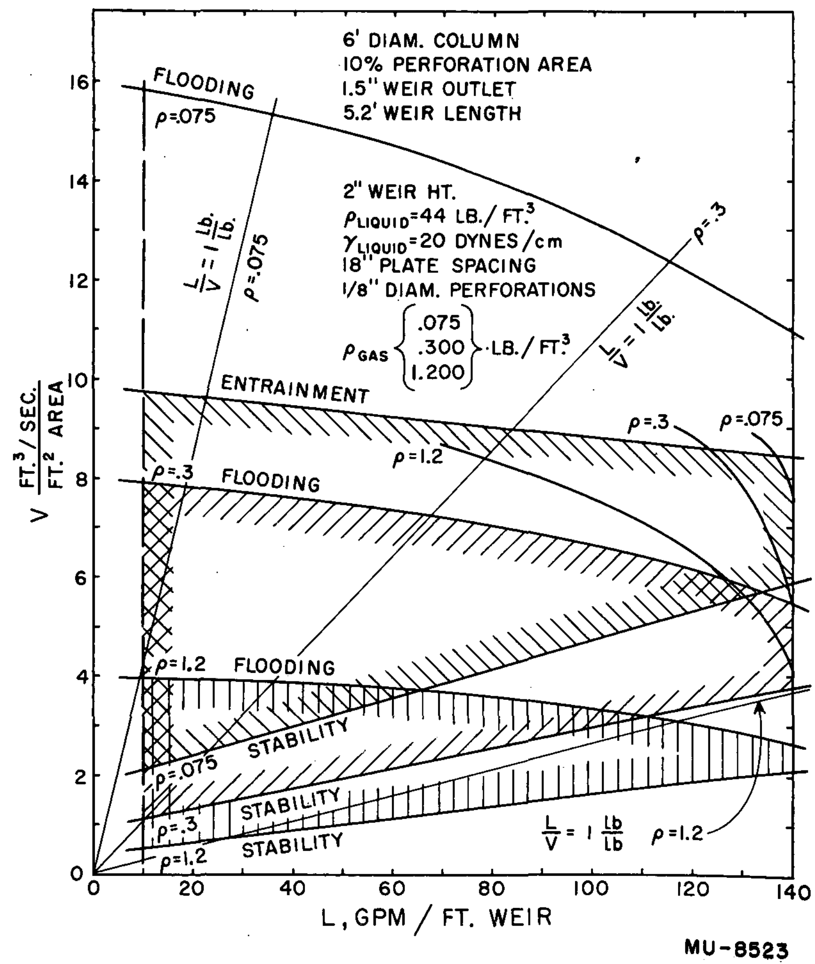

Fig. 38. Perforated Plate Column Operating Limits.

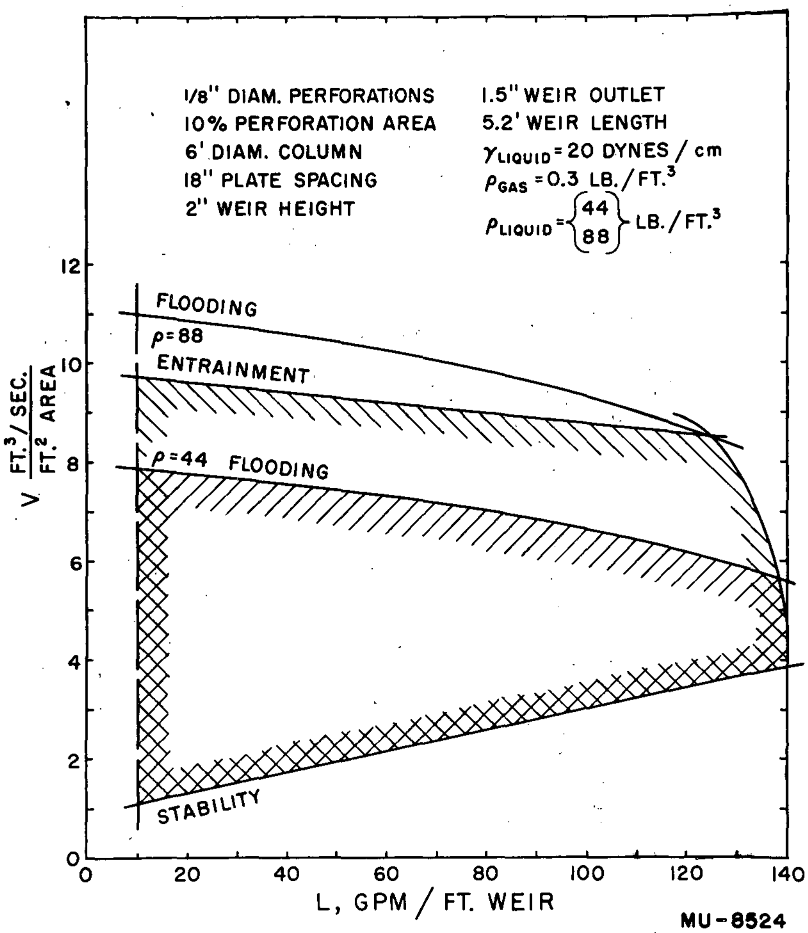

Fig. 39. Perforated Plate Column Operating Limits.

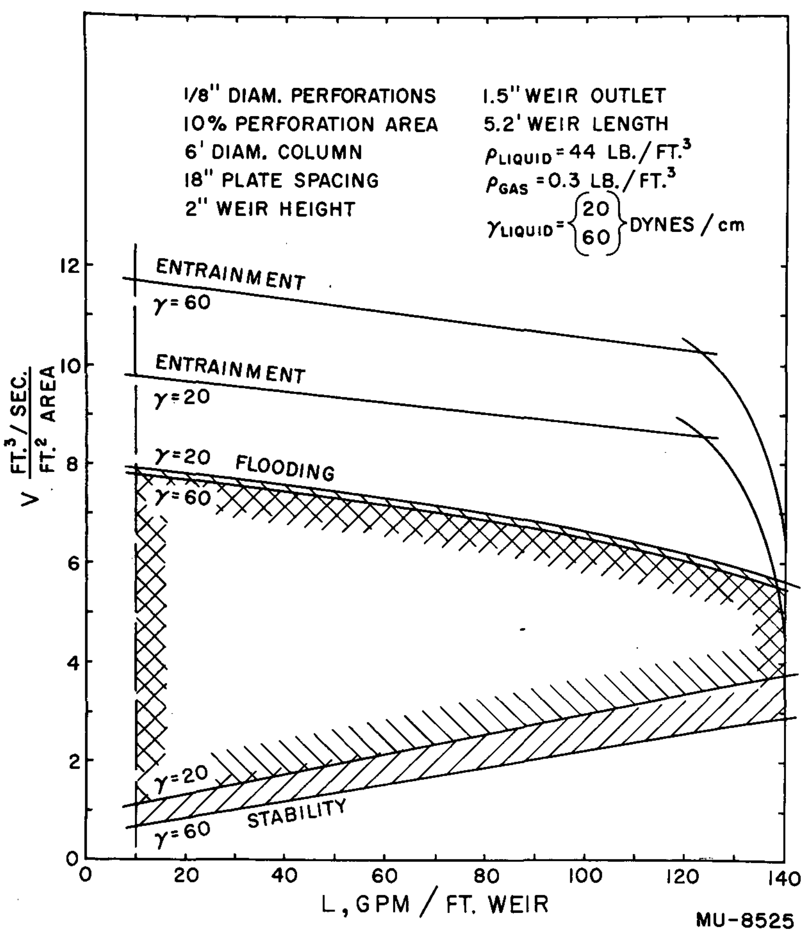

Fig. 40. Perforated Plate Column Operating Limits.

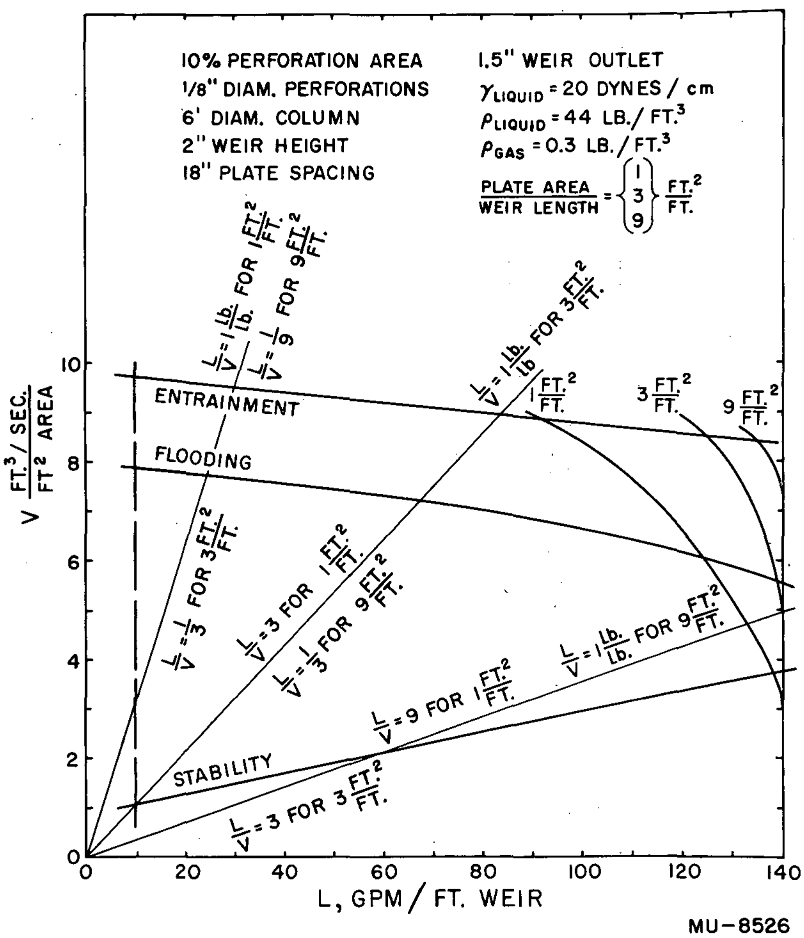

Fig. 41. Perforated Plate Column Operating Limits.

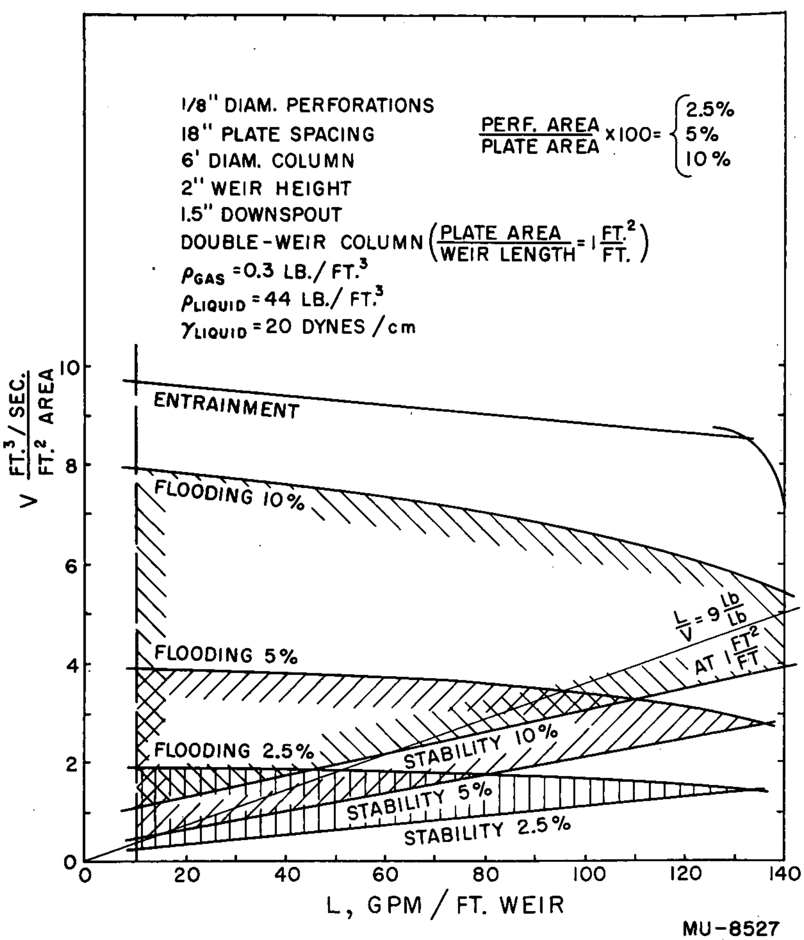

Fig. 42. Perforated Plate Column Operating Limits.

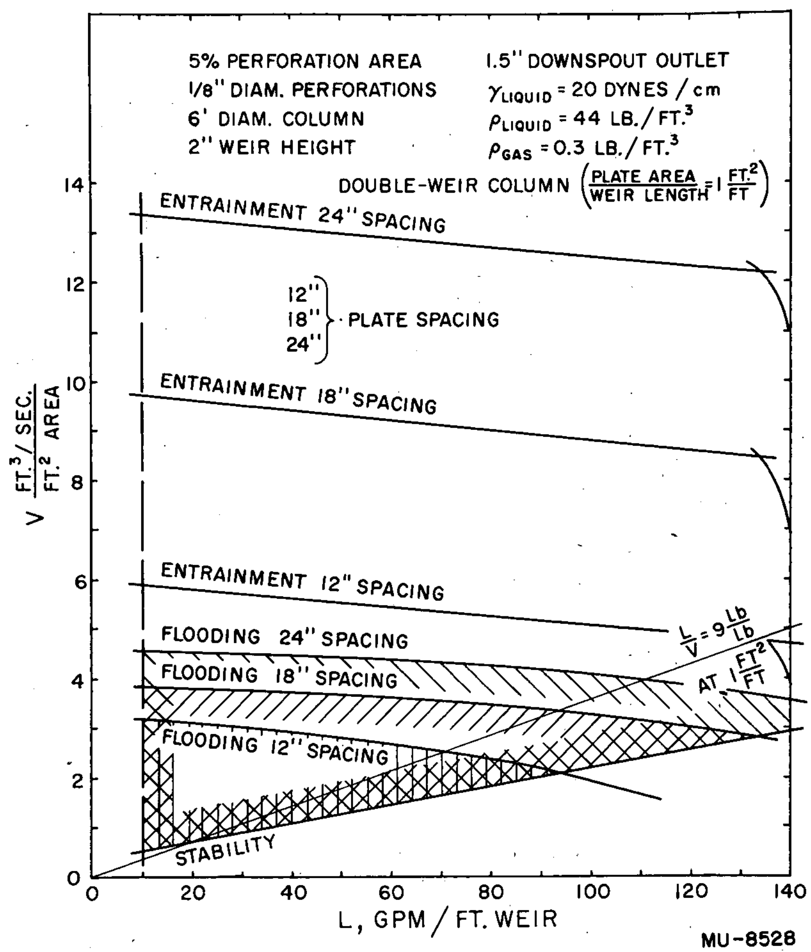

Fig. 43. Perforated Plate Column Operating Limits.

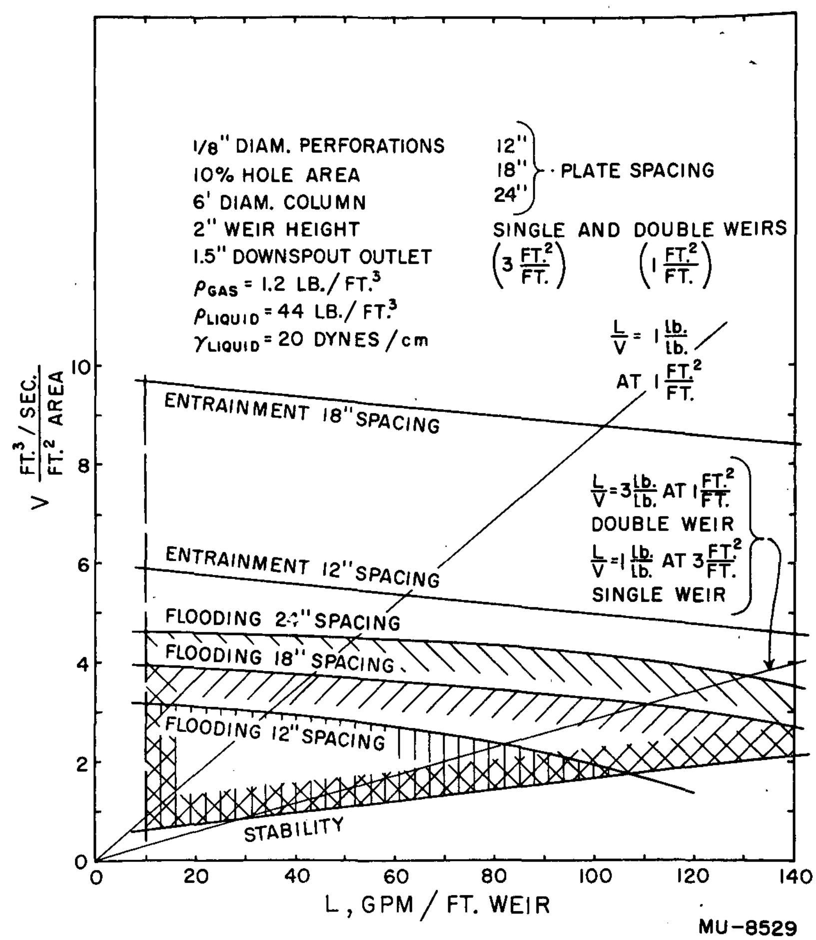

Fig. 44. Perforated Plate Column Operating Limits.

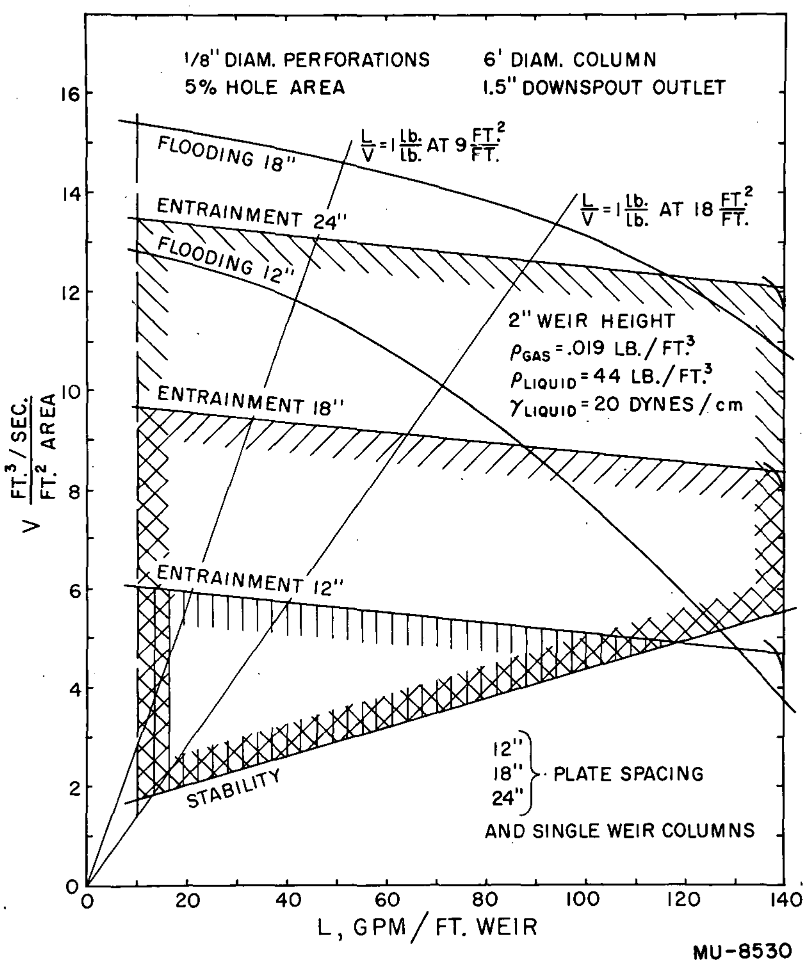

Fig. 45. Perforated Plate Column Operating Limits.

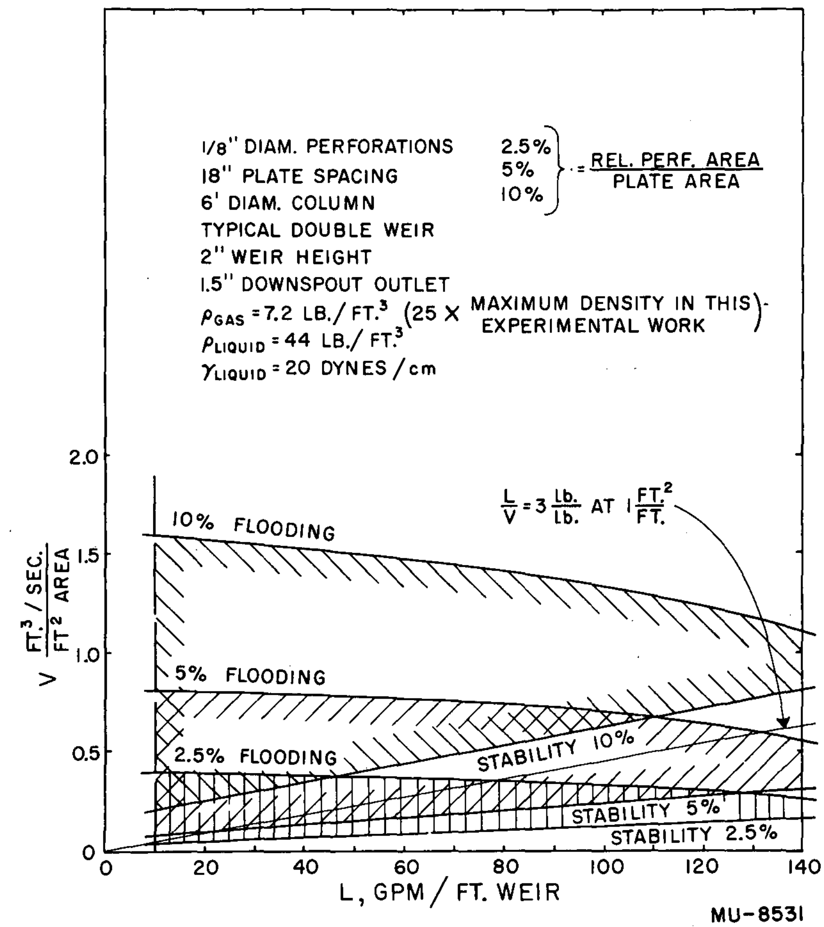

Fig. 46. Perforated Plate Column Operating Limits.

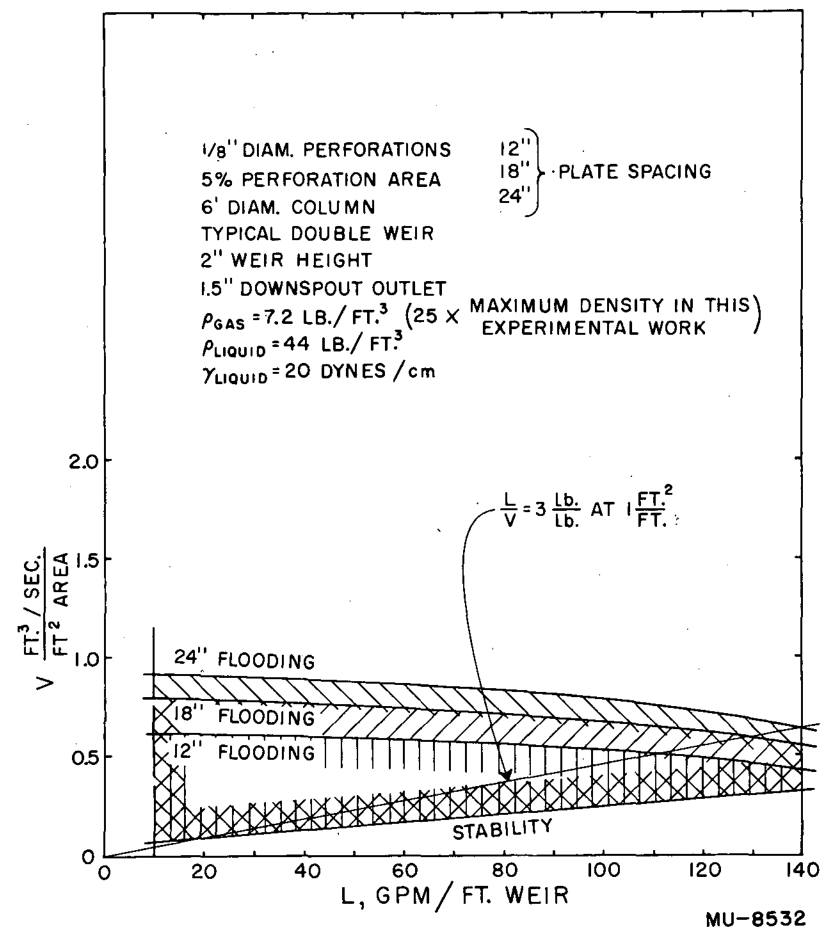

Fig. 47. Perforated Plate Column Operating Limits.

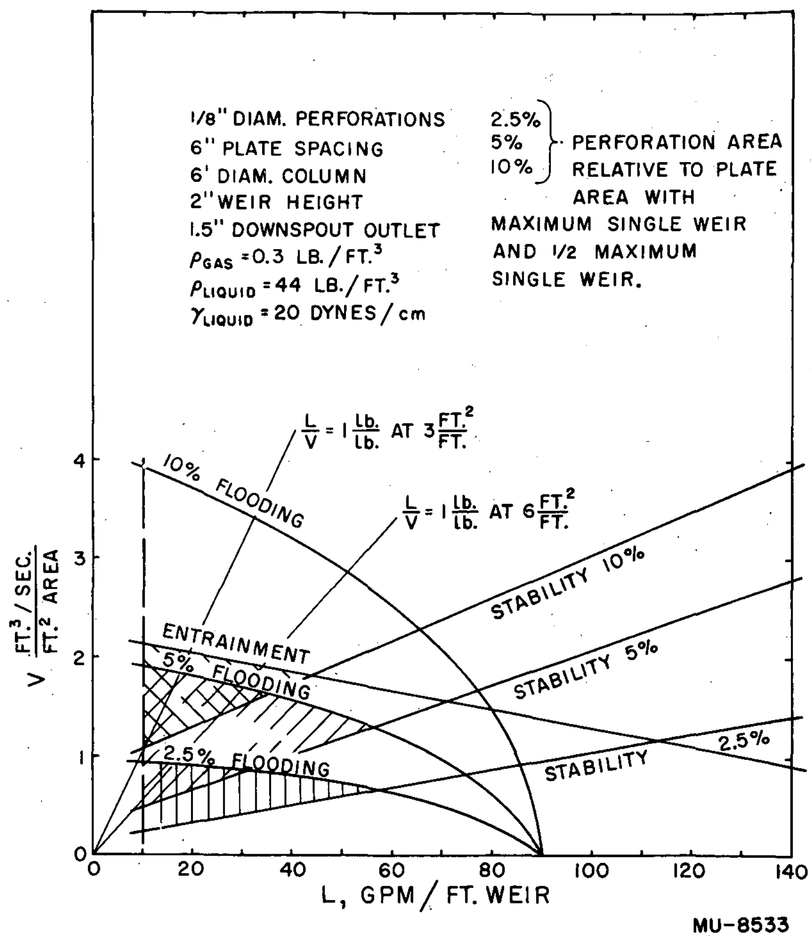

Fig. 48. Perforated Plate Column Operating Limits.

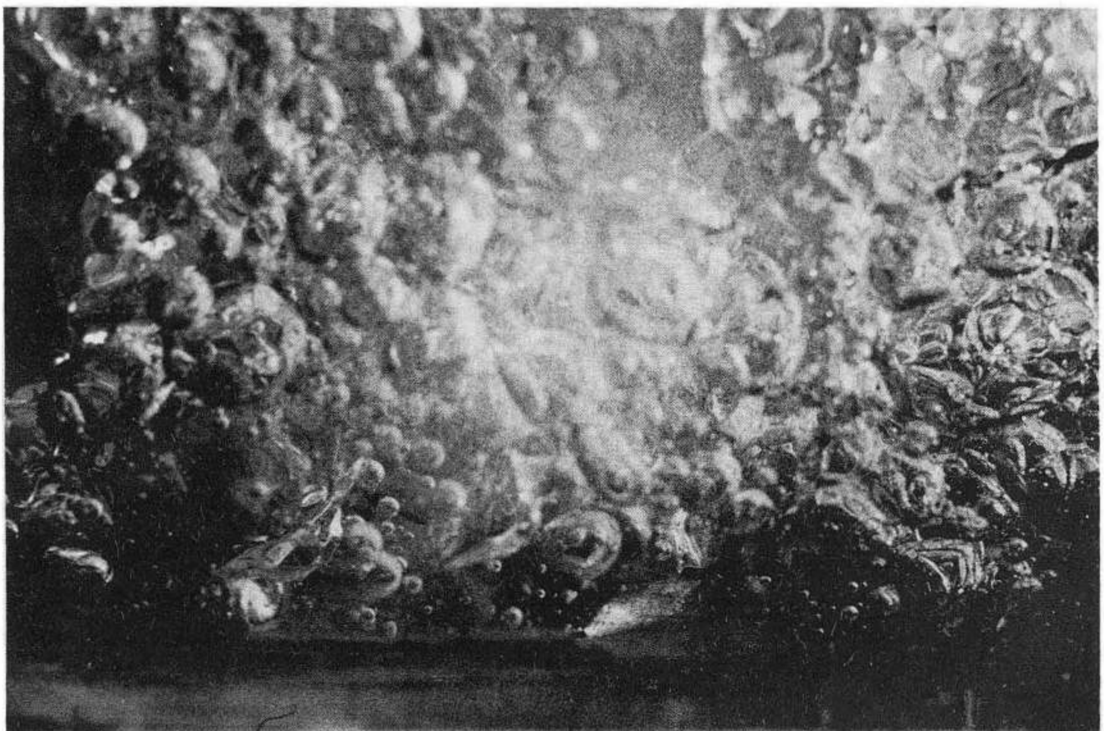

Fig. 49. 1/4-inch diameter perforations, 1/2-inch spacings, Air-Water System, Air velocity 50 ft/sec (3-1/2 x Magn.)

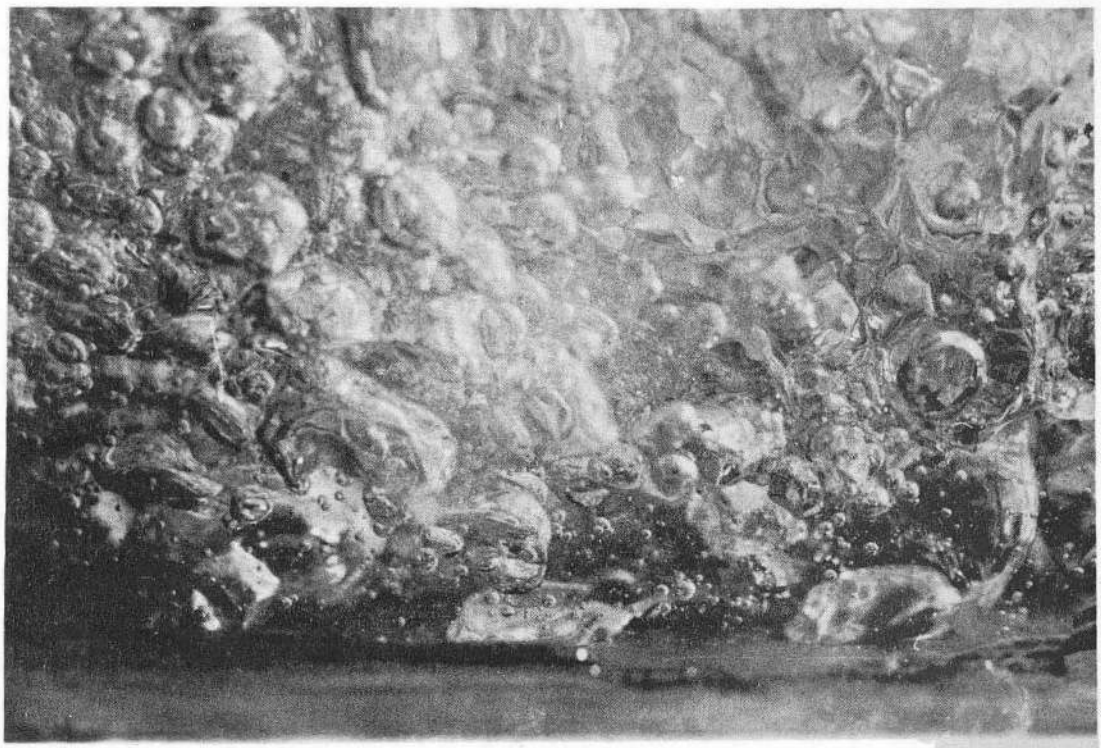

ZN-1048

Fig. 50. 1/4-inch diameter perforations, 1/2-inch spacings, Air-water system, air velocity 50 ft/sec (3-1/2 x Magn.)

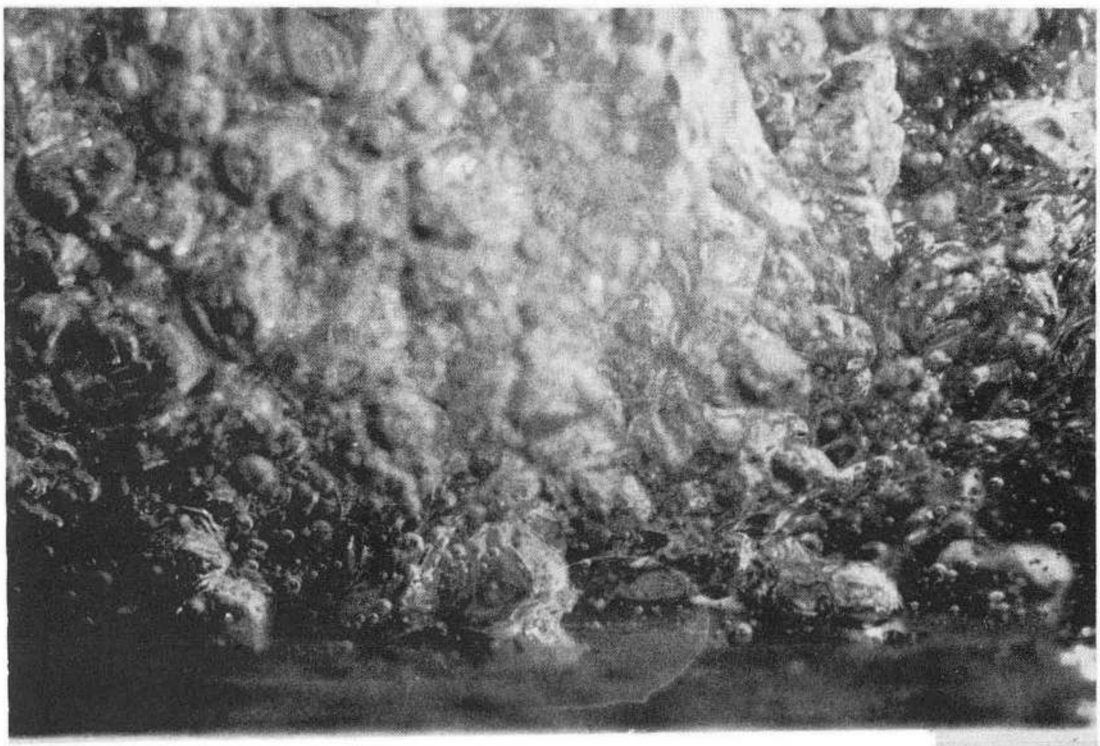

ZN-1049

Fig. 51. 1/8-inch diameter perforations, 1/2-inch spacings, Air-water system, air velocity 40 ft/sec. (3-1/2 x magn.)

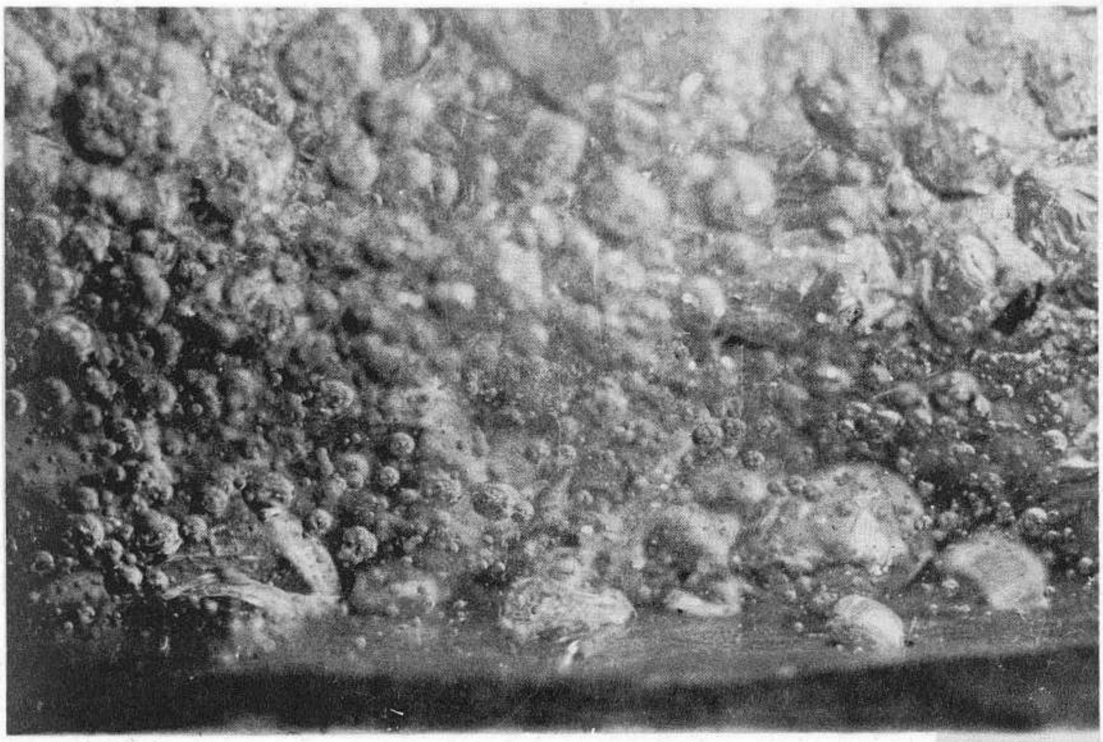

ZN-1050

Fig. 52. 1/8-inch diameter perforations, 1/2-inch spacings, air-water system, air velocity 40 ft/sec. (3-1/2 x magn.)

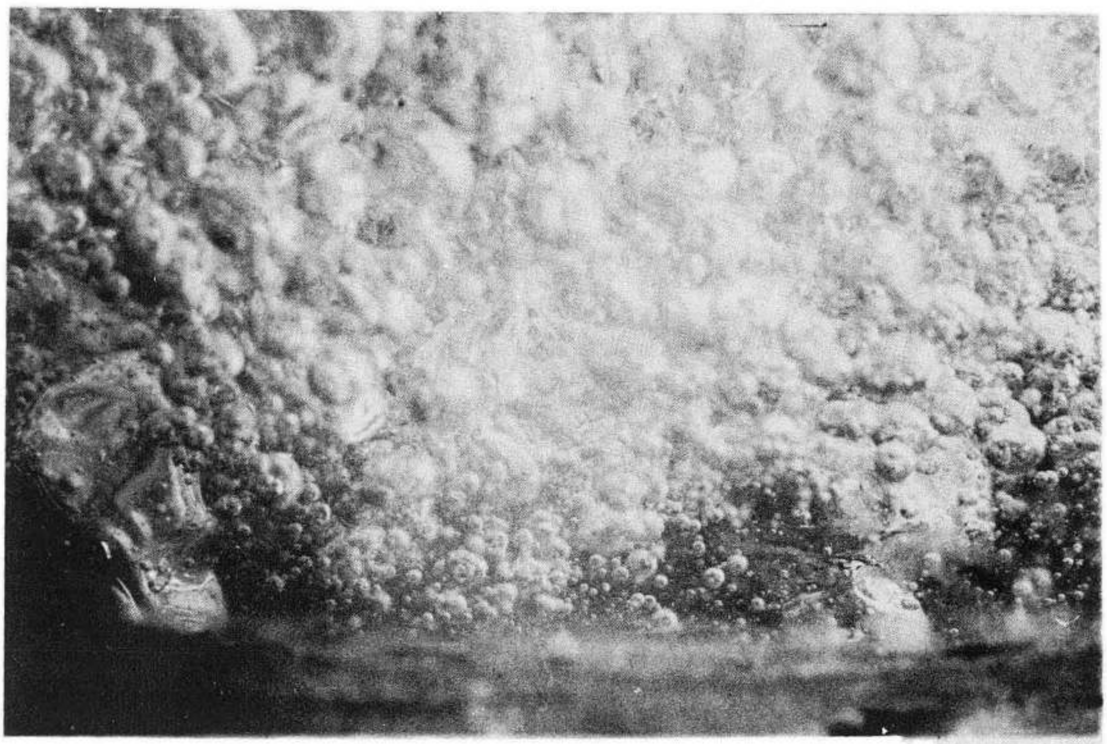

Fig. 53. 1/4-inch diameter perforations, 1-inch spacings, air-water system, air velocity 40 ft/sec. (3-1/2 x magn.)

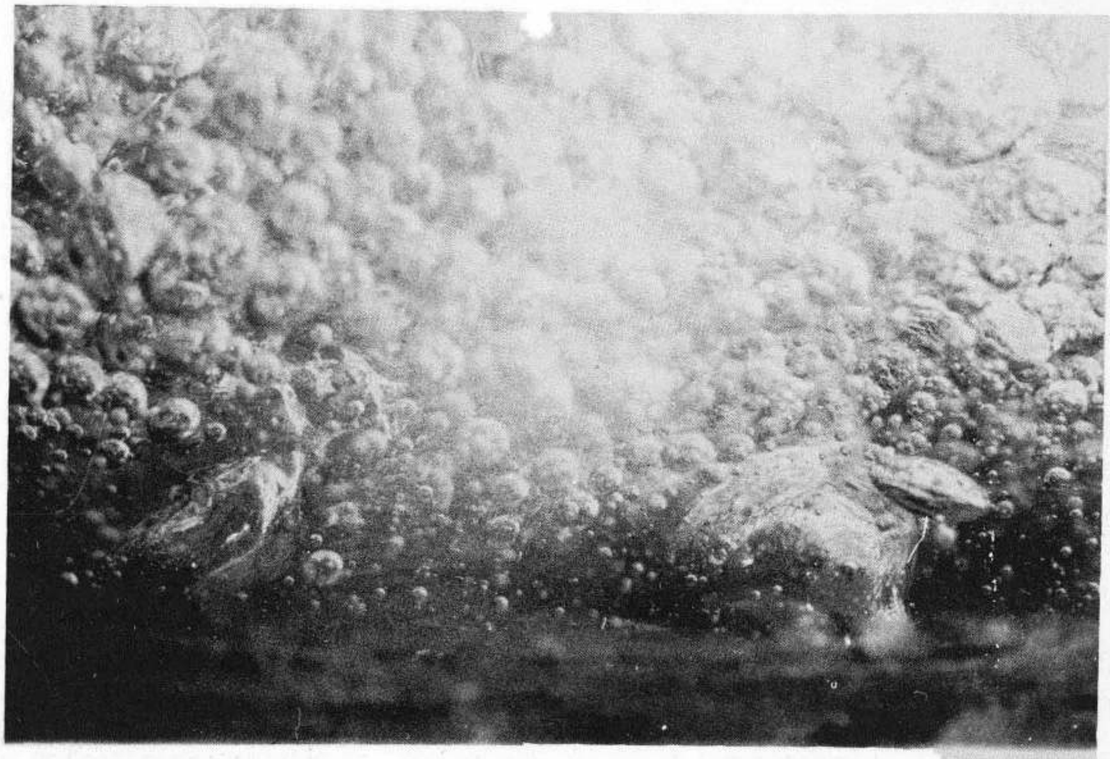

ZN-1052

Fig. 54. 1/4-inch diameter perforations, 1-inch spacings, air-water system, air velocity 40 ft/sec. (3-1/2 x magn.)

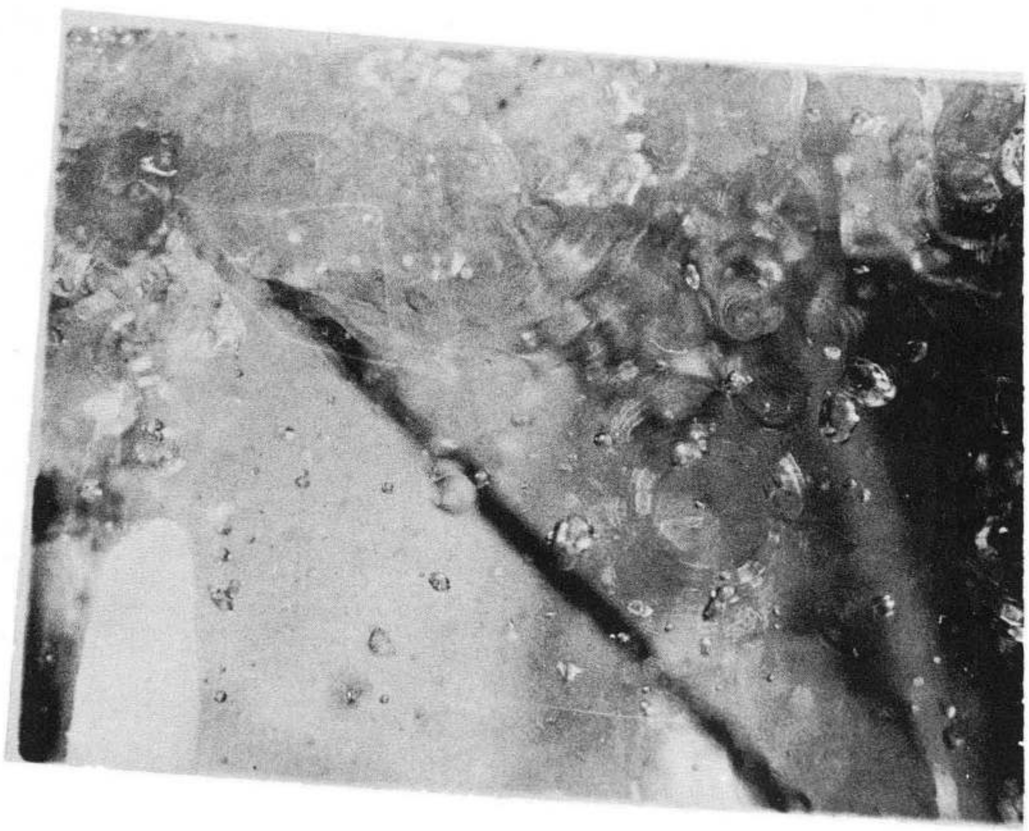

Fig. 55. Surface of Froth, Air-Water System.
Column Gas Velocity 3 ft/sec (full scale).

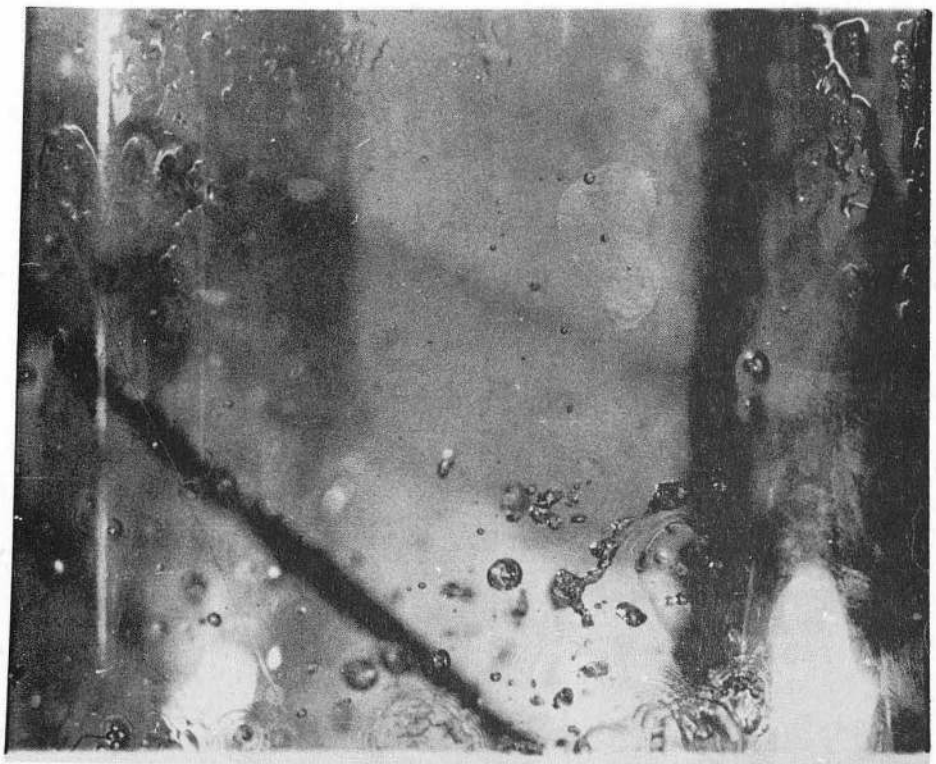

ZN-1054

Fig. 56. Entrained Liquid Region, 1 inch above froth surface, Air-Water System, Column Gas Velocity 3 ft/sec (full scale).

ZN-1055

Fig. 57. Froth, Air-Water System, Column
Gas Velocity 3 ft/sec (full scale).

Table I

Configuration of Perforated Plates

(All Holes in Equilateral Triangular Spacing)

Plate Number	Thick-ness (Inches)	Hole Diam. (Inches)	Hole Spacing (Inches)	Number Holes	Area Per Hole (sq.ft.)	Total Hole Area (sq.ft.)	Percent of Total Column Area
I	1/8	1/8	1/4	433	.0000852	.0369	18.8
II	1/8	1/8	1/2	109	.0000852	.00929	4.9
III	1/4	1/4	1	31	.000341	.01056	5.4
IV	1/4	1/4	1/2	109	.000341	.0372	19.0
V	1/2	1/2	2	7	.00136	.00954	4.9
VI	1/2	1/2	1	31	.00136	.04226	21.5
VII	3/8	3/8	1 1/2	13	.000767	.00997	5.1
VIII	1/4	1/4	3/4	55	.000341	.0187	9.5
II A	1/8	1/8	1/2	109	.0000852	.00929	4.9

Table II

Properties of Liquids Used

(At Temperatures (°C) Noted by Each Value)

Liquid	Density gm/cc	Viscosity (cp)	Surface Tension (dynes/cm)	Relative* Wettability
Water	1.0 (20)	1 (20)	73 (20)	1
Glyc-water	1.22 (20)	~10 (20)	69 (20)	2.0
" "	1.14 (20)	~80 (20)	65 (20)	2.0
Water (Wetting plate because of residual glyc.)	1.0 (20)	1 (20)	73 (20)	~2.0
n-Butyl Alc.	0.81 (20)	3.0 (20)	24.6 (20)	4.2
CCl_4	1.60 (20)	0.97 (20)	27.0 (20)	4.2
n-Hexane	0.67 (20)	0.3 (20)	18.4 (20)	5.7
Kerosene (approximately C-12)	0.71 (20)	~1 (20)	~25 (20)	6.0

*Arbitrarily defined here on the basis of the diameter to which a given volume of liquid will spread on an aluminum plate. Water is the reference liquid.

Table III

Plate Stability Data

(1.8" liquid head on plate)

Plate	Liquid	Gas	Gas Velocity at Critical Stability: In Perforations ft/sec	Gas Velocity at Critical Stability: In Column ft/sec
I	Water	Air	35	7.5
II	"	"	25	1.3
III	"	"	30	1.5
IV	"	"	>50	>10
V	"	"	27	1.4
VI	"	"	>60	12
VIII	"	"	40	4.0
III	Water (wetting the plate)	"	21	1.1
III	Water-Glyc. (Visc. 80 cp)	"	21	1.1
III	Water-Glyc. (Visc. 10 cp)	"	21	1.1
III	n-butyl alcohol	"	23	1.2
III	carbon tetrachloride	"	24	1.2
III	kerosene (C-12)	"	15	0.8
III	n-hexane	"	14	0.7
III	Water	Freon-12	15	0.8
III	Water	methane	32	1.6

Table III-A

Plate Stability Data, Air-Water System

(1.8" liquid head on plate)

Effect of Perforation Diameter and Total Perforation Area:

5% Total Area		20% Total Area	
Perforation Diameter, Inches	Gas Velocity at Critical Stability ft/sec	Perforation Diameter, Inches	Gas Velocity at Critical Stability ft/sec
1/8	25	1/8	35
1/4	30	1/4	> 50
1/2 (normal)	27	1/2	> 60
1/2 (modified)	35		

Table III-B

Plate Stability Data, Gas-Water System

(1.8" liquid head on plate) (Plate III)

Effect of Gas Density:

Gas	Specific Density (relative to air)	Gas Velocity at Critical Stability ft/sec
Methane	0.55	32
Air	1.0	30
Freon-12	4.0	15

Table III-C

Plate Stability Data, Air-Liquid System

(1.8" liquid on plate) (Plate III)

Effect of Liquid Properties:

Surface Tension of 70 dynes/cm			Surface Tension of 20 dynes/cm		
Liquid	Relative Wettability	Gas Vel. Crit.St.	Liquid	Relative Wettability	Gas Vel. Crit.St.
Water	1	30	n-butyl alcohol	4.2	23
Water plus Glycerine, Visc. 1 cp	2	21	carbon tetra-chloride	4.2	24
Water plus Glycerine, Visc. 10 cp	2	21	kerosene	5.7	15
Water plus Glycerine, Visc. 80 cp	2	21	n-hexane	6.0	14

Table IV

Entrainment Data

Run No.	System	Plate	Plate Spacing (Inches)	Gas Velocity Column (ft/sec)	Gas Velocity Hole (ft/sec)	Entrainment Rate (cc liq/min)	Notes
1	Air-CCl_4	III	20	4.9	97	15.3	(1) (Air + CCl_4 vapor) density = .117 lb/ft^3.
2	"	"	"	4.5	89	11.3	(2) Evap. losses cause approx. 2cc/min error in entrainment.
3	"	"	"	4.2	83	8.3	(3) 1.8" liq. head.
4	"	"	"	3.8	76	4.5	
5	"	"	"	3.5	69	2.8	
6	"	"	"	3.2	63	1.3	
7	"	"	"	2.7	53	0.5	
1	Air-Hexane	III	20	5.1	101	70	(1) (Air + Hexane vapor) density = .100 lb/ft^3
2	"	"	"	4.8	95	40	(2) Evap. losses cause approx. 3 cc/min error in entrainment
3	"	"	"	4.4	88	22.5	(3) 1.8" liq. head
4	"	"	"	4.0	80	12	
5	"	"	"	3.6	72	7.5	
6	"	"	"	3.2	63	3.5	
7	"	"	"	2.7	53	0.8	
1	Air-Kerosene	III	20	5.3	105	72.5	(1) 1.8" liq. head
2	"	"	"	4.9	98	47.5	
3	"	"	"	4.5	90	33	
4	"	"	"	4.2	83	23	
5	"	"	"	3.7	74	15.5	
6	"	"	"	3.2	64	9	
7	"	"	"	2.8	55	5	
8	"	"	"	2.2	44	2	
9	"	"	"	1.7	33	1	

Table IV

(Page 2)

Run No.	System	Plate	Plate Spacing (Inches)	Gas Velocity Column (ft/sec)	Gas Velocity Hole (ft/sec)	Entrainment Rate (cc liq/min)	Notes
1	Freon-H_2O	III	20	3.3	64.5	8.8	(1) 1.8" Liq. Head
2	"	"	"	3.0	59.6	6.5	
3	"	"	"	2.75	55.0	4.3	
4	"	"	"	2.5	50.3	2.5	
5	"	"	"	2.2	46.3	1.8	
1	Air-H_2O	III	20	3.4	67	2.8	(1) 1.8" Liq. Head
2	"	"	"	3.9	77	5.8	
3	"	"	"	4.4	87	8.3	
4	"	"	"	4.8	95	11.0	
5	"	"	"	5.1	101	13.5	
6	"	"	"	3.3	67	8.3	(2) 3.9" Liq. Head
7	"	"	"	3.8	76	14.3	
8	"	"	"	4.3	85	22.5	
9	"	"	"	4.7	94	22	(3) 2.9" Liq. Head
10	"	"	"	4.3	85	16	
11	"	"	"	3.8	76	10.5	
12	"	"	"	3.3	67	5.8	
13	"	"	"	3.3	67	4.3	(4) 2.3" Liq. Head
14	"	"	"	3.8	76	7	
15	"	"	"	4.3	85	11.6	
16	"	"	"	4.7	94	16.3	
1	Air-H_2O	III	20	4.8	94.5	14.5	(1) 1.8" Liq. Head
2	"	"	"	5.1	101	20	(2) Stabilizing screens above plate on all runs of this series (1-19)
3	"	"	"	3.9	78	9.5	

Table IV

(Page 3)

Run No.	System	Plate	Plate Spacing (Inches)	Gas Velocity Column (ft/sec)	Gas Velocity Hole (ft/sec)	Entrainment Rate (cc liq/min)	Notes
4	Air-H_2O	III	20	3.4	67	5.3	
5	"	"	"	4.6	91	28.5)	
6	"	"	"	4.2	83	24.5)	
7	"	"	"	3.8	77	18.5)	(3) 3.8" Liq. Head
8	"	"	"	3.6	71	13.0)	
9	"	"	"	3.2	63	9.5)	
10	"	"	"	3.2	63	7.0)	
11	"	"	"	3.6	71	10.0)	
12	"	"	"	3.8	77	14.0)	(4) 3.1" Liq. Head
13	"	"	"	4.2	83	18.5)	
14	"	"	"	4.6	91	22.5)	
15	"	"	"	4.6	91	17.0)	
16	"	"	"	4.2	83	13.5)	
17	"	"	"	3.8	77	11.0)	(5) 2.4" Liq. Head
18	"	"	"	3.6	71	8.0)	
19	"	"	"	3.2	63	6.3)	
1	"	"	24	4.3	86	7.5)	(1) 3.9" Liq. Head
2	"	"	"	3.8	77	4.5)	
3	"	"	"	3.4	67	3.0)	
4	"	"	"	3.4	67	1.2)	1.8" Liq. Head
5	"	"	"	3.8	77	2.0)	
6	"	"	"	4.3	86	3.5)	
7	"	"	"	4.8	95	5.5)	

Table IV ·

(Page 4)

Run No.	System	Plate	Plate Spacing (Inches)	Gas Velocity Column (ft/sec)	Gas Velocity Hole (ft/sec)	Entrainment Rate (cc liq/min)	Notes
1	Air-H_2O	III	28	4.3	86	2.5)	(1) 3.9" Liq. Head
2	"	"	"	3.8	77	1.5)	
3	"	"	"	3.4	67	1.0)	
4	"	"	"	3.4	67	0.5)	1.8" Liq. Head
5	"	"	"	3.8	77	0.8)	
6	"	"	"	4.3	86	1.4)	
7	"	"	"	4.8	95	2.4)	
1	"	VII	20	5.3	111	11.5	1.8" Liq. Head
2	"	"	"	4.8	101	10.0	
3	"	"	"	4.3	92	7.4	
4	"	"	"	3.8	82	5.6	
5	"	"	"	3.4	71	2.5	
1	"	V	"	3.4	74	7.0	(1) 1.8" Liq. Head
2	"	"	"	3.8	85	18.0	
3	"	"	"	4.3	96	30.5	
4	"	"	"	4.8	105	48.0	
1	"	II	"	5.3	120	20.5	(1) 1.8" Liq. Head
2	"	"	"	4.8	108	17.5	
3	"	"	"	4.3	99	10.8	
4	"	"	"	3.8	88	6.2	
5	"	"	"	3.4	76	3.3	

Table IV

(Page 5)

Run No.	System	Plate	Plate Spacing (Inches)	Gas Velocity Column (ft/sec)	Gas Velocity Hole (ft/sec)	Entrainment Rate (cc liq/min)	Notes
1	Air-H_2O	VII	20	3.4	71	5.0	(1) 1.8" Liq. Head
2	"	"	"	3.8	83	10.0	(2) Stabilizing screens on plate
3	"	"	"	4.3	101	19.8	
4	"	"	"	5.2	110	26.5	
1	"	V	20	3.4	74	16.0	(1) 1.8" Liq Head
2	"	"	"	3.8	86	36.5	(2) Stabilizing screens on plate
3	"	"	"	4.3	104	68.5	
1	"	II	"	5.2	117	18.0	(1) 1.8" Liq. Head
2	"	"	"	4.8	107	14.0	(2) Stabilizing screens on plate
3	"	"	"	3.8	88	8.5	
4	"	"	"	3.4	76	5.3	
1	"	VIII	"	6.1	62	24.0	(1) 1.8" Liq. Head
2	"	"	"	9.1	93	125	
3	"	"	"	8.5	87	90	
4	"	"	"	8.0	82	67	
5	"	"	"	7.0	71	43.3	
6	"	"	"	11.0	112	600	
1	"	IV	"	12.1	64	1090	(1) 1.8" Liq. Head
2	"	"	"	11.8	62	827	
3	"	"	"	11.5	60	648	
4	"	"	"	11.2	58	545	
5	"	"	"	10.8	56	370	
6	"	"	"	10.2	54	270	
7	"	"	"	9.7	51	203	
8	"	"	"	8.6	45	110	

Table IV

(Page 6)

Run No.	System	Plate	Plate Spacing (Inches)	Gas Velocity Column (ft/sec)	Gas Velocity Hole (ft/sec)	Entrainment Rate (cc liq/min)	Notes
1	CH_4-H_2O	III	20	4.05	81	2.5	(1) 1.8" Liq. Head
2	"	"	"	3.95	79.2	2.5	
3	"	"	"	4.7	94.3	4.0	
4	"	"	"	4.15	82.8	3.0	
5	"	"	"	3.6	72	1.5	
6	"	"	"	2.95	59	0.9	
1	Air-H_2O	VIII	16	7.2	72	95	(1) 1.8" Liq. Head
2	"	"	"	8.0	80	165	
3	"	"	"	8.4	84	240	
4	"	"	"	8.9	89	310	
1	"	"	12	8.0	40	840	(1) 1.8" Liq. Head
2	"	"	"	7.2	28	550	
3	"	"	"	6.1	24	240	
1	"	III	8	3.4	68	580	(1) 1.8" Liq. Head
2	"	"	"	3.2	64	340	
3	"	"	"	3.0	60	260	
4	"	"	"	2.75	55	170	
5	"	"	"	2.4	48	105	
6	"	"	"	1.8	36	55	
1	"	"	12	2.8	56	13	(1) 1.8" Liq. Head
2	"	"	"	3.2	64	21	
3	"	"	"	3.4	68	30	
4	"	"	"	3.9	78	62	
5	"	"	"	4.4	88	85	
6	"	"	"	4.8	96	110	
7	"	"	"	5.4	108	135	

Table V-1

Pressure Drop Data

System - Air-H_2O

Plate - I

Run Series - I

Run No.	ρgas (plate) lb/ft^3	V Hole ft/sec	ΔP_t cm H_2O x 2.50	h liq cm H_2O x 2.50	ΔP dyn lb/ft^2	ΔH ft gas
1	.0777	32.8	14.00	10.75	2.62	33.8
2	"	27.0	13.40	10.70	2.20	28.4
3	"	21.1	13.20	10.70	2.04	26.3
4	"	16.4	13.05	10.70	1.92	24.8
5	"	32.8	11.25	7.85	2.77	35.7
6	"	26.9	10.65	7.85	2.29	29.5
7	"	21.0	10.45	7.85	2.12	27.3
8	"	16.3	10.30	7.85	2.00	25.8
9	.0768	33.9	9.95	6.35	2.94	38.3
10	"	33.6	10.00	6.35	2.98	38.8
11	"	27.1	9.30	6.35	2.41	31.4
12	"	21.3	8.80	6.40	1.96	25.5
13	"	16.4	8.70	6.35	1.92	25.0
14	.0755	33.1	16.55	13.35	2.61	33.7
15	"	26.9	16.10	13.35	2.24	28.9
16	"	20.9	15.95	13.35	2.12	27.3
17	"	26.9	16.05	13.35	2.20	28.4
18	"	32.2	19.20	15.85	2.74	35.3
19	"	27.0	18.50	15.85	2.16	27.9
20	"	20.9	18.10	15.85	1.83	23.6
21	.0775	30.9	21.90	18.85	2.49	32.1
22	"	26.9	21.55	18.85	2.20	28.4
23	"	21.2	21.05	18.85	1.79	23.1
24	"	30.1	24.65	21.85	2.29	29.5
25	"	26.7	24.55	21.85	2.20	28.4
26	"	20.8	23.90	21.85	1.67	21.5
27	"	28.9	27.65	24.85	2.29	29.5
28	"	26.9	27.50	24.85	2.16	27.9
29	"	21.1	27.00	24.85	1.75	22.6
30	.0775	37.3	2.30		1.88	25.1
31	.0748	34.1	1.95		1.59	21.3
32	"	28.6	1.45		1.18	15.8
33	"	24.1	1.10		0.90	12.0
34	"	20.8	0.90		0.74	9.9
35	"	17.2	0.67		0.55	7.4
36	"	32.4	1.77		1.44	19.3

Table V-1

(Page 2)

Plate - I

Series - VI

Run No.	ρ gas (plate) lb/ft^3	V Hole ft/sec	ΔP_t cm H_2O x 2.50	h liq cm H_2O x 2.50	ΔP dyn lb/ft^2	ΔH ft gas
1	.0734	92.3	13.85		11.34	154
2	.0733	79.4	10.65		8.68	118
3	.0727	69.1	8.05		6.60	90.8
4	.0723	55.5	5.25		4.30	59.5
5	.0723	45.3	3.55		2.91	40.2
6	.0716	32.0	1.85		1.51	21.1
7	.0761	27.4	14.65	11.85	2.29	30.0
8	.0761	41.1	16.90	11.80	4.18	55.1
9	.0761	51.3	18.90	"	5.82	76.4
10	.0763	61.8	22.20	"	8.51	112
11	.0764	71.0	24.90	"	10.7	140
12	.0770	66.2	31.80	19.70	9.91	129
13	.0769	55.4	29.10	19.80	7.61	99
14	.0769	45.5	26.40	"	5.41	70.2
15	.0768	30.9	23.70	"	3.19	41.8

Series - XII

Run No.	ρ gas (plate) lb/ft^3	V Hole ft/sec	ΔP_t cm H_2O x 2.50	h liq cm H_2O x 2.50	ΔP dyn lb/ft^2	ΔH ft gas
1	.0745	70.8	23.4	10.2	10.81	145.1
2	.0744	63.6	21.9	10.5	9.33	125.4
3	.0745	54.7	20.2	11.2	7.37	98.9
4	.0745	45.2	18.1	11.1	5.73	76.9
5	.0745	34.2	15.8	11.3	3.69	49.5

Series - XIII

Run No.	ρ gas (plate) lb/ft^3	V Hole ft/sec	ΔP_t cm H_2O x 2.50	h liq cm H_2O x 2.50	ΔP dyn lb/ft^2	ΔH ft gas
1	.0745	71.5	13.3		10.89	146.5
2	.0745	71.3	13.2		10.81	145.5
3	.0745	54.6	8.3		6.76	91.1
4	.0744	63.6	10.8		8.83	119.0

Series - XIV

Run No.	ρ gas (plate) lb/ft^3	V Hole ft/sec	ΔP_t cm H_2O x 2.50	h liq cm H_2O x 2.50	ΔP dyn lb/ft^2	ΔH ft gas
1	.0756	72.9			11.5	151.4
2	.0756	70.7			11.06	145.9
3	.0755	68.9			10.56	139.5
4	.0755	67.8			10.07	133.5
5	.0754	66.3			9.70	128.2
6	.0754	62.9			8.97	118.5
7	.0736	61.3			8.27	112.4
8	.0736	57.7			7.45	101.2
9	.0739	54.2			6.67	90.3
10	.0742	49.1			5.69	76.6
11	.0744	45.7			4.91	65.9
12	.0744	40.3			3.89	52.3

Table V-1

(Page 3)

Series - XIV (continued)

Run No.	ρ gas (plate) lb/ft^3	V Hole ft/sec	ΔP_t cm H_2O x 2.50	h liq cm H_2O x 2.50	ΔP dyn lb/ft^2	ΔH ft gas
13	.0744	34.6			3.24	43.5
14	.0746	28.9			2.74	36.7
15	.0747	23.5			2.33	31.2
16	.0754	62.4			8.89	117.9
17	.0754	58.1			7.78	103.2
18	.0754	51.1			6.55	86.8
19	.0753	44.6			5.32	70.6
20	.0752	36.1			4.01	53.3
21	.0752	29.5			3.03	40.3
22	.0749	45.6			5.28	70.5
23	.0749	41.4			4.75	63.4
24	.0745	45.0			4.67	62.7
25	.0745	41.8			4.30	57.7
26	.0745	36.9			3.52	47.3
27	.0746	44.3			4.83	64.7
28	.0746	40.0			4.30	57.6
29	.0745	35.0			3.60	48.3
30	.0749	66.0			9.42	125.8

Table V-2

Pressure Drop Data

System - Air-H_2O

Plate - II

Run Series - II

Run No.	ρgas (plate) lb/ft^3	V Hole ft/sec	ΔP_t cm H_2O x 2.50	h liq cm H_2O x 2.50	ΔP dyn lb/ft^2	ΔH ft gas
1	.0755	78.4	11.25		9.18	121.6
2	"	70.4	9.35		7.63	101.1
3	"	60.8	6.95		5.67	75.1
4	"	51.8	5.05		4.12	54.6
5	"	43.9	3.65		2.98	39.5
6	"	34.8	2.35		1.92	25.4
7	"	25.8	1.30		1.06	14.0
8	"	18.1	0.75		0.61	8.1
9	.0757	78.2	22.80	6.35	13.42	177.3
10	.0757	65.4	18.20	"	9.67	128.1
11	.0755	54.3	14.90	"	6.98	93.0
12	.0753	43.8	12.55	"	5.06	67.3
13	.0752	32.3	10.80	"	3.63	48.0
14	.0757	21.7	9.80	"	2.81	37.2
15	.0754	13.1	9.25	"	2.37	31.5
16	.0760	77.7	27.05	10.85	13.22	173.9
17	.0760	64.3	22.55	"	9.55	125.
18	.0759	53.8	19.40	"	6.58	92.6
19	.0757	43.4	17.25	"	5.22	69.0
20	.0756	31.7	15.50	"	5.79	50.1
21	.0756	22.9	14.65	10.85	3.10	41.0
22	.0756	13.1	14.00	"	2.58	34.1
23	.0756	76.0	32.40	16.85	12.69	166.3
24	.0763	64.8	28.90	"	9.83	129.0
25	.0762	53.3	25.65	"	7.18	94.3
26	.0761	42.7	23.45	"	5.39	70.9
27	.0760	32.0	21.65	"	3.92	51.5
28	.0760	21.6	20.80	"	3.22	42.2
29	.0763	12.7	20.35	"	2.86	3.75
30	.0762	67.8	38.15	24.85	11.08	138.8
31	.0778	57.0	35.20	"	8.45	108.5
32	.0777	47.9	32.80	"	6.49	83.6
33	.0776	37.8	30.70	"	4.77	61.4
34	.0776	29.7	29.50	"	3.79	48.8
35	.0776	22.1	28.70	"	3.14	40.5
36	.0776	13.0	28.20	"	2.74	35.3

Table V-2

(Page 2)

Run No.	ρ gas (plate) lb/ft^3	V Hole ft/sec	ΔP_t cm H_2O x 2.50	h liq cm H_2O x 2.50	ΔP dyn lb/ft^2	ΔH ft gas
Plate-II						
Series - VIII						
1	.0744	188	59.4		48.6	653
2	.0739	155	40.7		33.3	451
3	.0735	123.5	25.5		20.9	284
4	.0732	91	14.2		11.6	158
Plate - II-A						
Series - IX						
1	.0740	93.8	18.55		15.19	205
2	.0740	85.3	15.70		12.85	174
3	.0740	74.8	12.10		9.91	134
4	.0739	63.7	8.85		7.25	98.1
5	.0739	47.0	4.9		4.01	54.3
6	.0739	29.0	2.05		1.68	22.7
8	.0745	93.5	35.4	9.80	21.0	281
9	.0744	84.6	31.8	"	18.0	242
10	.0743	74.3	29.5	"	14.5	195
11	.0743	63.2	23.5	"	11.2	151
12	.0746	49.8	18.7	"	7.29	97.7
13	.0745	35.5	15.4	"	4.59	61.6
14	.0749	93.3	47.5	22.7	20.3	271
15	.0748	83.5	43.8	"	17.3	231
16	.0746	75.0	40.1	"	14.3	191
17	.0745	62.5	35.1	"	10.2	136
18	.0752	49.0	31.0	22.6	6.87	91.4
19	.0748	35.3	28.0	"	4.42	59.1
Plate - II-A						
Series - XVII						
1	.0736	93.8	35.6	9.70	21.2	288
2	.0736	86.8	32.9	9.65	19.0	258
3	"	81.1	30.3	9.70	16.9	229
4	"	73.5	27.3	9.75	14.4	196
5	"	67.2	24.7	9.85	12.1	165
6	"	59.8	22.0	9.9	9.87	134
7	"	51.3	19.3	10.0	7.62	104
8	"	42.4	17.1	10.1	5.73	77.7
9	"	31.8	15.2	10.1	4.18	56.6

Table V-3

Pressure Drop Data

System - Air-H_2O

Plate - II

Run Series - III

Run No.	ρ gas (plate) lb/ft^3	V Hole ft/sec	ΔP_t cm H_2O x 2.50	h liq cm H_2O x 2.50	ΔP dyn lb/ft^2	ΔH ft gas
1	.0763	68.0	20.30	5.55	12.03	157.7
2	.0760	54.7	16.15	"	8.65	113.8
3	.0758	41.9	13.10	"	6.16	81.3
4	.0757	31.9	11.00	"	4.45	58.8
5	.0757	26.0	9.80	"	3.47	45.8
6	.0757	18.7	9.00	"	2.81	37.1
7	.0757	13.0	8.70	"	2.57	33.9
8	.0757	16.3	8.95	"	2.77	36.6
9	.0756	68.0	25.30	11.05	11.63	153.8
10	.0753	55.2	21.80	"	8.77	116.5
11	.0753	42.8	18.70	"	6.25	83.0
12	.0753	31.5	16.50	"	4.45	59.1
13	.0760	24.7	15.50	"	3.63	47.8
14	.0759	20.2	14.90	"	3.14	41.4
15	.0759	18.1	14.85	"	3.10	40.8
16	.0759	15.3	14.70	"	2.98	39.2
17	.0755	67.5	31.10	17.05	11.46	151.7
18	.0754	54.6	27.60	"	8.61	114.2
19	.0756	41.9	24.60	"	6.16	81.5
20	.0756	31.1	22.50	"	4.45	58.9
21	.0767	24.6	21.50	"	3.63	47.7
22	.0768	19.5	21.00	"	3.22	41.9
23	.0772	16.3	20.70	"	2.98	38.6
24	.0751	63.8	36.55	24.05	10.21	136.0
25	.0750	52.6	34.15	"	8.24	109.9
26	.0749	43.7	31.90	"	6.41	85.6
27	.0749	35.0	30.15	"	4.98	66.5
28	.0761	26.9	28.80	"	3.88	50.9
29	.0761	20.5	28.05	24.05	3.27	43.0
30	.0744	69.8	10.90		8.90	119.6
31	"	55.8	6.95		5.67	76.2
32	"	46.0	4.75		3.88	52.1
33	"	38.8	3.40		2.77	37.2
34	"	30.8	2.15		1.76	23.7
35	"	25.6	1.55		1.26	16.9
36	"	20.8	1.15		0.94	12.6
37	"	15.6	0.88		0.72	9.7
38	"	11.5	0.67		0.55	7.4

Table V-4

Pressure Drop Data

System - Air-H_2O

Plate - IV

Series - IV

Run No.	ρ gas (plate) lb/ft^3	V Hole ft/sec	ΔP_t cm H_2O x 2.50	h liq cm H_2O x 2.50	ΔP dyn lb/ft^2	ΔH ft gas
1	.0738	90.9	14.15		11.60	157
2	.0736	79.6	11.05		9.05	123
3	.0736	68.5	8.15		6.66	90.4
4	.0734	54.8	5.15		4.22	57.5
5	.0734	44.1	3.35		2.74	37.3
6	.0733	34.9	2.10		1.72	23.4
7	.0733	24.0	0.90		0.74	10.1
8	.0755	28.0	13.6	11.0	2.1	28
9	.0755	39.5	15.5	"	3.7	49
10	.0756	51.1	17.8	"	5.6	74
11	.0754	58.2	12.55	"	7.0	93
12	.0754	69.2	22.2	"	9.2	122
13	.0758	66.7	29.4	18.8	8.7	115
14	.0758	60.6	27.9	"	7.4	98
15	.0756	51.4	26.1	"	6.0	79
16	.0754	40.0	23.8	"	4.1	55
17	.0754	27.9	21.9	"	2.5	33
Series XI						
1	.0746	69.4	21.35	10.4	8.96	120
2	.0745	61.6	20.0	10.9	7.45	100
3	.0745	52.8	17.9	10.5	6.06	81.3
4	.0745	43.7	16.1	10.8	4.34	58.3
5	.0746	32.5	14.0	11.0	2.45	32.8
Series XV						
1	.0746	59.9	18.85	10.45	6.88	92.2
2	.0746	73.0	22.20	10.55	9.54	128
3	.0745	71.1	21.65	10.40	9.21	124
4	.0744	66.9	20.10	9.95	8.31	112
5	.0746	62.4	19.85	10.75	7.45	98.5
1a	.0742	60.2	18.45	9.85	7.04	94.8
2a	.0741	73.9	21.95	10.15	9.66	130
3a	.0740	71.9	21.50	10.00	9.42	127
4a	.0746	67.0	19.9	9.65	8.39	112
5a	.0746	62.7	19.8	10.35	7.74	104

Table V-4

(Page 2)

Run No.	ρ gas (plate) lb/ft^3	V Hole ft/sec	ΔP_t cm H_2O x 2.50	h liq cm H_2O x 2.50	ΔP dyn lb/ft^2	ΔH ft gas
6	.0747	59.8	18.65	9.95	7.13	95.3
7	.0745	56.3	17.65	9.80	6.43	86.3
8	.0746	52.5	17.10	10.05	5.77	77.4
9	.0747	48.8	16.00	9.65	5.20	69.6
10	.0745	44.5	15.05	9.65	4.42	59.4
11	.0746	39.8	14.35	9.80	3.73	49.9
12	.0745	33.2	13.60	10.05	2.91	39.0
13	.0746	28.3	12.85	9.90	2.42	32.4
14	.0754	63.9	31.05	21.15	8.11	108
15	.0753	59.9	30.4	21.25	7.49	99.4
16	.0753	56.6	29.9	21.30	7.04	93.5
17	.0750	52.3	29.0	21.45	6.18	82.4
18	.0748	47.2	28.0	21.40	5.41	72.3
19	.0748	40.8	26.25	21.15	4.18	55.8
20	.0747	36.2	25.5	21.10	3.60	48.1
21	.0747	30.7	24.85	21.40	2.83	37.9
22	.0748	58.3	26.1	17.45	7.08	94.6
23	.0747	58.3	23.45	14.95	6.96	93.2
24	.0747	58.8	20.15	11.65	6.96	93.3
25	.0745	58.8	17.5	8.95	7.02	94.2

Table V-5

Pressure Drop Data

System - Air-H_2O

Plate - V

Series - V

Run No.	ρ gas (plate) lb/ft^3	V Hole ft/sec	ΔP_t cm H_2O x 2.50	h liq cm H_2O x 2.50	ΔP dyn lb/ft^2	ΔH ft gas
1	.0764	74.3	24.55	5.95	15.18	198.7
2	.0761	59.2	18.85	"	10.53	138.4
3	.0759	49.9	15.65	"	7.91	104.2
4	.0757	41.3	13.35	"	6.04	79.8
5	.0759	34.9	12.00	"	4.94	65.1
6	.0759	27.7	10.55	"	3.75	49.4
7	.0759	23.0	9.95	"	3.27	43.1
8	.0767	70.8	27.90	12.00	12.98	169.2
9	.0766	58.7	23.90	"	9.71	126.8
10	.0763	48.5	20.90	"	7.27	95.3
11	.0752	41.3	19.05	"	5.75	76.5
12	.0761	34.3	17.65	"	4.61	60.6
13	.0760	24.8	16.05	"	3.31	43.6
14	.0767	70.9	33.55	18.00	12.69	165.4
15	.0766	58.6	29.80	"	9.63	125.7
16	.0765	47.9	26.55	"	6.98	91.2
17	.0764	40.9	24.65	"	5.43	71.1
18	.0763	32.4	23.25	"	4.29	56.2
19	.0762	28.2	22.45	"	3.63	47.6
20	.0770	66.5	37.65	24.05	11.10	144.2
21	.0769	56.8	34.85	"	8.81	114.6
22	.0768	47.3	32.05	"	6.53	85.0
23	.0768	40.0	30.55	"	5.31	69.1
24	.0768	32.6	29.10	"	4.12	53.6
25	.0767	26.9	28.05	"	3.27	42.6
26	.0753	76.3	14.00		11.42	151.7
27	.0753	62.1	9.35		7.63	101.3
28	.0753	52.5	6.50		5.31	70.5
29	.0753	43.3	4.32		3.52	46.7
30	.0753	34.4	2.70		2.20	29.2
31	.0753	27.4	1.75		1.43	19.0
32	.0753	21.9	1.20		0.98	13.0

Table V-6

Pressure Drop Data

System - Air-H_2O

Plate - VI

Series - VII

Run No.	ρ gas (plate) lb/ft^3	V Hole ft/sec	ΔP_t cm H_2O x 2.50	h liq cm H_2O x 2.50	ΔP dyn lb/ft^2	ΔH ft gas
1	.0730	78.8	11.0		9.01	123
2	.0730	67.3	8.25		6.76	92.3
3	.0729	58.3	6.20		5.08	69.6
4	.0728	45.3	3.60		2.95	40.5
5	.0727	30.6	1.70		1.39	19.1
6	.0727	24.2	1.20		0.98	13.5

Series XVI

Run No.	ρ gas (plate) lb/ft^3	V Hole ft/sec	ΔP_t cm H_2O x 2.50	h liq cm H_2O x 2.50	ΔP dyn lb/ft^2	ΔH ft gas
1	.0752	35.9	15.7	12.2	2.87	38.2
2	.0751	43.1	17.95	12.65	4.34	57.8
3	.0752	48.9	19.0	12.40	5.41	71.9
4	.0753	54.1	20.1	12.60	6.14	81.5
5	.0753	58.3	20.85	12.40	6.92	91.8
6	.0753	62.0	22.1	12.80	7.62	101.2
7	.0753	39.2	20.85	16.50	3.56	42.2
8	.0753	43.9	22.40	17.00	4.42	58.6
9	.0753	47.8	23.10	16.80	5.16	68.5
10	.0752	51.8	24.4	17.20	5.90	78.4
11	.0754	55.6	25.3	17.30	6.55	86.8
12	.0754	59.5	25.75	16.95	7.21	95.6
13	.0756	53.3	29.40	22.10	5.98	79.1
14	.0756	57.6	30.1	22.40	6.31	86.4

Table V-7

Plate - VII

Series - X

Run No.	ρ gas (plate) lb/ft^3	V Hole ft/sec	ΔP_t cm H_2O x 2.50	h liq cm H_2O x 2.50	ΔP dyn lb/ft^2	ΔH ft gas
1	.0738	91.1	18.9		15.5	210
2	.0737	82.6	15.55		12.7	173
3	.0736	73.0	11.9		9.75	132
4	.0736	62.0	8.65		7.08	96.2
5	.0735	47.8	5.15		4.22	57.4
6	.0734	30.3	2.10		1.72	23.4

Table V-8

Pressure Drop Data

System - Freon

Plate - III

Series - III

Run No.	ρ gas (plate) lb.ft^3	V Hole ft/sec	ΔP_t cm H_2O	h liq cm H_2O	ΔP dyn lb/ft^2	ΔH ft gas
1	.321	65.7	16.02		32.8	102.1
2	.320	58.3	13.26		27.1	84.7
3	.319	53.7	11.16		22.8	71.6
4	.318	48.9	9.22		18.9	59.3
5	.317	43.9	7.32		15.0	47.3
6	.316	40.4	6.12		12.5	39.6
7	.316	32.7	3.82		7.82	24.7
8	.316	26.1	2.44		4.99	15.8
9	.316	20.5	1.50		3.07	9.7
10	.317	56.0	19.32	6.45	26.3	82.9
11	.314	50.9	17.00	6.48	21.5	68.5
12	.313	47.2	15.42	6.51	18.2	58.2
13	.313	39.8	12.86	6.46	13.1	41.8
14	.312	33.4	10.92	6.40	9.25	29.6
15	.312	27.1	9.36	6.36	6.14	19.7
16	.314	20.0	8.16	6.38	3.81	12.1

Table V-9

System - CO_2

Plate - III

Series - IV

1	.1038	110.8	15.42		31.1	304
2	.1035	104.9	13.80		27.8	273
3	.1033	97.0	11.62		23.4	230
4	.1031	88.3	9.56		19.2	190
5	.1032	80.2	7.76		15.5	154
6	.1030	69.3	5.80		11.5	115
7	.1028	58.2	4.06		7.90	80.8
8	.1025	48.4	2.76		5.24	55.1
9	.1029	38.3	1.80		3.27	35.8
10	.1029	28.7	1.06		1.76	21.1
11	.1023	97.5	18.16	5.03	26.5	259
12	.1022	89.5	16.16	"	22.4	219

Table V-9

(Page 2)

Run No.	ρ gas (plate) lb/ft³	V Hole ft/sec	ΔP_t cm H_2O	h liq cm H_2O	ΔP dyn lb/ft²	ΔH ft gas
13	.1021	81.6	14.26	5.03	18.5	181
14	.1019	73.6	12.42	5.03	14.7	144
15	.1017	64.5	10.76	4.98	11.4	112
16	.1020	55.7	9.46	4.96	8.80	86.3
17	.1023	45.5	8.26	4.96	6.34	62.0
18	.1023	37.0	7.46	4.96	4.71	46.0
19	.1021	27.9	6.80	4.96	3.36	32.9

Table V-10

System - Argon

Plate - III

Series - V

1	.1037	94.7	10.60		21.7	209
2	.1035	88.8	9.20		18.8	182
3	.1031	80.3	7.40		15.1	147
4	.1030	72.7	6.10		12.5	121
5	.1029	65.8	5.00		10.2	99.4
6	.1028	57.8	3.86		7.90	76.8
7	.1027	50.9	2.94		6.02	58.6
8	.1025	41.2	1.98		4.05	39.5
9	.1025	32.7	1.20		2.46	24.0
10	.1035	94.8	17.06	4.95	24.8	239
11	.1031	88.9	15.50	4.88	21.7	211
12	.1028	80.7	13.72	4.98	17.9	174
13	.1026	73.1	12.22	4.93	14.9	145
14	.1030	66.0	11.06	4.93	12.5	122
15	.1028	58.1	9.86	4.86	10.23	99.5
16	.1027	50.9	8.96	4.86	8.39	81.7
17	.1025	40.7	7.96	4.86	6.34	61.9
18	.1025	31.9	7.20	4.87	4.77	46.5

Table V-11

System - CH_4

Plate -III

Series - VI

1	.0377	114	5.96		12.2	323
2	.0378	106	5.14		10.52	278
3	.0377	101	4.56		9.33	247
4	.0377	93	3.96		8.10	215

Table V-11

(Page 2)

Run No.	ρ gas (plate) lb/ft^3	V Hole ft/sec	ΔP_t cm H_2O	h liq cm H_2O	ΔP dyn lb/ft^2	ΔH ft gas
5	.0377	85.5	3.28		6.71	178
6	.0376	78	2.70		5.52	147
7	.0376	68	2.08		4.26	113
8	.0376	57.3	1.48		3.03	80.5
9	.0375	46.5	0.96		1.96	52.3
9a	.0375	35.2	0.60		1.23	32.7
10	.0378	100	10.16	4.75	11.07	293
11	.0377	94	9.64	4.73	10.05	267
12	.0378	87	8.98	4.71	8.74	231
13	.0377	77.4	8.34	4.70	7.45	198
14	.0377	68.6	7.76	4.69	6.28	167
15	.0377	58.0	7.16	4.69	4.87	129
16	.0377	46.3	6.60	4.69	3.91	104
17	.0377	34.1	6.10	4.66	2.95	78.1

Table V-12

System - Glycerine (μ 80 cp)

Plate - III

Series - A

1	.0759	107	9.84		20.1	265
2	.0759	93.1	7.34		15.0	198
3	.0756	73.3	4.50		9.21	122
4	.0754	55.8	2.56		5.24	69.5
5	.0755	38.3	1.22		2.50	33.1
6	.0768	106	16.78	6.17	21.7	282
7	.0767	101	15.74	6.18	19.6	255
8	.0765	93.1	14.20	6.25	16.3	213
9	.0764	87.0	13.28	6.26	14.4	188
10	.0761	79.3	12.22	6.27	12.2	159
11	.0760	70.2	11.28	6.27	10.3	135
12	.0761	62.6	10.50	6.22	8.76	115
13	.0759	54.5	9.68	6.26	7.00	92.2
14	.0762	45.7	8.68	6.16	5.16	67.7
15	.0760	35.1	7.78	5.99	3.66	48.1
16	.0761	29.6	7.28	5.86	2.91	38.2

Table V-13

System - Glycerine (μ = 10 cp)

Plate - III

Series - B

1	.0760	106	15.52	5.37	20.8	273
2	.0758	98.6	14.08	5.43	17.7	234
3	.0756	90.7	12.62	5.20	15.2	201

Table V-13

(Page 2)

Run No.	ρ gas (plate) lb/ft^3	V Hole ft/sec	ΔP_t cm H_2O	h liq cm H_2O	ΔP dyn lb/ft^2	ΔH ft gas
4	.0756	85.0	11.72	5.17	13.4	177
5	.0756	75.4	10.32	5.14	10.6	140
6	.0756	68.3	9.46	5.14	8.84	117
7	.0756	59.1	8.68	5.14	7.24	95.8
8	.0755	49.9	7.82	4.99	5.79	76.6
9	.0757	40.9	7.16	4.96	4.50	59.4
10	.0756	28.2	5.96	4.44	3.11	41.1

Table V-14

System - H_2O (wetting plate)

Plate - III

Series - C

1	.0758	108	15.56	4.48	22.7	299
2	.0756	95.4	13.00	4.18	18.1	239
3	.0756	86.6	11.46	4.18	14.9	197
4	.0754	76.7	10.06	4.23	11.9	158
5	.0753	62.6	8.46	4.23	8.65	115
6	.0753	47.4	7.12	4.25	5.87	78.0
7	.0754	38.1	6.46	4.28	4.46	59.2
8	.0753	26.9	5.76	4.23	3.13	41.5

Table V-15

System - n-Butyl Alcohol

Plate - III

Series - D

1	.0771	107	14.64	3.26	23.3	302
2	.0768	100	13.24	3.28	20.4	265
3	.0767	90.1	11.44	3.26	16.7	218
4	.0767	83.9	10.44	3.24	14.7	192
5	.0767	74.1	8.88	3.22	11.6	151
6	.0766	63.0	7.34	3.22	8.43	110
7	.0766	55.3	6.24	3.35	5.91	83.0
8	.0765	43.5	5.64	3.43	4.52	59.0
9	.0765	32.8	4.76	3.35	2.88	37.6

Table V-16

System - CCl_4

Plate - III

Series - E

Table V-16

(Page 2)

Run No.	ρ gas (plate) lb/ft³	V Hole ft/sec	ΔP_t cm H_2O	h liq cm H_2O	ΔP dyn lb/ft²	ΔH ft gas
1	.1184	96.9	21.24	6.85	29.4	248
2	.1194	89.3	19.24	7.09	24.9	208
3	.1186	83.2	17.62	7.09	21.5	182
4	.1191	76.3	15.90	6.85	18.5	156
5	.1176	69.2	14.34	6.85	15.3	130
6	.1167	63.3	12.78	6.61	12.6	108
7	.1152	53.3	11.00	6.45	9.31	80.8
8	.1140	45.9	9.54	6.29	6.65	58.3
9	.1133	36.1	8.10	6.05	4.19	37.0

Table V-17

System - Kerosene

Plate - III

Series - F

1	.0778	105	12.84	2.95	20.2	260
2	.0777	98.0	11.50	2.95	17.5	225
3	.0775	90.0	10.04	2.95	14.5	187
4	.0774	82.5	8.94	2.95	12.3	158
5	.0772	73.5	7.74	2.95	9.80	127
6	.0772	64.1	6.60	2.95	7.47	96.7
7	.0772	54.7	5.64	2.95	5.50	71.3
8	.0771	43.5	4.84	2.91	3.95	51.2
9	.0770	33.0	4.24	2.91	2.72	35.3

Table V-18

System - n-Hexane

Plate - III

Series - G

1	.0999	101	14.44	2.56	24.3	243
2	.0999	95.1	12.98	2.56	21.3	213
3	.0999	87.5	11.40	2.43	18.4	184
4	.0999	79.5	9.84	2.43	15.2	152
5	.0995	72.1	8.50	2.36	12.6	126
6	.0993	63.3	7.08	2.36	9.66	97.3
7	.0992	53.1	5.60	2.23	6.90	69.6
8	.0989	40.8	4.24	2.26	4.05	41.0
9	.0984	29.5	3.44	2.26	2.41	24.5

Acknowledgments

The author is indebted to Professor D. N. Hanson and Professor C. R. Wilke for help and stimulus provided during the course of this investigation.

This work was performed under the auspices of the Atomic Energy Commission.